

**SUMMARY REPORT OF
GEOTECHNICAL INVESTIGATIONS;
9/86 THROUGH 2/88; MARICOPA
SUPERCONDUCTING SUPER COLLIDER
SITE; MARICOPA COUNTY, ARIZONA**

Arizona Geological Survey
Open-File Report 87-6

1987

Arizona Geological Survey
416 W. Congress, Suite #100, Tucson, Arizona 85701

*Prepared by
Engineers International, Inc., in association with
Department of Mining and Geological Engineering
Department of Civil Engineering & Engineering Mechanics
College of Engineering and Mines
The University of Arizona, and the
Arizona Geological Survey*

This report is preliminary and has not been edited
or reviewed for conformity with Arizona Geological Survey standards

LIST OF CONTRIBUTORS

Engineers International, Inc.

Robert A. Cummings
Larry A. Salhaney
Gregory D. Zeihen

Department of Mining and Geological Engineering

Robert Armstrong
Jaak Daemen
Ian W. Farmer
Mary E. Glynn
Navid Mojtabai
Ben K. Sternberg

Department of Civil Engineering and Civil Mechanics

Jay S. DeNatale
Edward A. Nowatzki

Arizona Geological Survey

Stephen J. Reynolds
Jon E. Spencer
John W. Welty

Arizona SSC Project

Steven J. Brooks

TABLE OF CONTENTS

EXECUTIVE SUMMARY	i
List of Figures	iv
List of Tables	v
1.0 INTRODUCTION	1
1.1 Purpose and Scope of Report	1
1.2 Approach	3
1.3 Participation	3
2.0 GEOLOGIC SETTING	5
2.1 Site Location	5
2.2 Geologic Setting	5
2.3 Groundwater	6
3.0 PROJECT DEVELOPMENT	8
3.1 Existing Geotechnical Data	8
3.2 Identification of SSC Data Requirements	8
3.3 Design of the Investigation	10
4.0 CONSTRUCTION SEGMENTS IN HARD ROCK	13
4.1 Description of Surface Studies	13
4.1.1. Seismic Refraction Surveys	13
4.1.2. Geotechnical Mapping	15
4.1.3. Geological Reconnaissance	16
4.2 Diamond Drilling	17
4.2.1. Drilling Program Overview	17
4.2.2. Core Logging Program	19
4.2.3. Hole Abandonment	19
4.3 Testing	19
4.4 Findings	21
4.4.1. Results of Core Drilling	21
4.4.2. Geological and Geotechnical Reconnaissance	32
4.4.2.1. Results of Surface Geotechnical Reconnaissance	32
4.4.2.2. Results of Geological Reconnaissance	42
4.4.2.3. Discontinuity Orientations	44
4.4.3. Distribution of Rock Mass Strength	45
4.4.4. Seismic Refraction Interpretation	54
4.4.4.1. Distribution of Detected Seismic Velocities	54
4.4.4.2. Correlation with Strength and Modulus	56
4.4.5. Forecast of Hard Rock Tunnelling Characteristics	58
4.4.5.1. Intrusive Assemblage	61
4.4.5.2. Volcanic Assemblage	63
5.0 Construction Segments in Alluvium and Conglomerate	66
5.1 Description of Surface Studies	66
5.1.1. Geophysical Surveys	66
5.1.2. In-Place Testing	67
5.1.3. Examination of Nearby Exposures	67

TABLE OF CONTENTS (cont)

5.2	Subsurface Studies	72
5.2.1.	Drilling	72
5.2.2.	In-Place Testing	74
5.3	Laboratory Testing	76
5.3.1.	Sieve Analyses	76
5.3.2.	Atterberg Limits Analyses	76
5.3.3.	Soil Classifications	76
5.3.4.	Direct Shear Testing	76
5.3.5.	Triaxial Testing	77
5.3.6.	Analysis of Collapse Potential	77
5.4	Hydrology	78
5.5	Findings	79
5.5.1.	Results of Drilling	79
5.5.2.	In-Place Testing Results	81
5.5.3.	Laboratory Testing Results	84
5.5.4.	Comparability of Fanglomerate Strength Data	94
5.5.5.	Seismic Refraction Interpretation	94
5.5.6.	Comparison of Fanglomerate Response and Seismic Strength	95
5.5.7.	Forecast of Fanglomerate Tunnelling Characteristics	96
5.5.7.1.	Open Cut Construction - Stability Analysis For 90 Degree, 60 Degree, and 45 Degree Slopes	98
5.5.7.2.	Soft Ground Tunnelling	101
6.0	CONSTRUCTION OF OTHER FEATURES	103
6.1	Shafts	104
6.2	Campus Area, Injector Complex, and Experimental Halls	105
6.2.1.	Physical Layout and Description	105
6.2.2.	General Soil Conditions	106
6.2.4.	Seismic Design Provision	110
6.3	Temporary Portals and Access Ramps	110
7.0	CONSLUSIONS	111
7.1	Ring Geology by Construction Units	111
7.2	Construction Costs	128
7.2.1.	Cut-and-Fill for Ring and Injector Tunnels	129
7.2.3.	TBM for Ring and Injector Tunnels	129
7.2.4.	Comparison of TBM Versus Cut-and-Fill	129
7.2.4.	Experimental Chambers	129
7.2.5.	Shafts	130
REFERENCES	138

EXECUTIVE SUMMARY

The proposed Superconducting Super Collider (SSC) site passes mainly through three types of earth materials: approximately 35 miles of indurated alluvium and fanglomerate, 10 miles of granitic rocks and 8 miles of volcanic and sedimentary rocks. Data were obtained from three main sources: (1) existing data sources, (2) field investigations including drilling and geophysics, and (3) laboratory testing.

The field drilling included seven diamond drill holes, four rotary holes and nine auger holes. The auger holes were advanced in the alluvial fanglomerates and included standard penetration tests. The drill core from volcanic and intrusive rocks was logged for lithology, RQD, fracture frequency, point load index, and other geotechnical parameters. Cores were tested for uniaxial and triaxial strength. Deaggregated samples of alluvium from rotary and auger holes were subjected to standard soil index tests.

Seismic refraction surveys were also carried out to describe the consistency and limits of the fanglomerates and alluvium. In addition, seismic data were collected to investigate the strength and consistency of the intrusive and volcanic bedrock types and the nature of their buried pediment surfaces (if any) and the extent and character of any measurable weathered zones at the tops of the bedrock surfaces. Geophysical borehole logs from the rotary holes were compared with seismic data. Seismic lines and boreholes were located so as to coincide, wherever feasible to do so.

To further document the suitability of indurated alluvium and fanglomerate for deep surface cuts and subsurface soft-ground tunnelling, field in-place tests were conducted in trenches and boreholes. Where a close spatial relationship could be achieved, these strength data were compared to nearby seismic profiles or logs from nearby boreholes, to establish the relationship of seismic velocity to laboratory and in-place material properties. In this way, confidence in the continuity of favorable construction indices throughout the ring was established.

The fanglomerates have the consistency of weak sandstone. Standard Penetration Tests (SPT) values in excess of 200 blows/foot, and seismic velocities in excess of 3000 feet/second, indicate compressive strengths greater than 500 psi for fanglomerates. Higher velocities and strengths were found in older, and generally deeper, fanglomerates. Locally, indurated alluvium of somewhat less, but still substantial, strength is found above the fanglomerates.

Geophysical surveys demonstrate the consistency of the properties of fanglomerates and alluvial deposits found around the ring. Both types of fanglomerates occur above the water table; local variations in water table or substantial perched water zones that could impact the behavior of these materials in construction have not been detected to date and are not expected under the prevailing climate and observed subsurface conditions.

The fanglomerate and alluvium are moderately-indurated, unfractured, dry, and remarkably uniform in their gross material properties. As such, they make nearly-ideal materials for SSC construction. In open cut, they will be readily ripped with conventional high-production earthmoving equipment and will stand for long periods in steep, near-vertical slopes. Underground, they are ideal soft-ground tunnelling media. They have sufficient cementation and strength to withstand the stress redistribution associated with tunnelling without exhibiting stability problems. They will be easily penetrated by machine and high rates of advance are expected.

The granitic rocks have strengths that range up to 30,000 psi and more, depending on weathering and local fracturing. Locally, aplite, pegmatite, and diabase dikes are present, as are quartz veins, but they are not a significant percentage of the total rock mass. The granites have generally low fracture frequency and high RQD whereas the quartz diorite has higher fracture frequency and lower RQD. Rock mass quality is generally good to excellent, as indicated by rock mass classification values. Rock mass classes vary in the vicinity of fracture zones and faults; fractured zones are ordinarily associated with increases in weathering intensity and decreases in strength. Faults and shears noted in core and outcrops are associated with similar strength variations. Faults noted consist mostly of crushed rock with little gouge and are dry. Shears and fractures in core commonly contain clay but infilling thicknesses are probably generally less than the dimensions of asperities or waviness along the fracture planes. The top surfaces of intrusive rocks exhibit weathering (discolored biotite, cloudy feldspars, somewhat lowered strength) that ranges from intense just below the alluvium or fanglomerate contact, to slight at depths of 100 ft or more. This argues against expectations of prevalent mixed-face conditions, in that the tunnel will pass through substantial transition zones. These zones separate fanglomerates and alluvium, which have the properties of weak to moderate sandstone, from the harder intrusive rocks.

The intrusive rock masses vary somewhat in weathering intensity and fracturing. Points in the rock mass that are distant from fractured zones exhibit the highest strengths reported and the fractured zones themselves, because of weathering associated with them, exhibit lower strengths. Field evidence suggests that in a horizontal tunnel, such variations in rock mass strength may be encountered at wide intervals. Correlated point load strengths from core reflect this variation: these strengths range from near 30,000 psi in the strongest material to less than 5,000 psi in the centers of the most weathered zones. Even intense weathering is not accompanied by extensive clay development, however; thus, squeezing or swelling conditions are not considered likely. Minimal or no support should be all that is required in the stronger zones. Bolts, mesh, and shotcrete may be necessary in the weaker zones. Although some fractured areas may be found to be damp, local climatic conditions, drillhole data, and experience with other underground excavations in southern Arizona argue strongly that this should be the maximal extent of water encountered in the intrusive sections.

The volcanic rocks are comprised of basalt, granite-clast conglomerates, and welded tuff. The conglomerates exhibit drilling behavior, laboratory strengths, and field seismic velocities that are comparable to the fanglomerates. Field mapping and core drilling show that fracturing is

scarce to absent in conglomerates. The basalt is thickly-bedded, massive, and its vesicularity is variable. No ashfall, cinder, or flow-top zones have been identified by field mapping and core drilling completed to date in this material. The basalt is sparingly-fractured and most fractures are either rough, curved, or healed with calcite, so these should detract little from overall rock mass strength. Laboratory and point load tests indicate a compressive strength in the neighborhood of 8,000 psi, which is not strong for massive basalts, and probably results from weathering. The basalts are the most competent units present in the volcanic assemblage, but they are not so strong that problems with advance rates would be expected during tunnelling. The tuffs and conglomerates also present favorable tunnelling characteristics. Although the conglomerates are porous and some of the tuffs also contain porous zones, the tunnel would be above the regional and local water tables, and no large inflows are expected. An unlikely and worst-case scenario would include the potential effects of locally perched water zones associated with the few washes in the area. Such zones would pose no construction problems and long-term measures should also be simple (panning, weep holes, or possibly local grouting).

Empirical design approaches were used in conjunction with rock classifications at the tunnel horizon to estimate support requirements and overall tunnel progress. Nothing was discovered to indicate difficulties in tunnelling or cut-and-fill.

This report details the hard rock investigations to reach the conclusions described above. Details of investigations of conglomerate and soil deposits may be found in Nowatzki et.al. (1987; 1988). Details of geophysical investigations will be found in several reports (Sternberg and Esher, 1987; Bryan et.al., 1987; and Sternberg et.al., 1988). All geophysical data and geotechnical test data such as hole logs and test sheets, can be obtained through the references cited.

List of Figures

Figure 1	Locations of Investigations	(pocket)
Figure 2	Location Map of Maricopa and Sierrita Sites	2
Figure 3	Site Geologic Map	(pocket)
Figure 4	Geotechnical Characteristics Borehole MD1R	22
Figure 5	Geotechnical Characteristics Borehole MD3R	23
Figure 6	Geotechnical Characteristics Borehole MD5	24
Figure 7	Geotechnical Characteristics Borehole MD10	25
Figure 8	Geotechnical Characteristics Borehole MD11	26
Figure 9	Geotechnical Characteristics Borehole MD12	27
Figure 10	Geotechnical Characteristics Borehole MD13	28
Figure 11	Comparison of Scanline and Traverse Mapping Results, Espanto Mountains	33
Figure 12	Joint Distribution By Degrees - Drillhole MD11	36
Figure 13	Surface Joint Distribution By Degrees - Drillhole MD11 Vicinity	37
Figure 14	Joint Distribution By Degrees - Drillhole MD10	38
Figure 15	Surface Joint Distribution By Degrees - Vicinity of MD5	39
Figure 16	Surface Joint Distribution By Degrees - Southwest of MD10	40
Figure 17	Joint Distribution By Degrees - Drillhole MD5	41
Figure 18	Site-Wide Distribution of Seismic Velocities Versus Depth	55
Figure 19	Velocity Profiles for Refraction Line DST420	57
Figure 20	Comparison of Compressive Strengths Obtained from Seismic Velocities and Various Strength Tests	59
Figure 21	Sketch of Field Slope Testing Set-Up, Maricopa Site	68
Figure 22	View Looking South In Sacaton Pit	69
Figure 23	Iron-Stained Fanglomerate at Sacaton Pit	70
Figure 24	View Looking at West Side of Sacaton Pit	71
Figure 25	Caliper Log, MR-1	75
Figure 26	A Typical Field Slope Failure Surface Geometry	82
Figure 27	Results of Fanglomerate Pressuremeter Testing	85
Figure 28	Typical Pressure-Displacement Curve for Dilatometer Testing	86
Figure 29	Collapse Potential, MA12	92
Figure 30	Collapse-Susceptibility Diagram	93
Figure 31	Seismic Velocities Versus Depth, Construction Unit 1	113
Figure 32	Seismic Velocities Versus Depth, Construction Unit 2	114
Figure 33	Seismic Velocities Versus Depth, Construction Unit 3	116
Figure 34	Seismic Velocities Versus Depth, Construction Unit 4	119
Figure 35	Seismic Velocities Versus Depth, Construction Unit 5	121
Figure 36	Seismic Velocities Versus Depth, Construction Unit 6	122
Figure 37	Seismic Velocities Versus Depth, Construction Unit 7	123
Figure 38	Seismic Velocities Versus Depth, Construction Unit 8	126
Figure 39	Seismic Velocities Versus Depth, Construction Unit 9	127

List of Tables

Table 1	Drilling Program -- Maricopa Site	18
Table 2	Maricopa Site Geotechnical Traverses	34
Table 3	Laboratory Compression Tests on Core Samples	47
Table 4	Summary of Maricopa Rock Properties	48
Table 5	UCSS and Point Load Index for Various Core Intervals	50
Table 6	Assignment of Rock Mass Ratings to Strength Categories	51
Table 7	Rock Mass Properties Corresponding to Strength Category	53
Table 8	Fanglomerate Drilling Program, Maricopa Site	73
Table 9	SPT Blow Count Data, Stage I Drilling Program (1987)	80
Table 10	Values of Cohesion Back-Calculated from Field Slope Testing	83
Table 11	Fanglomerate Material Properties from Dilatometer Testing	87
Table 12	Results of Laboratory Sieve and Atterberg Limits Analyses	89
Table 13	Results of Laboratory Strength Testing	90
Table 14	Results of Pseudo-Consolidation Testing for MA12	91
Table 15	Comparison of Elastic Moduli Obtained from SPT Blow Counts with Moduli Obtained from Seismic Surveys	97
Table 16	Safety Factors as a Function of Slope Height and Slope Angle	99
Table 17	Maricopa Shafts	104
Table 18	Summary of Maricopa Site Construction Units	112
Table 19	Construction Method Summary for Construction Units	131
Table 20	Estimated Cut-and-Fill Construction Costs Per Foot	132
Table 21	Summary of TBM Costs	133
Table 22	TBM Unit Costs Per Foot	134
Table 23	Experimental Chambers and Injector Complex Estimated Construction Costs	135
Table 24	Estimated Shaft Unit Costs	136
Table 25	Access Shaft E7 Cost Summary	137

1.0 INTRODUCTION

1.1 Purpose and Scope of Report

The specific requirements of the Department of Energy's (1987) Invitation for Site Proposals come under several headings. Volume 3 of the proposal is to provide supporting information on geology and tunnelling including a general description of geology, and specific information on various rock and soil characteristics that may affect the tunnel. These include:

- a) Identification and description of significant geologic features that may pose problems to construction or long term operation.
- b) Location and extent of soft clay, unconsolidated sand, or other soil conditions that may pose problems to tunnelling, excavation, or foundations.
- c) Locations of data sources such as borings and seismic surveys.
- d) Identification of potential groundwater problems.
- e) Description and location of relevant soil and rock units, including potential construction methods associated with geologic structures and anomalies.
- f) Information about the physical and mechanical properties of the rock and soil masses in sufficient detail to estimate the type of construction equipment needed, excavation rates, and support requirements.

The major feature of the proposed Superconducting Super Collider (Department of Energy, 1987) is a collider ring, approximately 53 miles in circumference, in which the basic constituents of matter are created and studied at a total energy of 40 trillion electron volts (TeV). The collider ring will be oval in plan (Figure 1 (in pocket)) and will be placed inside a circular tunnel about 10 ft in diameter and with center-line level at least 30 ft below ground surface. The tunnel will be connected to the surface by alternating service and access shafts at approximately 2 1/2 mile intervals (Figure 1). Other features include an injector complex of four cascaded accelerators, campus laboratory areas above the injector complex, and a site infrastructure of roads and utilities. There are two interaction regions on the east side of the ring and 4 on the west. The most important feature, however, is the collider ring tunnel and a major requirement of the technical evaluation criteria for proposals to build the Superconducting Super Collider (SSC) is evidence that the tunnel can be built satisfactorily. Particular criteria are:

1. Suitability of the topography, geology and associated geohydrology for efficient and timely construction of the proposed SSC underground structures.
2. Stability of the proposed geology against settlement, seismicity, and other features that could adversely affect SSC operations.

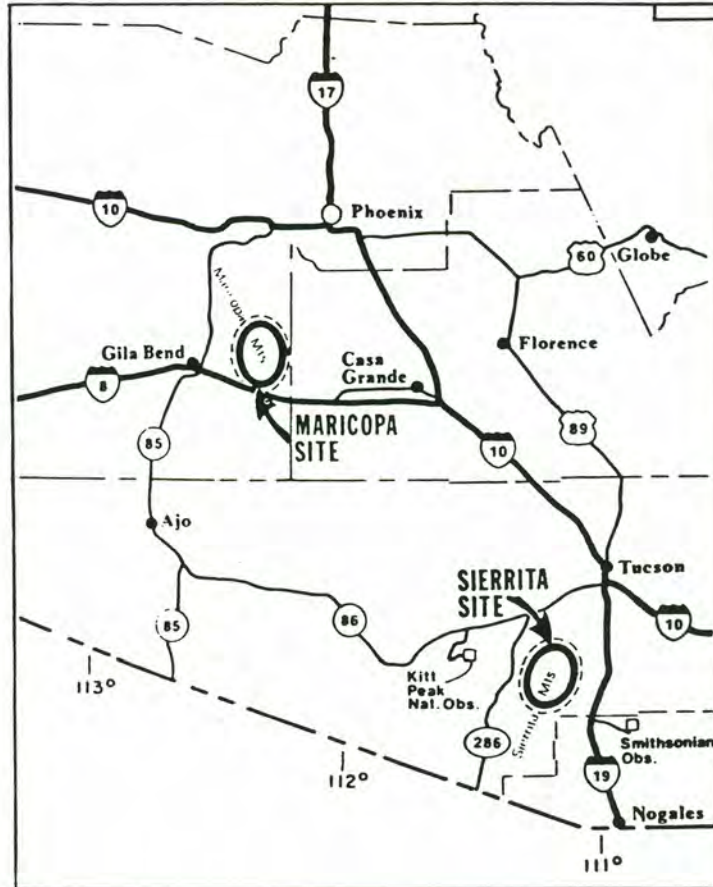


Figure 2 - Location map of Maricopa and Sierrita Sites (Cunningham, 1987).

3. Installation and operational efficiency resulting from minimum depths for the accelerator complex and interaction regions.
4. Low risk of encountering major problems during construction.

For the Arizona proposal, one site was selected from about 20 original candidates. Most of the other sites were eliminated because of their remote locations. The site selected (Figure 2) is located around the Maricopa Mountains 35 miles southwest of Phoenix. The requirement for shallowness and efficient construction necessitated a major part of the tunnel being driven in the typical southwestern Cenozoic alluvial deposits which form a major part of the surface of Arizona.

The pediments around the Maricopa and mountains where the site is proposed have generally thin deposits of cemented fanglomerates. Water tables are deep and pumping has been, and will continue to be, at low levels. This fact enables exploitation of the unusual and favorable engineering properties of the fanglomerates to achieve major construction benefits.

1.2 Approach

In order to obtain the above information for this site, investigations into literature and data sources of the site was carried out. As described in 3.1, little prior data were found to exist. Hence, a careful reconnaissance geotechnical investigation was needed.

The geotechnical characterizations reported upon herein therefore draw upon data obtained from three main sources:

- (a) Existing published and unpublished data sources on the site
- (b) Field investigation, including drill logs, field tests, field mapping and geophysics
- (c) Laboratory testing

The detailed rationale for the program is found in 3.3, Program Formulation.

1.3 Participation

This report was prepared by the staff of Engineers International, Inc., in association with members of the Mining and Geological Engineering and Civil Engineering Departments of the University of Arizona, and the Arizona Geological Survey. EI's portion of the work was done under EI's contracts (Nos. KR 87-2762-CIV and KR 88-0388-CIV) to the Arizona Department of Commerce.

For Engineers International, the Project Manager was Robert A. Cummings, P.E., who supervised the field work, analyses, and report preparation. Also for EI, Gregory D. Zeihen performed field geological mapping and

drill-site geotechnical logging. Other drill-site logging work was done by Gregory Weeks of EI. Larry A. Salhaney of EI assisted in data processing and computer work, and, along with the personnel mentioned above, participated in report writing.

The University of Arizona participated to a considerable extent in the work. Mary E. Glynn, Navid Mojtabai, and John Corey assisted in geotechnical core logging. Ms. Glynn also performed the considerable task of summarizing the early site work together with data from the first phase of field work conducted during 1987. Mr. Mojtabai also prepared the stereonetts included in this report. Geomechanics laboratory tests were done at the University of Arizona under the supervision of Robert Armstrong and Dr. Jaak Daemen. Overall supervision of the effort by the University of Arizona Mining and Geological Engineering Department was by Dr. Ian W. Farmer who offered valuable advice and insight to the project.

Conclusions and findings reported upon herein depend to a considerable extent on the work of others. These studies are referenced in the report; however, special mention should be made of the investigation of general geology by Steve Reynolds, Jon Spencer, and John Welty of the Arizona Geological Survey; of hydrogeology by Steve Brooks of the Arizona SSC Project; of site geophysical signatures by Dr. Ben Sternberg of the Mining and Geological Engineering Department at the University of Arizona; and of the behavior of alluvial deposits by Drs. Edward Nowatzki and Jay DeNatale of the Civil Engineering Department at the University of Arizona.

Drilling services were provided by two organizations. Joy Manufacturing Company, Drilling Division, Tucson office, performed all the diamond core drilling. Alluvial overburden drilling was completed by Sergeant, Hauskins, and Beckwith, Inc., of Phoenix, which also provided foundation recommendations for the campus-area facilities.

For the Arizona SSC Project, John W. Welty was the field coordinator. Mr. Welty developed the field program using the various consultants' recommendations for field data collection and test site location, handled all the detailed logistical planning, obtained the necessary permits and served as the contract administrator for the drilling. In addition, Mr. Welty assisted in field geological reconnaissance and core logging. Archeological inspections of drilling and seismic test sites were done by Arizona State University. The Arizona SSC project Manager is Mr. Don Morris.

Work reported upon herein began in 1986, with preliminary studies by others. Engineers International became involved with the start of core drilling (Stage I investigations) in the spring of 1987. Work continued through February, 1988 (Stage II investigations).

2.0 GEOLOGIC SETTING

2.1 Site Location

The Maricopa site tunnel alignment circles the southern Maricopa Mountains and passes through the northern Maricopa Mountains, so that about 35 miles of the tunnel are in fanglomerates and about 18 miles are in intrusive and volcanic rocks (Figure 3, in pocket). The injector complex and campus are along the eastern arc of the collider ring. Elevations along the surface trace of the collider ring range from 1,170 to 2,300 ft. The collider ring will be tilted 0.3 degrees to the southwest to allow - as will be shown later - shallow excavation for the injector complex and interaction regions.

2.2 Geologic Setting

Previous geologic studies of the Maricopa Mountains region are rare. The first reconnaissance geologic map of the area was completed in 1987 at the request of the Arizona SSC Project (Cunningham et al., 1987). Prior to this the Maricopa Mountains had been discussed only in a cursory fashion as part of the regional efforts of the U. S. Geological Survey (Ross, 1923; Kahle et al., 1978; Hollett and Garrett, 1984; Peterson et al., 1985) and the Arizona Geological Survey (Wilson et al., 1957; Morrison, 1984). The following descriptions and conclusions are drawn from these sources as well as from independent studies carried out by Arizona SSC Project team members.

The Maricopa Mountains are composed predominantly of Proterozoic plutonic and metamorphic rocks. The oldest rock unit, Proterozoic Pinal Schist, occurs in the southern Maricopa Mountains. The schist has been intruded by Proterozoic granitic rocks, of which most of the range is composed. The plutonic rocks consist of two separate granitic plutons and a dioritic pluton. A sequence of Tertiary sedimentary and volcanic rocks overlies the Proterozoic basement in the southeastern corner of the range. No Paleozoic or Mesozoic lithologies are recognized in the Maricopa Mountains.

The Pinal Schist occurs as a northeast-trending strike belt and as isolated pendants of higher-metamorphic-grade schists which are in fault contact or intrusive contact with the younger Proterozoic plutons. The Pinal Schist generally consists of fine- to medium-grained biotite-muscovite quartzo-feldspathic schist. Within the Pinal Schist are concordantly intruded pegmatite dikes of Precambrian (?) age.

The Proterozoic granites consist of an older medium- to coarse-grained porphyritic granite which is intruded by dikes and irregular masses of leucocratic medium-grained granite. The dioritic pluton is generally a mesocratic biotite-hornblende tonalite to quartz diorite. All three Proterozoic plutonic rock types range from undeformed to well foliated. Within the central region of the range several small Proterozoic gabbroic

bodies occur within the porphyritic granite. At places, small quartz-rich pegmatites, thin diabase dikes, and small bodies of an aplitic-textured fine-grained granite may be found.

The Tertiary sequence consists of a gently southwest-dipping stack of sedimentary and volcanic rocks that form an asymmetric, southeasterly-plunging trough that disappears beneath younger sediments. The lowermost unit consists of a poorly sorted dominantly granite-clast conglomerate that was derived from Proterozoic basement. Field relations suggest that the basal conglomerate is in depositional contact with the basement. Above the lower conglomerate lies a sequence of dense, variably-vesicular basalt flows. Above the basalt occurs a granite- and schist-clast conglomerate unit that contains smaller clasts than the basal conglomerate. The middle conglomerate locally contains a basal sandstone and is intercalated with locally-great thicknesses of vesicular basalt. A welded tuff overlies the middle conglomerate along an angular unconformity and is probably unconformably overlain by an upper conglomeratic unit that is poly lithologic and contains local interbeds of tuffaceous sandstone and basalt. The thickness of each unit has not been measured, and may vary considerably. The total thickness of the Tertiary section is in excess of 1,250 ft.

Structures recognized in the Maricopa Mountains include brittle faults, mylonitic and/or cataclastic shear zones, metamorphic foliations and lineations, and bedding in the Tertiary units. More specifically, northwest- or northeast-trending mylonitic and/or cataclastic shear zones are locally common within the two Proterozoic granites, especially near their mutual contacts; however, only a few of these zones are wider than 10 ft. In the southern Maricopa Mountains, brittle faults containing up to 10 ft of breccia and gouge occur along two separate fault systems. The western fault is a Precambrian mylonite zone that contains gouge evidencing Tertiary reactivation and that places Proterozoic porphyritic granite against Pinal Schist. The eastern fault system consists of multiple splays that juxtapose Tertiary conglomerates against Pinal Schist. Neither of the faults is expected to persist as far as the collider ring alignment.

Foliation attitudes within the Proterozoic basement, although not systematically studied, generally strike northeast and dip steeply (>60 degrees). In the center of the range northwest-striking attitudes associated with northwest-trending mylonitic shear zones also are found. Lineations in the plane of foliation generally trend north-northwest and sense of shear, where determined, indicates southeast side up. No major folds occur in the range, but small-scale folds are common in the Pinal Schist.

2.3 Groundwater

Because of the lack of prior development in the area of the site, ground water elevation data are sparse along and within the tunnel alignment. As a result, the ground water table has been estimated over much of the site by using linear interpolation and extrapolation techniques combined with geological and hydrologic knowledge of the area. The site's simple geology, combined with experience from other similar basins and the available data, suggest that the aquifers have a predictable and consistent water-table gradient in areas of little or no pumping. High confidence in

the estimated values, along with the site's overall great depth to water in relation to the tunnel elevation, strengthens the statement that no part of the tunnel will be in saturated material. The depth to water appears to be 300 feet or greater around the entire site. (State of Arizona, 1987)

3.0 PROJECT DEVELOPMENT

3.1 Existing Geotechnical Data

Prior to this investigation, very few geotechnical data existed on the Maricopa Mountain Ranges due to the lack of development in the area. However, there are some geotechnical data concerning the fanglomerate surrounding the range, that were collected for siting studies of a waste isolation facility in the area. In addition, considerable experience exists with surface construction in fanglomerates and cemented younger alluvium in Arizona, as will be alluded to frequently in this report.

A summary of the main sources of geologic and geotechnical data utilized in the investigation, both historical and current, is given in the State of Arizona's site proposal to the Department of Energy (State of Arizona, 1987).

Data on fanglomerates collected from site investigations for the Palo Verde Nuclear Generating Station (Fuigo 1975), amongst other sites, indicate that below depths of 5 to 20 ft, the fanglomerate acts as a moderately strong rock. The area of the site is generally held to contain fanglomerates with "relatively strong cementation, generally continuous" by the Western Soil and Water Research Committee (1964).

Rock geotechnical conditions in the vicinity of the site were even less-well-known, prior to the Arizona SSC Project's investigations. The area had been mapped sufficiently to surmise the rock types and likely geotechnical conditions by analogy with other, better-studied areas elsewhere in the State. Evaluation of this mapping produced confidence that the rock masses in the area would be dry, competent, and generally unaltered, and therefore suitable for major construction. Further, the evaluations concluded that major faulting and highly-stressed rock would not be likely. On this basis, the decision to further investigate the site was made.

3.2 Identification of SSC Data Requirements

The ultimate purpose of the preliminary investigation, field investigation and laboratory testing program was to provide information which would allow reasonable estimates of tunnel stability and support requirements, and preliminary choice of tunnelling method, to demonstrate the feasibility of constructing the SSC facility at the Maricopa site. Further, an objective was to support preliminary estimates of construction cost and construction time to be made in the site proposal, and to identify any effects on the forecasted costs and schedules that would accrue from site investigations.

It was recognized early in the project that the Maricopa site offered the major advantage of cut-and-fill construction to appreciable depths at

rapid rates and low unit costs, owing the presumed properties of the fanglomerates found at the site. This presumption was based on considerable experience in construction of open cuts in fanglomerates elsewhere in the State. The most important projects include several world-class open-pit copper mines and the Central Arizona Project.

The open-pit mines exhibit benches in fanglomerates up to 50 ft in height that have been remarkably stable for decades. The principal limitation to bench height is the reach of shovels the mines use for ore production; the 50-ft height represents a double-benching process because the single-pass excavation limit is commonly 20 to 25 ft.

The Central Arizona Project documented the constructability of very long open-cut projects that cross fanglomerates from different source areas, and showed that this had little effect on overall construction cost or method. In this way the CAP demonstrates that confidence may be had in construction appraisals of the Maricopa fanglomerates.

Temporary cuts deeper than these have not been required for major construction in Arizona so these limits do not represent upper bounds on the achievable depth and slope steepness in fanglomerate. It was recognized that the SSC's open-cut requirements of the fanglomerates were less stringent than for the mines or the CAP, in that the stability of the excavations would only need to be assured for the construction period. Therefore, there is basis for expecting that deeper, steeper cuts could conservatively be forecasted for SSC construction than had been constructed before in the State. It was important that the investigation be able to evaluate this expectation.

In siting the SSC, the approach taken was to position the ring and campus complex near to the surface over as much length as possible to take advantage of the favorability of cut-and-fill construction in fanglomerate. In particular, it was desired to position the campus complex where its near-surface construction would involve only fanglomerate.

Once this was accomplished, the task of the geotechnical investigation was to document the consistency of the fanglomerate's strength, cementation, and the absence of soil-related problems such as swelling or collapsing tendencies. Parameters were needed to describe the fanglomerate's response in excavated slopes. The strength of the material was needed to forecast the best method of excavation, particularly the amenability to excavation by scrapers or a Holland Loader system (a very high-productivity excavator used with great success on the CAP, and discussed in 5.5.7.1). Since the high strength of fanglomerate comes in large part from its undersaturation, it was desirable to assure that the water table would not be intercepted in the excavations. The generality of the fanglomerate condition was investigated through surface geophysics and was "calibrated" to strength values for stability assessments through drilling, laboratory testing, and various in-place strength tests.

The topography requires some deep tunnelling for completion of the SSC collider ring. Both hard rock (volcanic flows and intrusive rocks) and soft rocks (conglomerates of volcanic association and fanglomerates) would be involved in deep tunnelling.

Preliminary tunnel stability and support design can be assessed on the basis of empirical rock characterization indices such as the Geomechanics Classification (RMR) (Bieniawski, 1973) and the NGI Rock Quality Index (Q) (Barton, Lien, and Lunde, 1974). Compressive strength is also sometimes used as an index in weaker rocks through the stability ratio (rock strength/geostatic stress).

The choice of tunnelling method is -- for a long tunnel such as the collider ring--probably limited to full-face tunnel boring machines. In this case it is important to estimate machine progress. Support is one of the factors which determines this; drillability is another. Drillability is usually expressed in terms of rock strength or fracture toughness with modifications for abrasive wear and fracture frequency in the rock. This is the basis of the method used to assess tunnel progress for this investigation (see Sections 4.4.5 and 5.5.7.2).

For assessment of both stability and progress, the basic information needed includes rock characteristics such as compressive strength and seismic velocity (for computation of modulus). Rock mass characteristics should include the number and orientation of the major fracture sets; the fracture frequency and the fracture surface characteristics; and RQD. Geometric characteristics should include tunnel depth and tunnel orientation. Density should ideally be included, but rock mass densities or unit weights can often be judged with sufficient accuracy, making detailed measurements unnecessary.

With this basic information -- at the tunnel horizon -- together with information on geologic hazards such as faults or the presence of water, it should then be possible to estimate the support requirements and drillability indices. This report brings this information together from available data and investigation data. Some of the data are more accurate than others, and some of the data have been derived using site-specific correlations, but essentially the conclusions reached in Sections 4 through 7 represent reasoned estimates of the characteristics and behavior of the rock at the tunnel horizon.

3.3 Design of the Investigation

The overall purpose of the investigation was to develop sufficient geotechnical data for an assessment of site feasibility, focusing on areas where little prior data were available. Initial data requirements were identified on the basis of the findings of reconnaissance geologic mapping (Cunningham, et.al., 1987), hydrogeological studies done specifically for the SSC, prior area studies, and reconnaissance (helicopter-supported) by construction engineers and tunnel specialists. The following issues and data requirements were used in setting up the program:

- (1) Obtain geotechnical information for hard rock tunnel concepts in the intrusive and volcanic sections of the tunnel (mapping, lab testing, and core drilling).

- (2) Locate the limits of the hard rock tunnel segments so as to identify construction units based on commonality of construction methods (drilling, mapping, and geophysics).
- (3) Investigate the consistency of the fanglomerate and intrusive assemblage to be crossed by the ring (drilling and geophysics).
- (4) Develop reliable correlations between fanglomerate geophysical signatures and fanglomerate engineering behavior (in-place testing, laboratory testing).
- (5) Utilize hydrogeological investigations being done by others to assess groundwater conditions in the tunnel areas (drilling, literature assessment).
- (6) Assess shaft-sinking conditions at known shaft sites (mapping, geophysics).
- (7) Assess near-surface soil conditions in the campus area for surfaced-based construction of ancillary facilities (drilling, lab and in-place testing).
- (8) Identify any special or problematic conditions that could be associated with portals or with transitions from one rock to another, especially from rock into fanglomerate or vice versa (geophysical data, drilling).
- (9) Assess design and constructability for surface-based tunnel construction (cut and fill) in fanglomerate, especially excavation method, likelihood of encountering difficult bedrock in surface cuts, potential for water-related problems, and required excavation sideslopes (geophysics, drilling data, results of hydrogeologic studies by others, laboratory testing, and in-place testing).

To meet these requirements, a program of drilling, geophysics, field mapping, and literature studies was undertaken, as described below. Sections 4 and 5 of this report detail the methods used and the results obtained.

Results of the investigations are discussed separately from the methods and approaches. Only those methods involving the hard rock investigation are given full detail in this report. Investigations of the fanglomerates were conducted by others and only the summarized results of those investigations are included herein, for completeness. In order to keep the report to manageable size, raw data such as field notes, core logs, and geophysical traces are not included. For those interested in this level of detail, the Arizona SSC Project has all the raw data on file.

Summaries of other findings that impact overall design and constructability are also given. Details of such other studies are found in the referenced documents.

The resulting field investigation consisted of six parts:

- (a) Laboratory testing of surface grab samples performed early in the project to indicate the range of rock strengths at the site.
- (b) Geophysical surveys around the alluvial/conglomerate part of the proposed ring to generalize and extend drilling and mapping data, and to identify depth to bedrock and characteristics of the material. The most important of these was seismic velocity. Surveys were correlated with ground truth and with measured material properties.
- (c) Auger holes MA1 to MA6 and MA10 to MA13 to investigate alluvial deposits around the ring. Large-diameter holes were drilled to provide personnel access for in-place observation.
- (d) Rotary boreholes MR1, MR2, MD6, MD7 to investigate deep alluvial deposits and the water table to the north and south of the proposed alignment.
- (e) Diamond drill holes (MD1R, MD3R, MD5, MD10, MD11, MD12, and MD13) to investigate bedrock geology in the Northern and Southern Maricopa Mountains and just to the east of the proposed collider ring in the Booth Hills.
- (f) Mapping of surface discontinuities through detailed fracture surveys and reconnaissance traverses to determine main joint set orientations, spacings, lengths, and roughnesses.

4.0 CONSTRUCTION SEGMENTS IN HARD ROCK

Diamond drilling, seismic refraction geophysics, surface mapping, and laboratory testing were used to converge on a clear representation of the rock masses to be crossed by the "Hard Rock" portions of the SSC facility. The rock masses are readily-understood in terms of their geotechnical properties for tunnelling. In general, the rock masses were found to be of excellent quality and amenable to rapid and efficient excavation by machine boring methods.

The first parts of this section detail the methods used to obtain this understanding. The results of these investigations are presented, combined, analyzed, and compared in Section 4.4.

4.1 Description of Surface Studies

4.1.1. Seismic Refraction Surveys

Seventy-six seismic refraction sites were occupied between 1986 and 1988 at the proposed Maricopa SSC site. The primary purpose of these seismic measurements was to determine the depth distribution of seismic velocities and thereby estimate the geotechnical properties of the materials through which the proposed SSC tunnel would pass.

A series of reports (Sternberg and Esher, 1987; Bryan, et.al., 1987; and Sternberg, et.al., 1988) compile seismic data, a documentation of the instrumentation and field procedures that were used, and a summary of the interpreted seismic models (cross sections).

Instrumentation

The seismic system was a Geometrics model ES-1225 12-channel digital signal enhancement seismograph. With this system, the 12 traces are visible on a CRT for preview and may also be printed on a built-in printer. One-thousand data points per channel are stored, the sample interval can be varied from 25 to 1000 microseconds, and the gain for each channel can be varied from 0 to 66 db. Although stacking of successive records can be done with this unit, this feature was not utilized in this survey. The geophones were 14-hertz Model PE-3 or Model L10A 374-ohm land seismometers. Non-shielded geophone cables with takeouts at 120 foot intervals were used, except where greater resolution of near-surface layers was required. The seismograph parameters for each record are summarized in the Header Records which are reproduced in appendices to the reports referenced above.

A computer was used to record the digital data from the seismograph. An RS-232 connection was used to transfer data from the ES-1225 to the

computer. The computer was also used to process the data (first break picks and layered earth interpretation). SeisView Software (from Geometrics, Inc.) was used for this processing. The accuracy of SeisView was checked by comparing it with other published calculations, (such as Mooney, Harold M., Handbook of Engineering Geophysics, Bison Instruments, Inc., 1973).

Field Procedures

Geophone cables with takeout intervals of 120 feet were used for most of the sites. "Weathering shots" used much shorter spacings to confirm that no complications from extremely low-velocity near-surface layers was occurring. Since the seismograph recorded twelve channels simultaneously, the total length of the spread was 1320 ft. A few weathering layer recordings were made with geophone intervals of 5 ft. Two lines with 50 ft geophone spacings were recorded near ring mile 42 to look at the transition in velocities at the bedrock boundary in granitic terrane. Some double-shots (24 geophones over 2,640 ft) were also recorded in the basin at the north end of the ring.

At each site, the seismograph and computer were first set up at one end of the cable and a forward seismic profile was recorded. The shot was placed at the end of the spread nearest the recording truck and generally about 20 ft from the #1 geophone. The recording truck was then moved to the other end of the spread to record a reversed profile.

The explosive charge consisted typically of 4-5 pounds of Iremite 80. The blasting caps that were used were "zero-delay" caps. A two-person auger was used to drill the shot holes. The shots were generally buried 3 to 4 ft deep.

Detailed seismic refraction data are not included in this report. The referenced reports include, in order for each site:

- o File Headers for the forward and reversed profiles used in the interpretation. The file header summarizes all the cable layout and seismograph setup information.
- o First break lists for each channel for the forward and reversed profiles used in the interpretation.
- o Plot of the locations of the first break picks, superimposed on the variable-area seismic record for the forward profile.
- o Plot of the locations of the first break picks, superimposed on the variable-area seismic record for the reversed profile.
- o Plot of the travel-time (combined forward and reversed profiles) with superimposed least-square lines fit to the travel-time segments. Below this plot is the layered earth interpretation. The vertical depth scale

is in feet; the velocities are in feet per second; the dip angles are in degrees.

- o Table showing the input data and the calculated model parameters. Distance is in feet, velocity in feet/second, and dip in degrees. The travel-time intercept with the axis at the far end of the plot (for both forward and reverse profiles) was calculated by hand. The reciprocity (in percent) was then calculated as the difference between the forward and reverse intercepts.

The identification code for the sites is as follows: site codes begin with DST (for Desertron), followed by a location code for the location along the ring (e.g. 103 for Ring mile 10.3), followed by an N, S, E, or W for the location of the shot point relative to the spread (e.g. N for the north end of the spread), and finally, the record number (e.g. 2). The complete code as it exists on the computer floppy disk files and the printouts would therefore be DST103N2 for this example. Sites that were off the ring used an identification code which was descriptive of the geographic location (e.g. LOSHOFNS for Lost Horse, Forward Shot, North-South line).

The floppy disk files, field notes, and field maps are on file at the Department of Mining and Geological Engineering of the University of Arizona.

The interpreted cross-sections are summarized in the referenced reports, which also contain corresponding travel-time plots. The interpreted lines were picked in order to satisfy both the first-break points (in a least-squares sense) as well as satisfying reciprocity.

A possible limitation of the seismic refraction method is the potential complication due to low-velocity layers. An implicit assumption in this analysis is that each succeeding layer has a higher velocity than the layer above it. Although this is generally a reasonable assumption in this area, where the assumption does not hold, the depths to layers in the model could be overestimated.

4.1.2. Geotechnical Mapping

In strong rocks such as the plutonic rock masses found at the Maricopa site, fracturing can be expected to govern rock mass behavior at the shallow to moderate depths anticipated for the SSC facility. To generalize and expand the data base on fracturing that had been developed from the drill core, a series of surface scan lines and geotechnical traverses was carried out. The procedures for geotechnical traverses differed from those for scan lines.

Scan line data were collected by stretching a tape along the outcrop, measuring the azimuth and inclination of the tape and then recording the strike, dip, and tape intercept of each fracture intersecting the tape. Because it was necessary to record data from natural outcrops (there are no excavated faces near the ring at the Maricopa site) the choices of sites, line orientations, and line lengths were limited. To reduce orientation

bias, it is desirable to collect data from three orthogonal lines of equal length at the same site. From most natural slopes, this is not possible. Furthermore, weathering, colluvial material, and debris tend to preferentially obscure shallow-dipping and flat fracture expressions on natural slopes. In order to alleviate these drawbacks as much as was practical, preferred outcrops for scan lines were well-fractured and free-standing with at least one steep face, commonly on a ridgecrest.

A different method from scanlines, the geotechnical traverse, was used to broaden the fracturing assessment and thereby study the consistency of fracturing around the ring. Scan lines are unsuitable for reconnaissance for several reasons. By their nature, scan lines offer refined statistical expressions of fracturing but cover little area. Outcrops suitable for scan lines cannot always be found where the data are needed. Scan lines are also time consuming and tedious to complete. The geotechnical traverses conducted for this project covered more terrain more rapidly, albeit at the expense of some statistical accuracy. Traverses were planned so as to follow a variety of azimuths and inclinations. As each clearly in-place, fractured outcrop was encountered during a traverse, all the fracture orientations within that outcrop were measured and recorded, the number of fractures belonging to each recognized set was noted and recorded, and the distance over which each set occurred, taken perpendicular to the plane of the set orientation, was also measured and noted. In this way an approximate average spacing could be calculated.

Spacing values obtained from scan lines and traverses may represent a non-conservative estimate, because weathering tends to obscure some fractures, especially healed ones. Outcrops where fracture sets were measured were more resistant to erosion and therefore probably include a lower proportion of densely-fractured zones than does the rock mass in general. Fracture swarms with spacings of a few inches to fractions of inches were occasionally noted on slopes at those places where gaps in colluvium and brush allowed exposure of the weathered surface bedrock. During detailed site investigation for specific projects, it will be desirable to investigate the rock mass more thoroughly through trenches and/or angle drilling.

Locations of scan lines and traverses are given on Figure 1 (in pocket). There were 27 main survey locations, as follows.

- (a) Espanto Mountains (Lines 1, 2, 3; Traverse 1)
- (b) Maricopa Mountains (Lines 4, 5, 6, 7; Traverses 2, 3, 4, 6, 7)
- (c) Booth Hills (Traverse 5)
- (d) Northwest Ring Area (Traverses 8, 9, 10, 11, 12, 13)
- (e) Southeast Intrusive Terrain (Traverses 14, 15, 16, 17, 18, 19)
- (f) Southeast Volcanic Terrain (Traverses 23, 24, 25, 26)
- (g) Southwest Volcanic Terrain (Traverses 21, 22)
- (h) Southwest Granitic Terrain (Traverses 21, 22)

4.1.3. Geological Reconnaissance

Surface geological reconnaissance was carried out in several areas of the Maricopa site to supplement existing geological and geotechnical information. Commonly, both the traverse method described above, and the

basic field mapping of units and major discontinuities, were incorporated in this step. The ring alignment was concentrated upon, and special emphasis was placed on the southeast side of the ring (near the Booth Hills), the southern portion of the ring (especially in the Tertiary volcanic sections), the southwestern vicinity of the ring, and the northwestern ring alignment.

Brief descriptions of the surface exposures in these areas is presented in Section 4.4.2.

4.2 Diamond Drilling

4.2.1. Drilling Program Overview

Seven diamond drill holes have been bored on the Maricopa site in support of the SSC site investigations. The approximate locations of these are shown graphically on Figure 1 (in pocket). All holes were drilled to the depth of the ring projected for that location, except in the case of MD1R. Borehole MD1R penetrated strata that were not necessarily flat-lying and was therefore deepened to intercept deeper strata that could be intercepted at tunnel depth elsewhere. Table 1 provides important borehole information.

Wireline methods were used on all diamond coreholes. Boreholes MD1R, 3R, and 5 were drilled during the summer of 1987. In these holes, core was retrieved with a 5-ft double-tube core barrel, with a solid inner tube. In order to assure that the recovered core was being logged as accurately as possible with respect to the incidence of fracturing and breakage of core, a change to split-inner-tube, 5-ft core barrels was made when holes MD10 through MD13 were drilled in the winter of 1988. This saved considerable logging time that would have been spent fitting the core back together for accurate measurements of fracture spacing/fracturing orientation relationships, RQD, and percentage recoveries. It also improved confidence in the characterizations of fractured or weathered zones, which were seen in the split tube to have more integrity than is apparent after extrusion (usually with much beating on the inner tube by the driller's helper) from a solid inner tube.

The softer rocks in the volcanic sequence were generally drilled with diamond-set bits. The harder intrusive rocks were drilled with both set and impregnated diamond bits. Bit performance in the granites seemed to be better with the impregnated bits.

All the diamond holes were drilled with direct circulation of a water-polymer drilling fluid. Although a cellulose lost-circulation additive (shredded paper) was on hand at all times, it was never used as no significant circulation loss was encountered in any of the bedrock portions of the holes. Minor losses occurred through casing joints and at the casing-to-bedrock interface, chiefly because of the difficulty in establishing a reliable gauge in the weathered bedrock top surface. Circulation losses from such sources were estimated at less than 5 percent. For example, MD10, a 700-ft-deep hole that took 10 days to drill and that exhibited the most severe circulation loss of all, showed no increase in loss once the top of

Table 1 - Drilling Program--Maricopa Site

<u>Hole No.</u>	<u>Approx Collar Elevation</u>	<u>Approx Tunnel Depth</u>	<u>Total Depth</u>	<u>Size</u>	<u>Lithology</u>
MD1R	1840	420	1,250	NX	Volcanic sequence
MD3R	1520	120	125	NX	Quartz diorite
MD5	1480	450	475	NX	Granite
MD10	1770	700	700	NX	Granite
MD11	1200	100	100	NX	Granite
MD12	1740	310	350	NX	Volcanic sequence
MD13	1560	125	125	NX	Quartz diorite

bedrock had been reached at 30 ft and casing had been set: total fluid consumption for this hole was in the range of 2,500-3,000 gal, including water loss for non-drilling purposes, such as rinsing equipment.

4.2.2. Core Logging Program

Cores and drilling were logged in detail for:

- o lithological description, weathering, alteration, and rock fabric
- o drill string penetration rate
- o RQD and fracture frequency
- o point load index and estimates of strength
- o discontinuity directions and surface properties (roughness, filling).

Holes MD10 through MD13 were logged at the drill site throughout. The other holes were logged at the drill site as the hole penetrated the ring horizon, and other portions were logged in the laboratory.

Because a trained engineering geologist was present at all times during drilling of holes MD10 through MD13, it was possible to ensure that accurate drilling times were measured for each run. For these holes only the actual drilling times were measured -- time required for chuck resetting and core retrieval were not included. Also, run-by-run variations in rig downpressure were noted. For holes MD1R, MD3R, and MD5, these parameters were tracked by the drillers, and the level of care exercised by the geologist cannot be assured. Although the driller penetration times are available in the SSC files and are qualitatively interesting, they may contain errors of from 10 to 50 percent and are therefore not used in computing the penetrability indices reported in 4.4.1.

4.2.3. Hole Abandonment

Auger holes, rotary drillholes, and diamond drillholes were all abandoned and filled in accordance with Arizona Department of Water Resources regulations. Drill sites were cleaned and reclaimed in order to restore them as closely as possible to their undisturbed states.

4.3 Testing

Sampling and point-load testing were performed concurrently with, and as an integral part of, the core logging.

Point load tests were run as frequently as feasible, but minimally as each apparent change of rock strength, not rock type; was presented in the core. Some intervals were purposely not point-load tested in order to preserve them for potential future sampling. Other zones were not amenable to point-load testing because of core condition, rock weakness, or fracturing. For these, the probable point load index was estimated from results in surrounding core and from experience. Point load indices obtained from each run were averaged and are shown on the logs. Estimated values are clearly

differentiated on the logs and on the downhole parameter logs given in 4.4.1. In addition to the scattered tests for strength profiling, point load tests were also concentrated around samples removed for laboratory strength testing. This enables a correlation to be made between laboratory-derived compressive strength and the point load indices without the uncertainty of accounting for distance, lithology, or weathering changes in the core. The derivation of this correlation is discussed in 4.4.3.

Early in the program, grab samples were obtained from helicopter-supported reconnaissance of the general site area. These data are reported in 4.4.3. Refinements to the ring location occurred subsequently, and many of the lithologies represented in this data base are no longer involved in the ring geology.

Laboratory testing consisted of confined compression tests on basalt, granite, conglomerate, and quartz diorite encountered in MD1R, MD3R, MD5, MD11, and MD10. A diabase dike encountered in MD10 was also sampled and tested: diabase dikes are found, but are generally scarce, in the granites. An aplitic phase of the granite was encountered in MD5 and MD10 in scattered locations; however, this phase represents a minor component of the core in these boreholes and, as indicated by surface mapping, of the rock masses expected to be intercepted by the ring. Furthermore, the rock masses corresponding to this phase appeared on the surface to be more densely fractured than the coarse-grained granite. In MD10 only one intact specimen of this type was obtained for testing and this specimen was silicified and anomalously strong. For the reasons cited above, this is not considered for present purposes to be a significant deficiency in the sampling and testing program.

Confined compression test methods were used exclusively so that critical strength data under confined conditions could be obtained. Unconfined equivalents were derived from the normal stress-shear stress diagrams (Mohr diagrams, see 4.4.3). This approach has the advantage of reducing the mixing of failure modes usually represented in suites of data from unconfined compression and Brazilian tensile strength tests. (For these fractured rock masses, tensile rock strengths are of little interest.) Hence the strength data used in the analyses to follow are relevant to shear failures, the mode in which rocks are ordinarily the weakest.

Compression tests were performed strictly according to ISRM and ASTM criteria for length-to-diameter ratio, end parallelness, end-to-axis perpendicularity, and end smoothness. The only exceptions to the end smoothness criteria were the much-weaker conglomerates, which were hand-trimmed to avoid the rigors of conventional specimen preparation. In such rocks, the end smoothness is generally overridden by the low strength, however.

Test depths and confining pressures are presented along with test results in 4.4.3.

4.4 Findings

4.4.1. Results of Core Drilling

The data are summarized in Figures 4 through 10, showing the distributions of subjective strength, penetration index (when available), RQD, and point-load index with depth in the boreholes. Detailed geotechnical logs are not provided in this report but copies are available through the Arizona SSC Project.

Each of these four parameters reflects different but related features of rock quality. RQD (Rock Quality Designation) is widely-accepted in the literature. It represents the cumulative length of core pieces greater than four inches divided by the total length of each run.

"Subjective strength" is a visual rock mass strength assessment that is logged graphically on a scale of zero to ten. The low end, zero, would be exemplified by a disaggregated or non-lithified rock such as an uncemented conglomerate or intensely fractured and altered granite. Such rock would have little or no rock mass strength. The high end, ten, is exemplified by a rock that would be very hard, very strong, unfractured, and essentially unweathered. In order to assure that consistent values were assigned to these criteria, each geotechnical engineer involved in logging was acquainted with upper and lower endpoints of the measurement and was made clear as to what examples from the site fell into the intermediate area. Some of the subjective portion involved the evaluation of the combination of weathering, mineralogy, strength, and discontinuities. This was refined by cross-checking logs and making comparisons with different holes to assure that consistent results were being obtained among all core logging personnel.

Point load indices were measured with a standard commercial point load instrument. The point load index (I_s) is the force required to break a core sample divided by the square of the distance between the points. There are restrictions as to length-to-diameter ratio and a correction is applied for distances between the points when the distance differs from 54 mm. A more detailed discussion can be found in Hoek and Brown, (1980). Core and sampling requirements permitting, at least one test was attempted per run, and a large volume of point load data resulted. Nevertheless, some intervals were not tested. For these, an index range was estimated. Estimated values are indicated on Figures 4 through 10 by a detached bar above the graphed value.

Penetration index is a derived parameter calculated from the penetration rate and the downhole pressure. In effect, the penetration index is the time rate of advance of the drill normalized with respect to the weight of the drill string, taking into account the downpressure, the drillstring weight, and the bouyant force of the mud on the drillstring.

Figures 4 through 10 show that all four parameters correspond for all rock types. From these figures it is possible to see how RQD and point-load index combine to reflect changes in rock mass strength as evidenced by both the subjective strength index and the penetration index. Usually, but not always, high RQD correlates with high point-load strength.

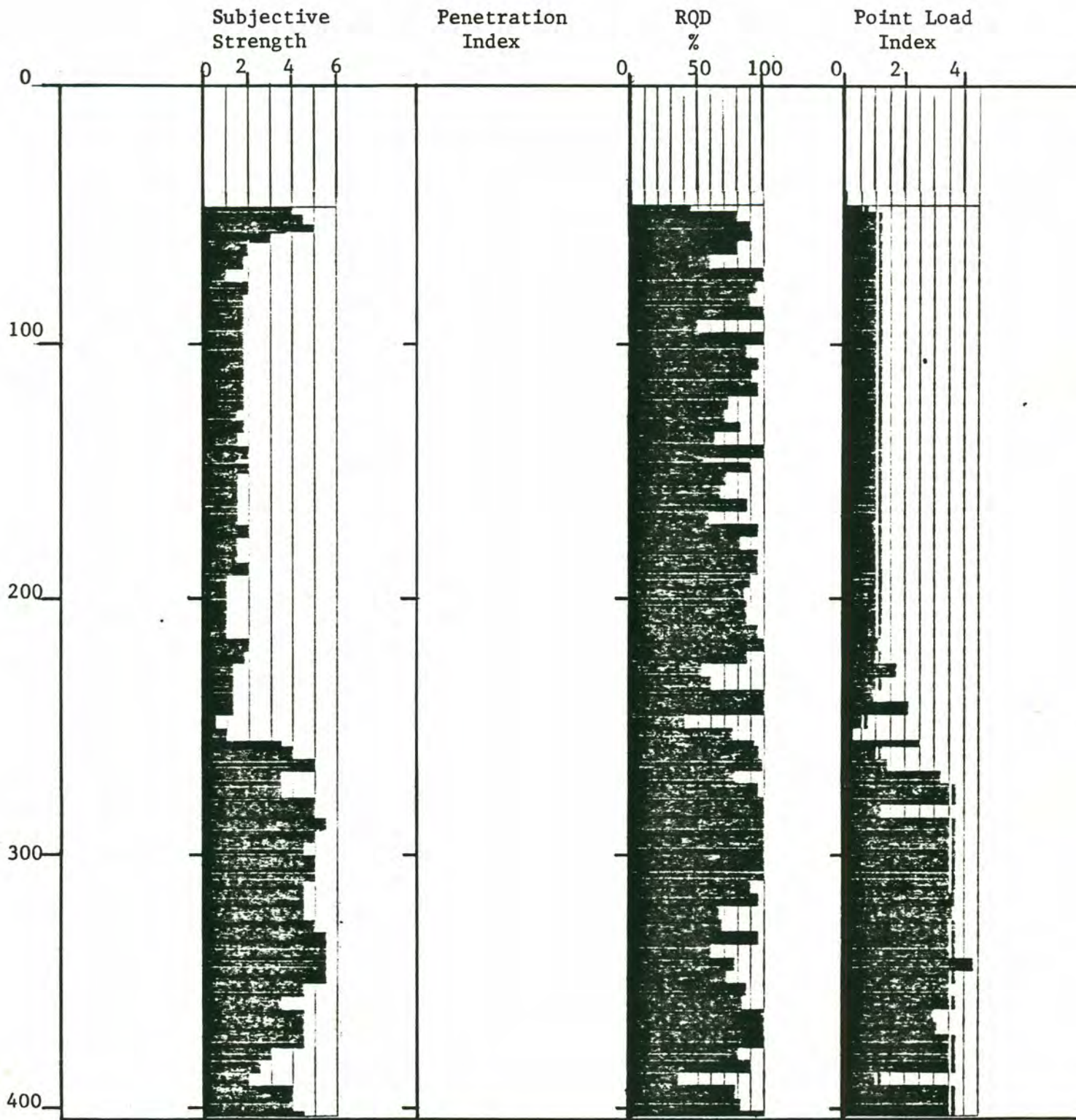


Figure 4. Geotechnical Characteristics, Borehole MD1 R

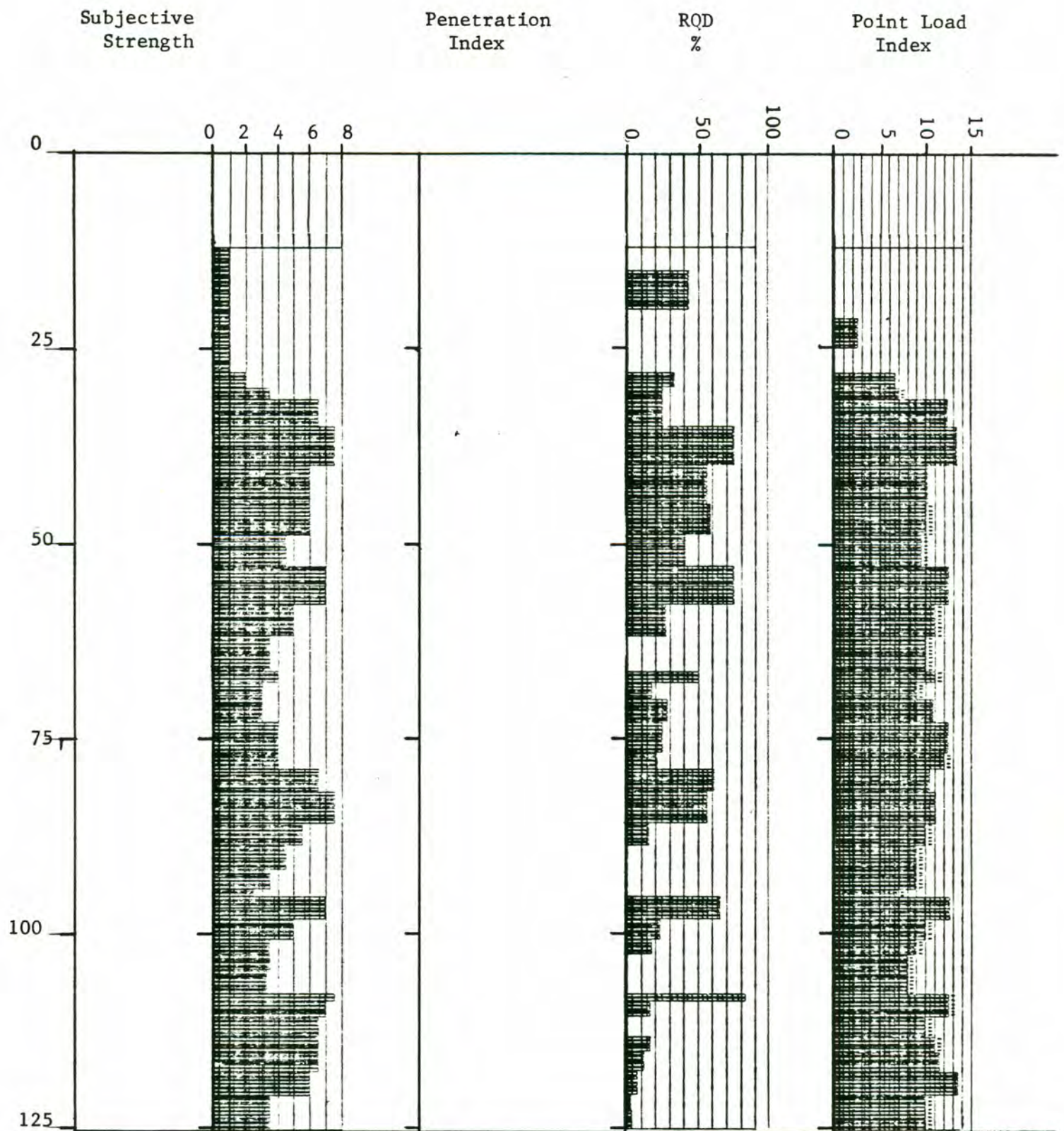


Figure 5. Geotechnical Characteristics, Borehole MD3R

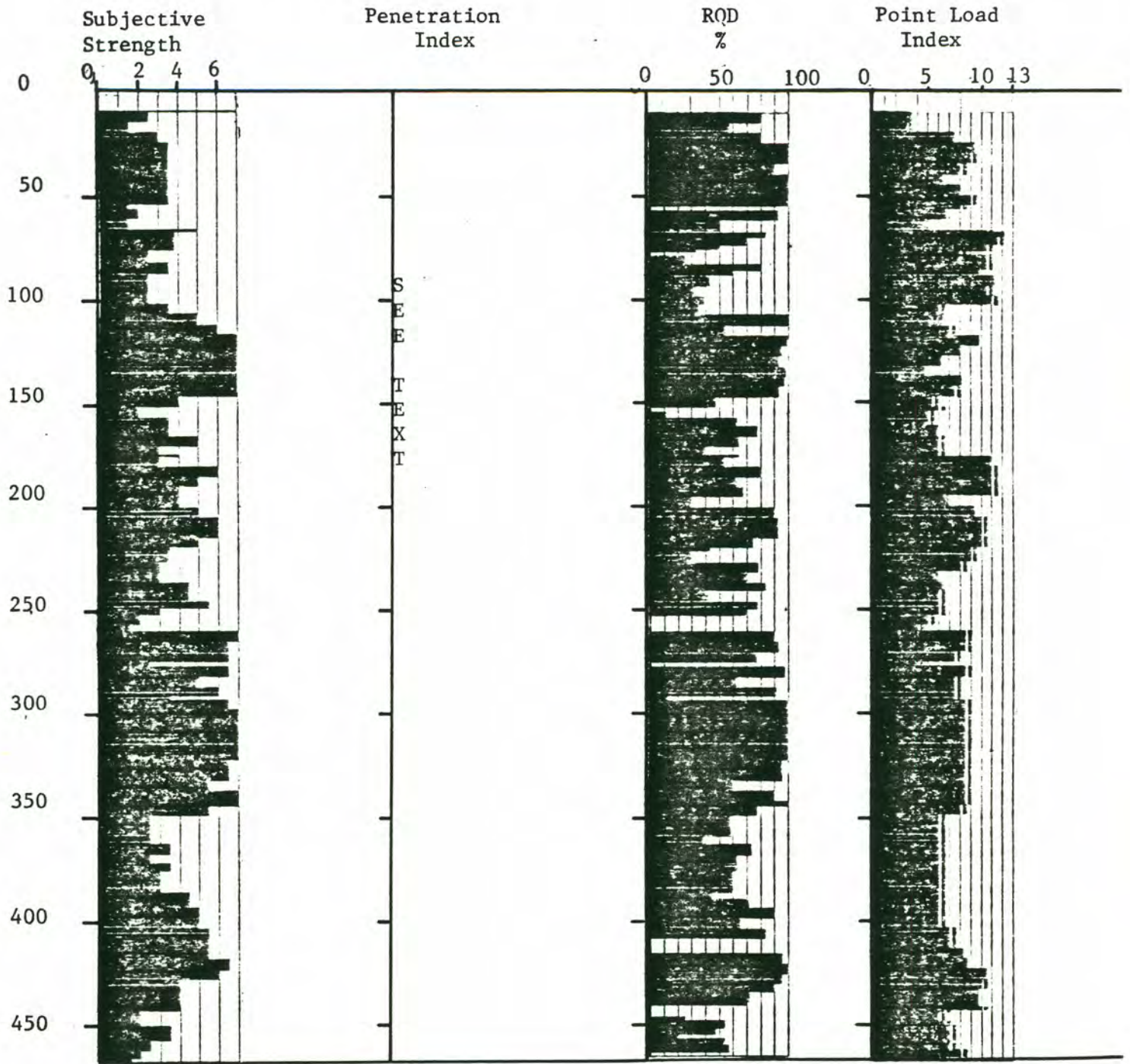


Figure 6. Geotechnical Characteristics, Borehole MD5

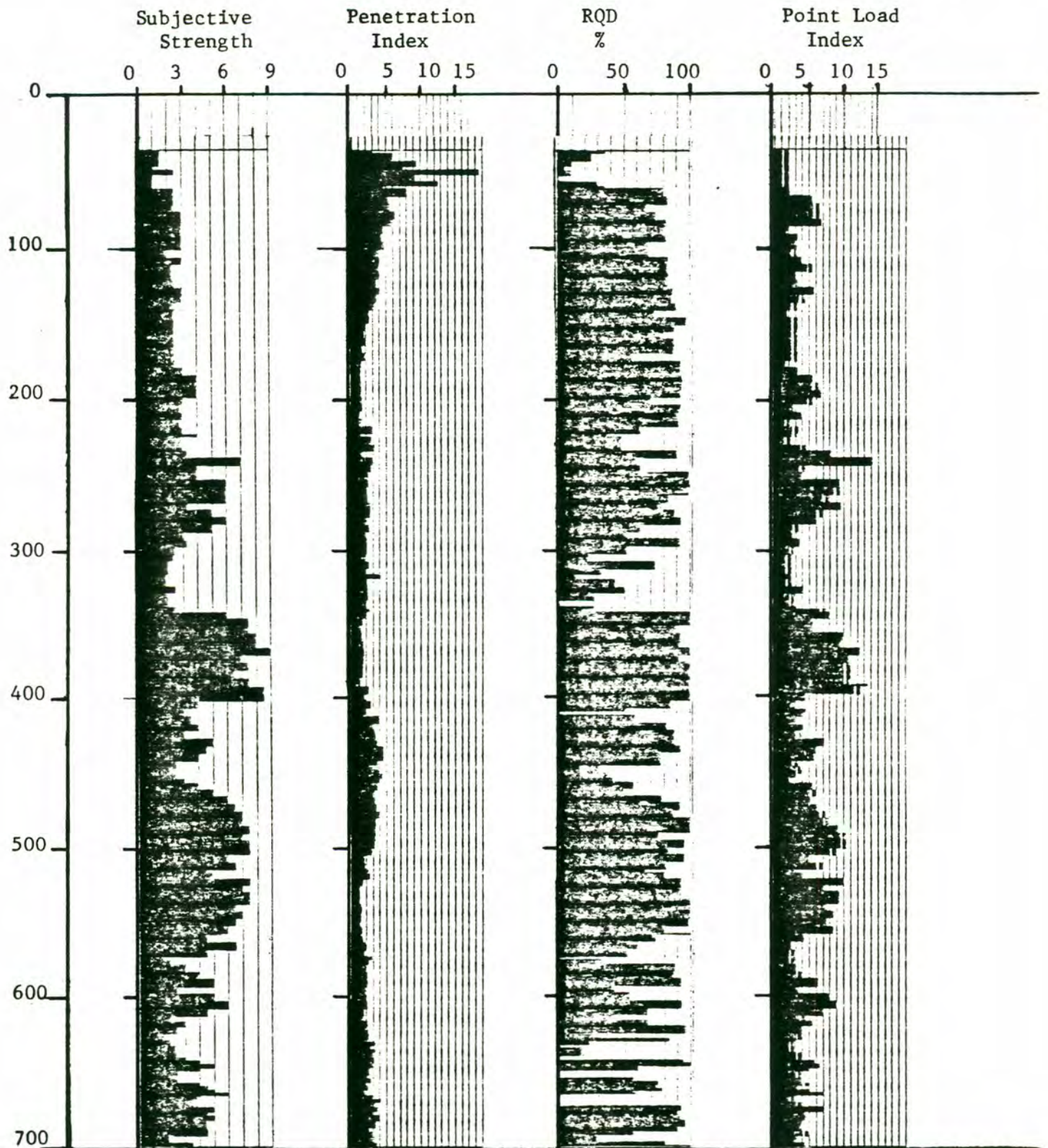


Figure 7. Geotechnical Characteristics, Borehole MD10

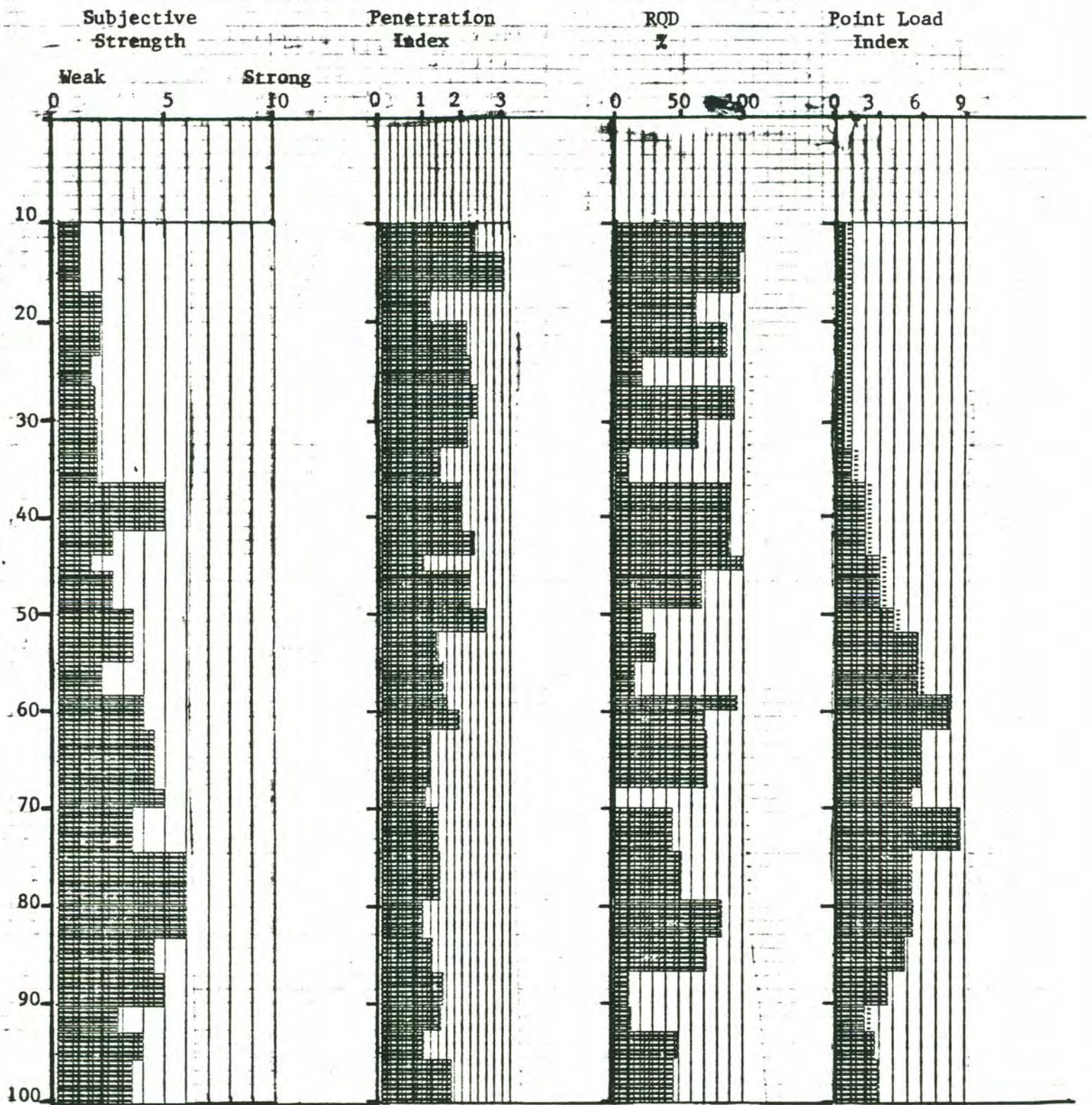


Figure 8. Geotechnical Characteristics, Borehole MD11

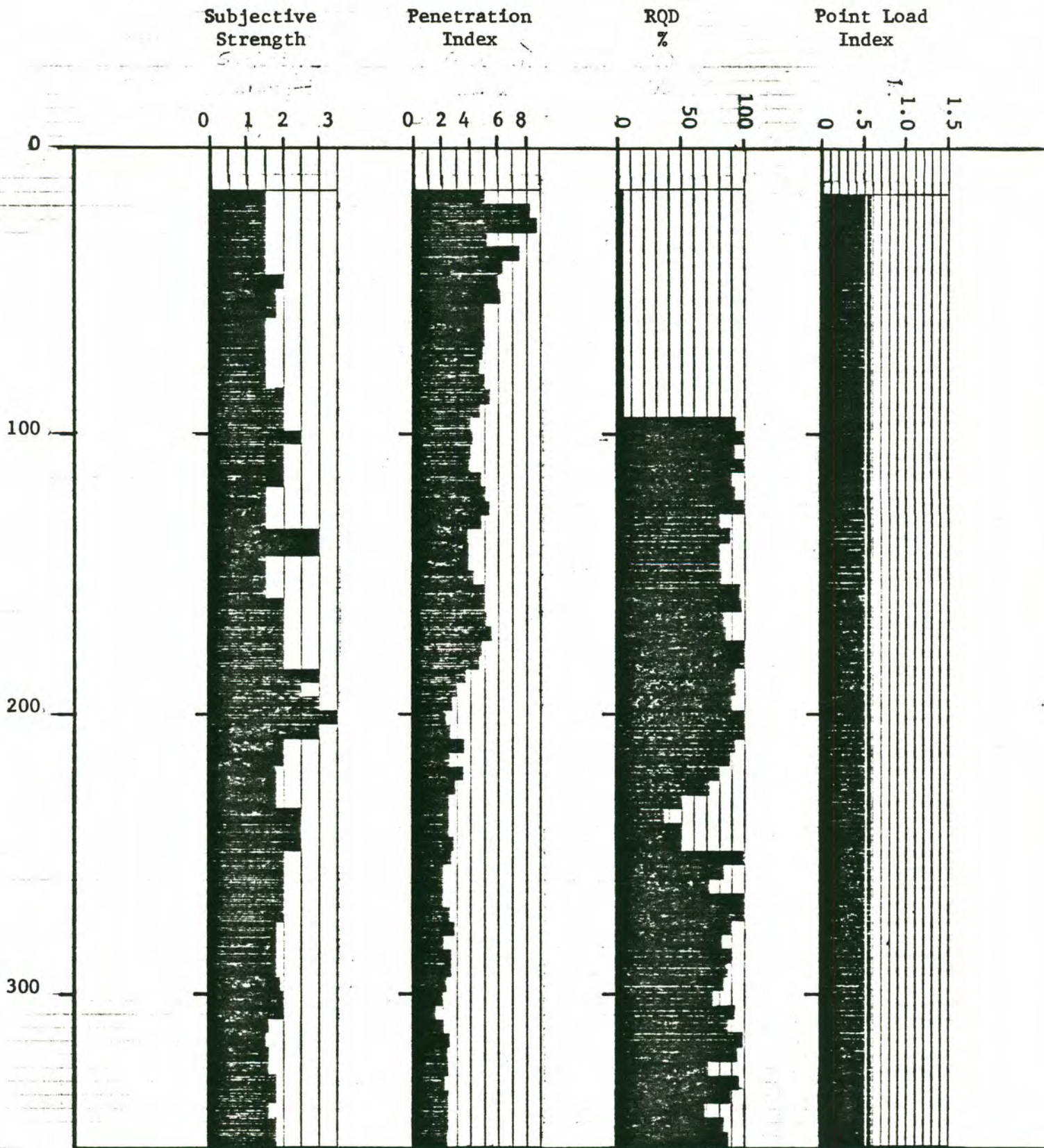


Figure 9. Geotechnical Characteristics, Borehole MD12

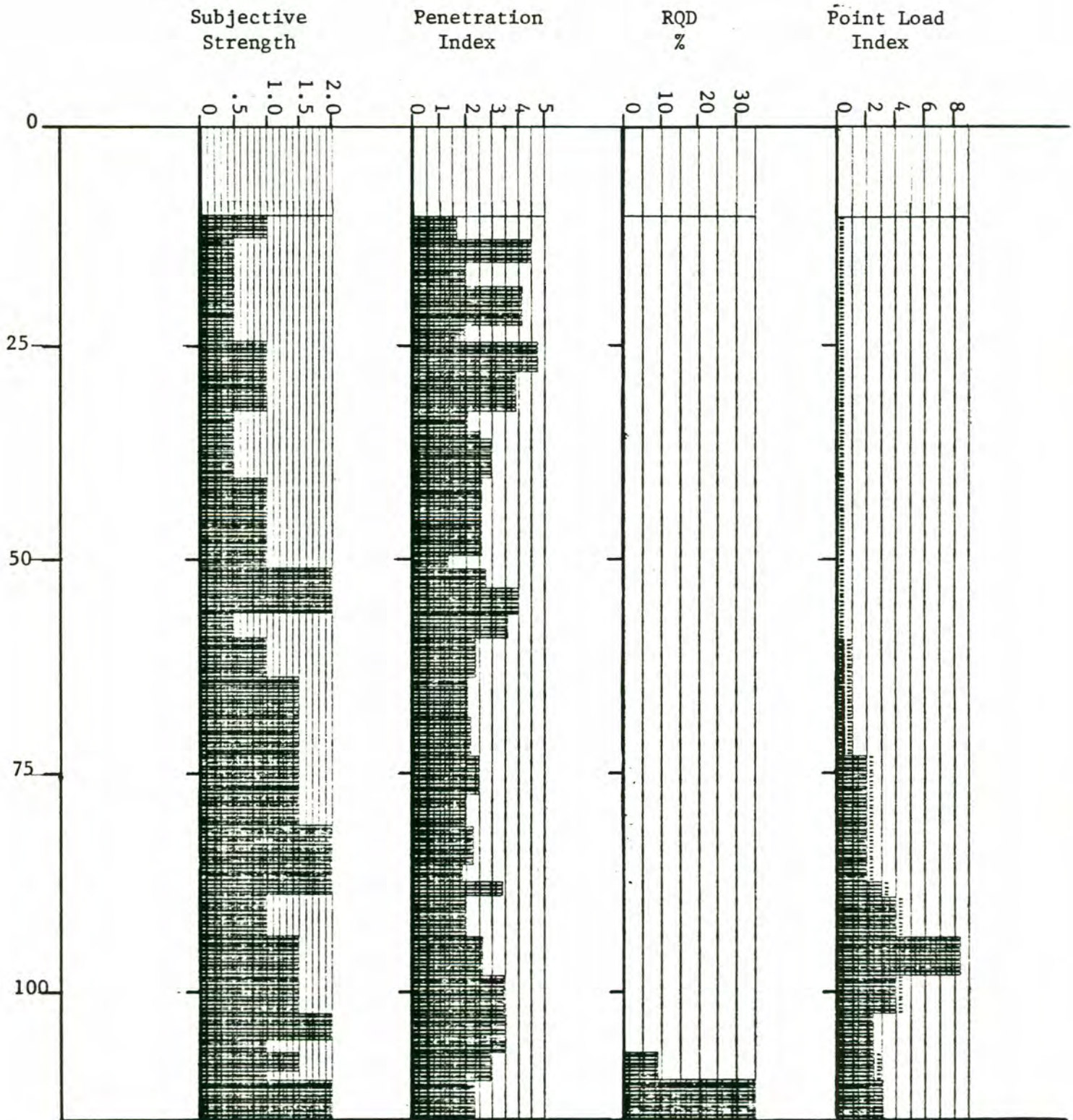


Figure 10. Geotechnical Characteristics, Borehole MD13

RQD values in conglomerate and fanglomerate were generally high, but rather sporadic, due to the lack of jointing in those materials and the major role of porosity and cementation in controlling core integrity. In both fanglomerate and conglomerate recovered as core, it was impossible to obtain point-load tests on fresh core because these materials became very weak after saturation with drilling fluid. A nominal point-load value of 0.5 was therefore assigned.

Both granite and Booth Hills quartz diorite show a distinct tendency towards strong and weak zones with more pronounced areas of low RQD in the quartz diorite. This could be due to the more mafic mineralogy of the diorite, which allows more pervasive weathering to occur in jointed regions. A comparison of MD5 and MD10 suggests a spacing of 100 feet between jointed zones. Discussions later in this report point out that this spacing might not be typical of rocks masses beneath topographic highs.

The poorer rock quality in the lower 150 feet of MD10 is strongly atypical of the intact granite as seen in surface outcrops and other drillholes. Surface mapping suggests that this is probably indicative of joint intersections, or a joint spacing decrease that was expressed by the presence of the valley where the drillhole was collared. Topographic control by joints is demonstrated by saddles and valleys associated with decreases in joint spacing and a strong tendency for saddles and valleys to parallel one of several major, roughly east-west, joint sets (see Figure 3, in pocket).

Comparison of the penetration indices for boreholes MD10 through MD13 shows relatively high values initially, gradually decreasing as fresher bedrock is encountered. Once in bedrock, gradational increases and decreases, roughly correlative with subjective strength and RQD, are seen. The pertinent feature of this comparison is the indication that changes in material strength occur gradually and over distances of the order of tens of feet.

Summaries of Core Geology

Borehole MD1R was begun on 4 May 1987 and is in NE 1/4, SE 1/4, SE 1/4, Sec 2, T7S R1W. The hole passes from overburden into ash flows, through arkosic sandstone conglomerates approximately 250 ft thick, and through a 350-ft-thick section of massive, only slightly vesicular basalt. The core was examined in detail to a depth of 400 ft, roughly 60 feet below tunnel depth. Conglomerate and basalt facies below tunnel depth were not logged geotechnically, but appeared to present little if any difference in engineering properties. Borehole MD1R was deepened with the intent of identifying the depth and nature of the basement contact with the Tertiary section. This contact had not been intercepted when the drilling was terminated at 1,250 ft for economic reasons.

From the log it may be concluded that the conglomerate is fairly weak (strength estimates 2000-5000 psi) but not jointed. The range of RQD of 70-95% and fracture frequency of 2-3 per foot represents core breakage at matrix-particle interfaces which may or may not be imposed during drilling.

Particles up to 6 in. in core dimension comprise 60% of the rock and are contained in a sandy matrix. Because of stratigraphic dip, the tunnel will be in conglomerate for a considerable distance. It should be noted that the apparent strength of conglomerate at the time of logging is low because of saturation with drilling fluids. When unsaturated to dry, this rock is much stronger, as is expected at depths above the water table.

At the depth of the tunnel in MD1R, the basalt is moderately strong (strength estimates of 7-12,000 psi) and has high RQD (up to 100%) and low to moderate fracture frequency (0.6-1 per foot in core).

Borehole MD3R was begun on 11 May 1987 in the SE 1/4, NE 1/4, NE 1/4, Sec 29, T5S R1E. This borehole was rotary drilled through overburden to 20 ft. It then passed through weathered granodiorite from 20 to 125 ft. The top part of the hole, a probable weathered shear zone, contains a few fragments of strongly weathered schist.

The granodiorite is a strong rock (strength estimates 24,000-31,000 psi) but this strength is mitigated for tunnelling by zones of alteration and dense fracturing which effectively reduce RQD to below 50% and increase fracture frequencies to 4-7 per foot, in core. Most of the fractures are calcite-filled and breaks may have been imposed by the drilling process. Weathering, which is intense at the top of the core, was found to decrease considerably with depth.

Borehole MD5 was collared on 14 May 1987, in the SE 1/4, NE 1/4, NW 1/4 Sec 25, T4S, R3W. It passes through 475 ft of weakly foliated porphyritic granite. This has medium to high strength (point load estimates of strength range from 11,000 to 29,000 psi with those near the tunnel horizon at 450 ft all exceeding 20,000 psi), high RQD (normally in the range of 70% to 100%) and low fracture frequencies. Fractured zones are normally associated with zones of heightened weathering up to 1 ft thick. Highly fractured zones (4 to 5 fractures per ft) occur just below the approximate tunnel horizon.

Borehole MD10 was begun on 18 January, 1988 and drilled to a total depth of 700.5 feet. The drillhole is southwest of Ring Mile 49 and is on the ring alignment in the SE 1/4, SE 1/4, NE 1/4, Sec 17, T4S, R2W. This hole was cased to a depth of 30 ft and core drilled to the final depth utilizing a 5 ft split-inner tube core barrel for sample recovery. Percent recovery was above 95 in almost all runs. RQD was consistently above 80% below the weathered zone (ending about 55-80 feet below surface) except in the more-heavily-jointed intervals described below.

The main rock type encountered is a porphyritic granite showing minor variations in composition, such as equigranular and biotite-rich zones; however, diabase dikes were cut during drilling from 235 to 239.9; 400 to 406.9 ft and 584.4-584.9 ft. From 30 ft to 60 ft gravelly clay and heavily weathered rock were encountered. The interval from 60 to 110 ft is strongly weathered but is also heavily jointed and contains crushed zones. Several other zones of heavy jointing and crushed and broken rock (with or without slickensides) were noted: these intervals were 280-339 ft (ave RQD = 45), 438-459 ft (ave RQD = 54), 574-593 ft, 613-654 ft (ave RQD = 42) and 667-677 ft (ave RQD = 19). Both steep joints (0-20 degrees) and notable vertical

fractures and flat joints were commonly encountered in this hole. Fresh granite in this hole appeared quite strong, and subsequent testing showed unconfined strength in the 20,000 to 30,000 psi range (see 4.4.3). This drillhole was bottomed in porphyritic granite at 700.5 feet. As mentioned earlier, this hole may have been collared in a structurally-controlled topographic low.

Borehole MD-11 was begun on 22 January, 1988 at a location just north of the Maricopa Road and about 400 feet southwest of Ring Mile 42 in SE 1/4, SW 1/4, NW 1/4, Sec 13, T5S, R3W. At a depth of 10 feet the hole was cased and the remainder cored to a final depth of 100 feet. Samples were recovered with a 5-foot, split-inner-tube core barrel with recoveries routinely above 90 percent. RQDs were generally low in the entire hole owing to persistent jointing below the weathered zone; however, both point load tests and confined compression tests indicated strong rock (unconfined strengths of near 20,000 psi). The interval from 10-14 ft generally is red clay, gravel, granite fragments, and caliche. Actual "C" horizon material was encountered from 14 to about 30 feet, the granite being strongly weathered, but with recognizable joints containing clay. Jointed, porphyritic granite was the only rock type encountered in the hole. Two friable, biotitic zones were cut, one at about 60 feet, and another at around 74 feet. Heavily-jointed and broken zones were logged at 33-36.5, 55-58.3, and 92 to 93 feet. The granite porphyry is silicified from approximately 30 feet to around 75 feet, and the hole bottomed in jointed granite at 100 feet. This hole was collared in a topographic low between two buttes, and structural control here is probable.

Borehole MD12 was begun on 18 January, 1988. The location is NW 1/4, NW 1/4, NW 1/4, Sec 12 T7S, R2W and about 300 feet east of Ring Mile 28. The hole was drilled to 14 ft, then cased and cored to the final depth of 354 ft. A 5-ft, split-inner-tube core barrel was used, with recovery consistently near 100%. The rock type encountered was a very-poorly-sorted fanglomerate made up principally of subangular to subrounded metamorphic clasts and minor granitic and volcanic clasts. No jointing was apparent and the clasts were commonly matrix-supported in caliche-cemented, arkosic sand and gravel. Core strength in newly-retrieved core was quite variable owing to the variable intensity of calcite cement, but in general, pieces longer than 8-12 in. could easily be broken by hand. The strength of this material seems to be considerably higher when fully dry. (Cored fanglomerate specimens were tested in the laboratory; see 5.5.3.) Fractures in core were along clast-matrix boundaries and rarely along contacts of poorly-sorted and well-sorted materials. The drillhole bottomed in fanglomerate at 354 ft.

Borehole MD13 was the last of the four Stage II Maricopa Site Evaluation diamond holes and was begun on 26 January, 1988. The hole was drilled on NW 1/4, NW 1/4, SW 1/4 Sec 33 T5S R1E approximately halfway between Ring Mile 15 and Ring Mile 16 and at interaction region K2. MD13 was cased to 10 ft and core drilled to a final depth of 125 ft with a 5-ft split inner-tube core barrel for sample recovery. Recovery was generally 90 to 100 percent, but substantial losses occurred during several runs owing to the material being drilled. Lithologic changes from clay to fragments of hard, moderately weathered diorite made full recovery of core a problem in several cases. Sandy silty clay and well-to-poorly sorted conglomerate made up the major footage of the hole, but badly weathered diorite was intercepted in

the final 15 ft. From 10 ft to 50 ft clay with sand and gravel beds was the only material encountered. In places (i.e. 39 feet) manganese-oxide-coated fissures were noted in the clay. The interval from 50 to about 110 ft contained matrix-supported clasts of sub-rounded to subangular diorite and was generally very poorly sorted. Heavily weathered diorite with recognizable jointing was drilled from 110 to 120 ft and weathering decreased in the final 5-ft run. Joints tended to be steeper than 30 degrees and contained clay and/or crushed rock: many joints were clean. Strength of core was generally low, most samples being a plastic clay although caliche cement and rock fragments improved competency near the bottom of the hole. The hole was stopped at a depth of 125 ft.

4.4.2. Geological and Geotechnical Reconnaissance

4.4.2.1. Results of Surface Geotechnical Reconnaissance

As described in Section 4.1.2., initial reconnaissance involved scanlines (1-7) and traverses (1-7). A comparison of the scanlines and traverses from the Espanto Mountains indicated that the scanlines compared favorably with traverses in indicating joint distributions. Figure 11 compares lower-hemisphere contoured pole plots and indicates that significant joint sets are identified with both methods.

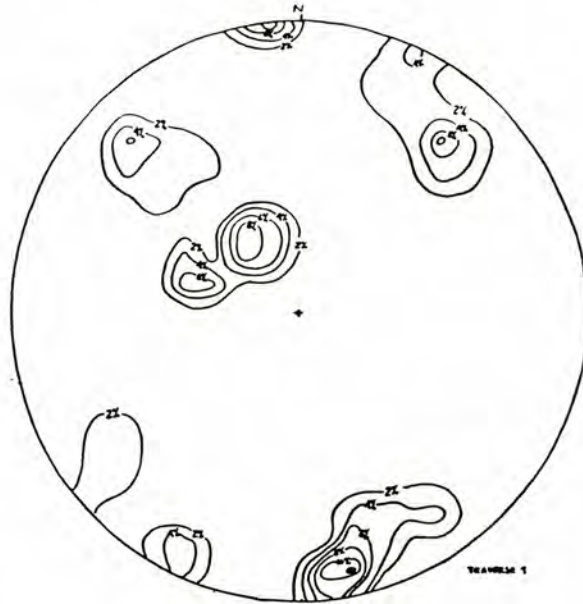
During follow-up investigations, traverses 8 through 26 were completed, concentrating more on the southern part of the ring. Figure 1 (pocket) of this report indicates locations of all scanlines and traverses, in addition to showing auger, rotary, and diamond drillholes, and geophysical survey traces. Contoured stereograms were compiled for Traverses 1-17, 19 and 22-26. In some cases, too few joints were encountered to be statistically significant.

Table 2 lists traverse number, locations relative to ring miles (RM), major rock types with minor rock type in parentheses, and whether or not a stereogram is associated with the traverse.

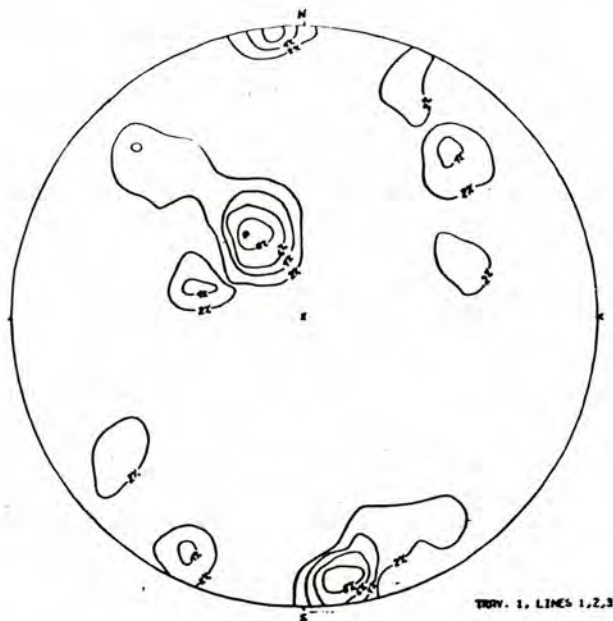
Fractures in the granites were generally limited to three major joint sets with orientations differing strongly between ranges and slight variations within structural domains.

On Traverse 8, a fault in a saddle was suspected in the field and proven by a comparison of stereograms upon either side of the structure. This is the only fault found with a clear cross-cutting relationship to the tunnel alignment and the paucity of such findings together with the total traversed length (on the order of 18 miles) suggests that major structures will not cause significant delay in tunnel construction.

Jointing in the Booth Hills quartz diorite seemed to also be limited to 3-4 sets. Differences in joint set directions seemed to be superficially resolvable by simple planar rotation of stereograms from different traverses. Pinal Schist shows a shallowly southward-dipping, irregular contact with the intrusive quartz diorite on the eastern part of the ring. Stereograms of lower-hemisphere pole plots of joints suggest that with the



Traverse 1



Traverse 1, Scanlines 1, 2, 3

Figure 11 - Comparison of scanline and traverse mapping results, Espanto Mountains.

Table 2 - Maricopa Site Geotechnical Traverses

<u>Traverse No.</u>	<u>Location</u>	<u>Rock Type</u>	<u>Stereogram</u>
T-1	.25 mile NE of RM5	Xg	yes
T-2	RM 50-50.5	Xg	yes
T-3	1 mile E of RM41	Xg	yes*
T-4	.5 mile W of RM 47	Xg	yes*
T-5	RM 13.2 EW	Xd	yes*
			(also separate)
T-6	.75 mile W of RM 42	Xg	yes*
T-7	.75 mile NW of RM 46	Xg	yes*
T-8	RM 45.5 -RM 46.5	Xg	yes
T-9	RM 46.75 -RM 47.5	Xg	yes*
T-10	" " "	Xg	yes*
T-11	RM 42 MD11 area	Xg	yes
T-12	RM 47.8-RM 48.6(MD10)	Xg	yes
T-13	RM 49.3 (N of MD10)	Xg	yes
T-14	RM 15.6 (SE of MD13)	Xd	yes
T-15	.25 mile W of RM 14	Xd	yes
T-16	SE of RM 14	Xd	yes
T-17	RM 16.5	Xd	yes
T-18	.5 mile E of RM 16.5	Xd (Xp)	no
T-19	1 Mile E of RM 18.25	Xp	yes
T-20	2.5 Miles E of RM 20.2	Xp	no
T-21	.75 Miles SW of RM 29	Xg (Xp,Tc,Tv)	no
T-22	SW of RM 31	Xg (Tv,Tc)	yes
T-23	RM 23.2-23.4	Tbu. (Tc)	yes
T-24	.25 Miles SE of RM 22.4	Tbu (Tc) Twt)	yes
T-25	RM 21.8	Tbm. (Tc)	yes (Tbm combined)
T-26	RM 223.2 and North	Tbm, Twt	yes (Twt combined)

RM = Ring Mile

Xg = Precambrian granite

Xd = Quartz diorite

Xp = Precambrian Pinal Schist

Tv = Tertiary volcanics

Twt = Tertiary welded tuff

Tb = Tertiary basalt (u = upper, m = middle)

* Combined into one plot

exception of the foliation, jointing in the Pinal Schist is of similar orientation to the major joints in the quartz diorite. The foliation is probably consistent in strike on a large scale, but chevron and isoclinal folds with wide variations in strike are present on a scale of tens of feet.

In the strong volcanic rocks, such as basalts and the welded tuff, four joint sets are commonly well developed, and even basalt flows separated by several hundred feet of conglomerate show distinctly similar joint pole distributions. Flat joints are present in all units but are most pronounced in the welded tuff which displays a "flaggy" outcrop in the field due to nearly-horizontal cooling/flowbanding joints.

In an attempt to relate jointing seen in drill core with surface traverses, a simple comparison of dip angles from both data sets was made. Figures 12, 13, 14, 15, 16, and 17 show graphs of joint number versus ranges of dip. In general, there is good agreement between surface and subsurface joint sets, which is often expressed at significant distances from the drill holes. When examining the graphs, however, it should be realized that a directional bias is introduced into both data sets, with vertical drill holes showing a low incidence of vertical fracturing and a high incidence of horizontal jointing. Conversely, a relatively-horizontal surface traverse will show a higher relative incidence of vertical fractures and lower numbers of horizontal fractures. The figures have not been corrected for such bias.

Field examination of joint sets reinforced observations from drillholes suggesting that joint frequency varies in broad zones. Comparisons of RQD, point-load indices, and subjective strength vs depth showed an approximately 100-ft spacing of weaker, more highly jointed zones, in MD5 and MD10. Zonation of jointed rock noted in MD11 compared favorably with a 50-foot spacing noted in the upper portion of MD5. In the field, heavily-jointed areas were often exposed as saddles on ridges or in scoured areas of arroyos. Spacing between highly-jointed zones at the surface appears to be on the order of 500 to 1000 feet in the granite on the northwest part of the ring.

The granite on the southwestern part of the ring has a similar fabric with strongly jointed zones about 1000 feet apart. A strong east-west trend to aplite and pegmatite dikes is also present.

Heavily-jointed zones were also found during surface mapping of the Booth Hills quartz diorite. Surface expressions of highly jointed zones are roughly 500 ft, and changes in rock composition seemed to have no effect on it. Highly jointed zones as estimated from MD3R appeared to be roughly 25 feet apart, but spacing was quite irregular.

The surface measurements of jointed-zone dimensions are probably more relevant to the tunnel orientation than are those made in vertical drill-holes. Also, fracturing may be more prevalent in the drillholes because of their locations. In general, surface mapping suggests that zones of increased fracturing, which may be expressed in the subsurface as zones of depressed rock quality, may be encountered at scales up to thousands of feet at most places but will be more but will be more closely-spaced, on the order of hundreds of feet, in major structural trends.

Figure 12 - JOINT DISTRIBUTION BY DEGREES

DRILLHOLE MD11

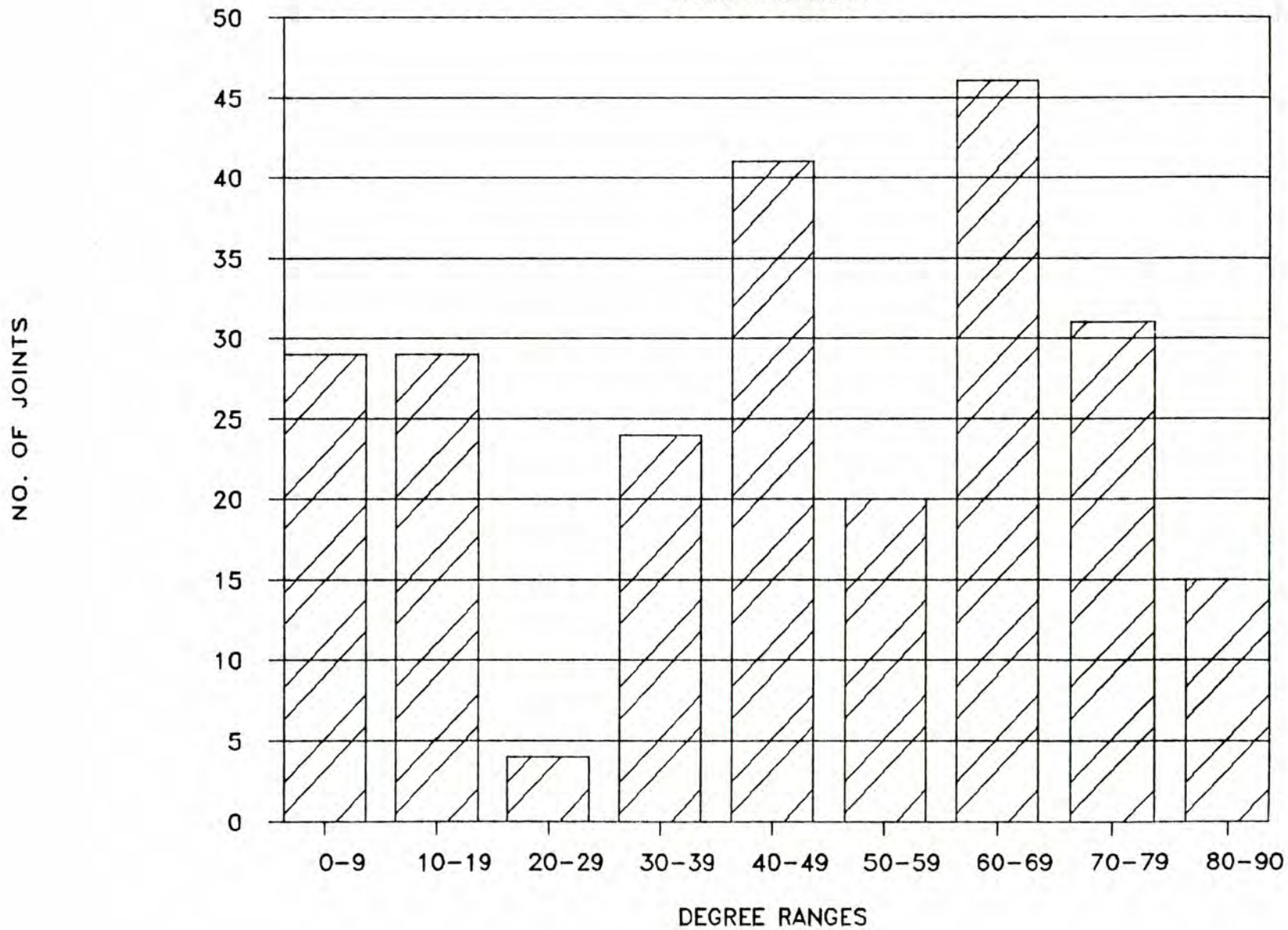


Figure 13 - SURFACE JOINT DISTRIBUTION BY DEGREES

DRILLHOLE MD11 VICINITY

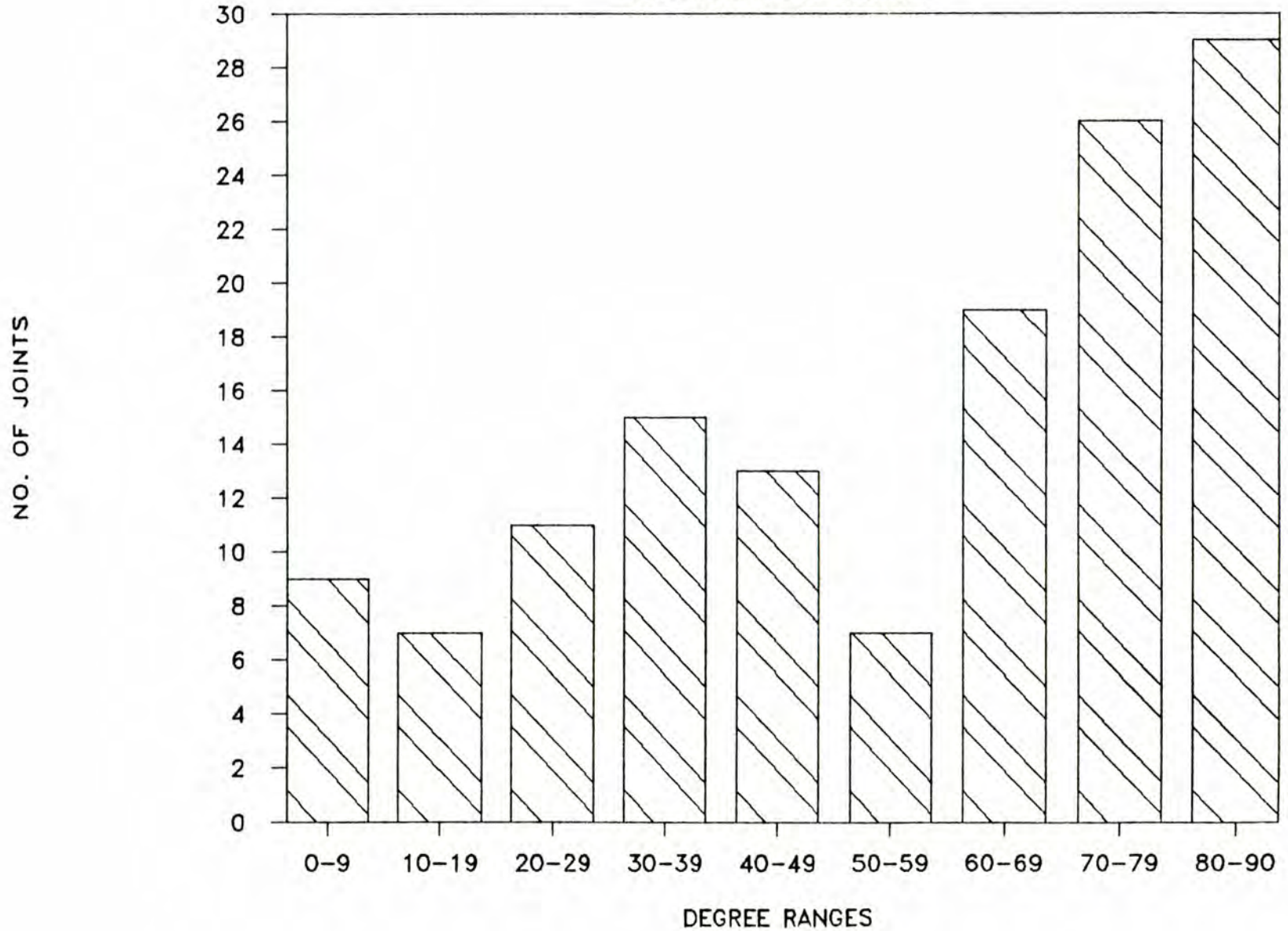


Figure 14 - JOINT DISTRIBUTION BY DEGREES

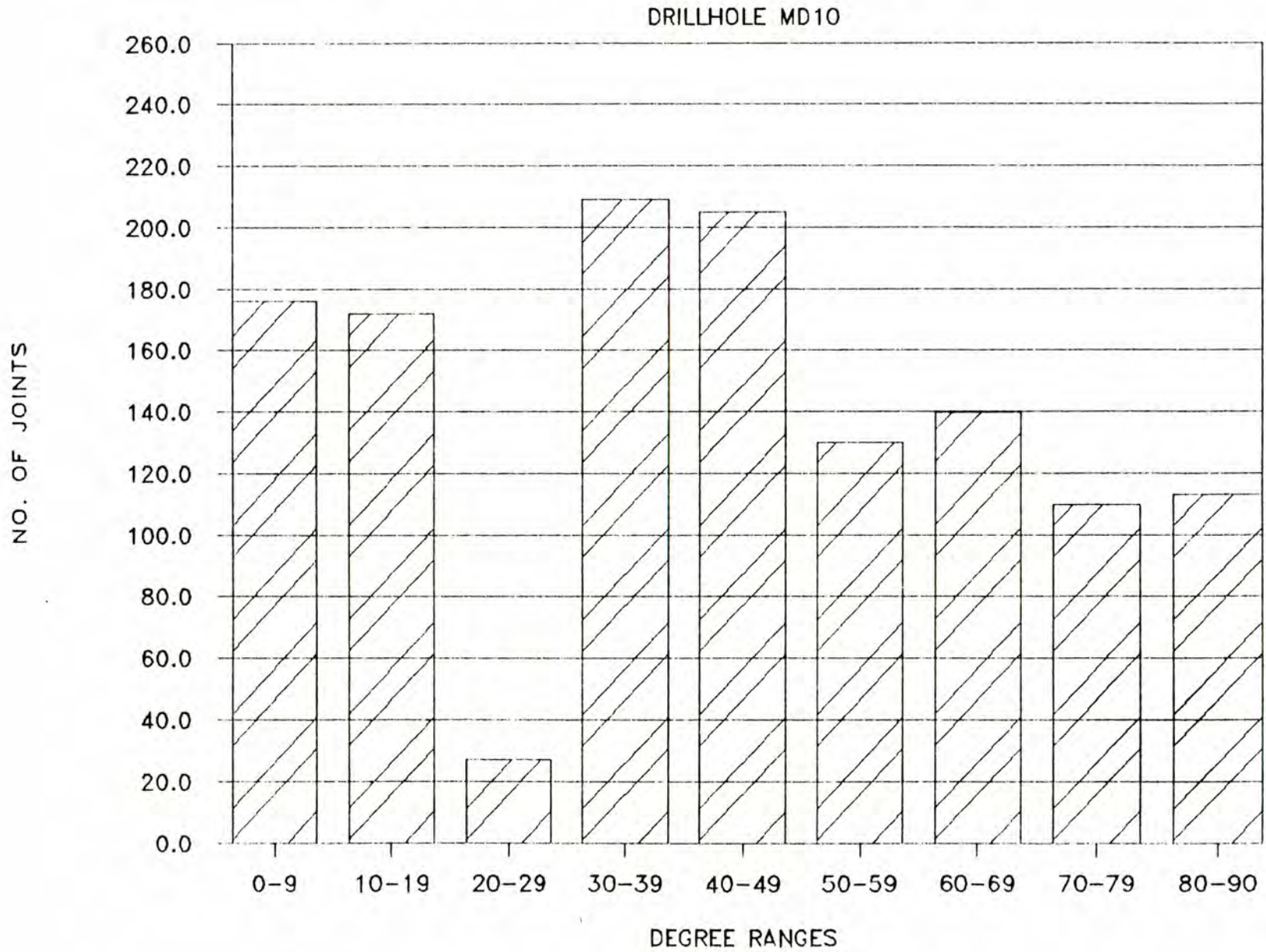


Figure 15 - SURFACE JOINT DIST.--SOUTH OF FAULT

VICINITY MD5 (MD10)

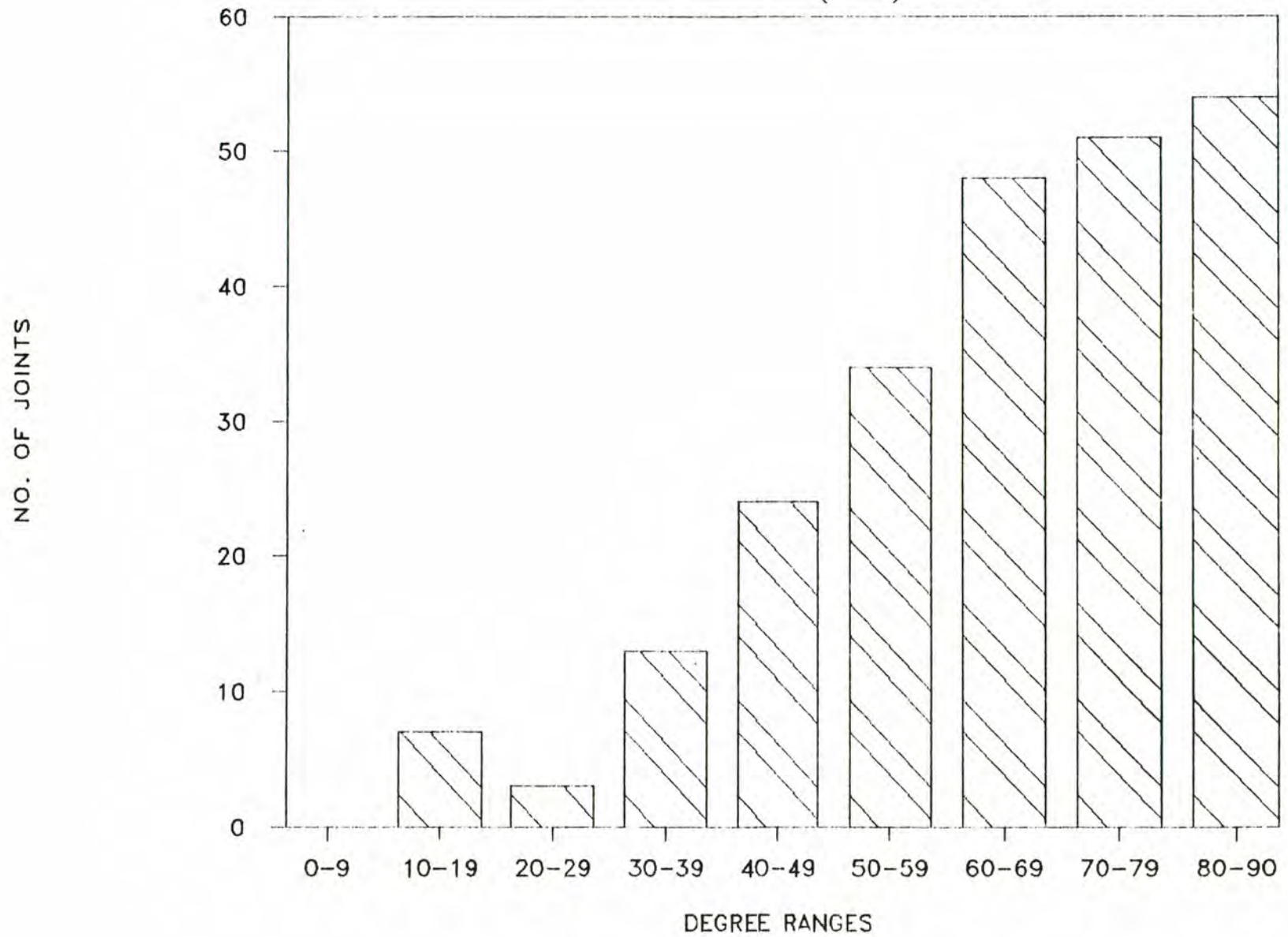


Figure 16 - SURFACE JOINT DISTRIBUTION BY DEGREES

DRILLHOLE MD5 & SW OF MD10

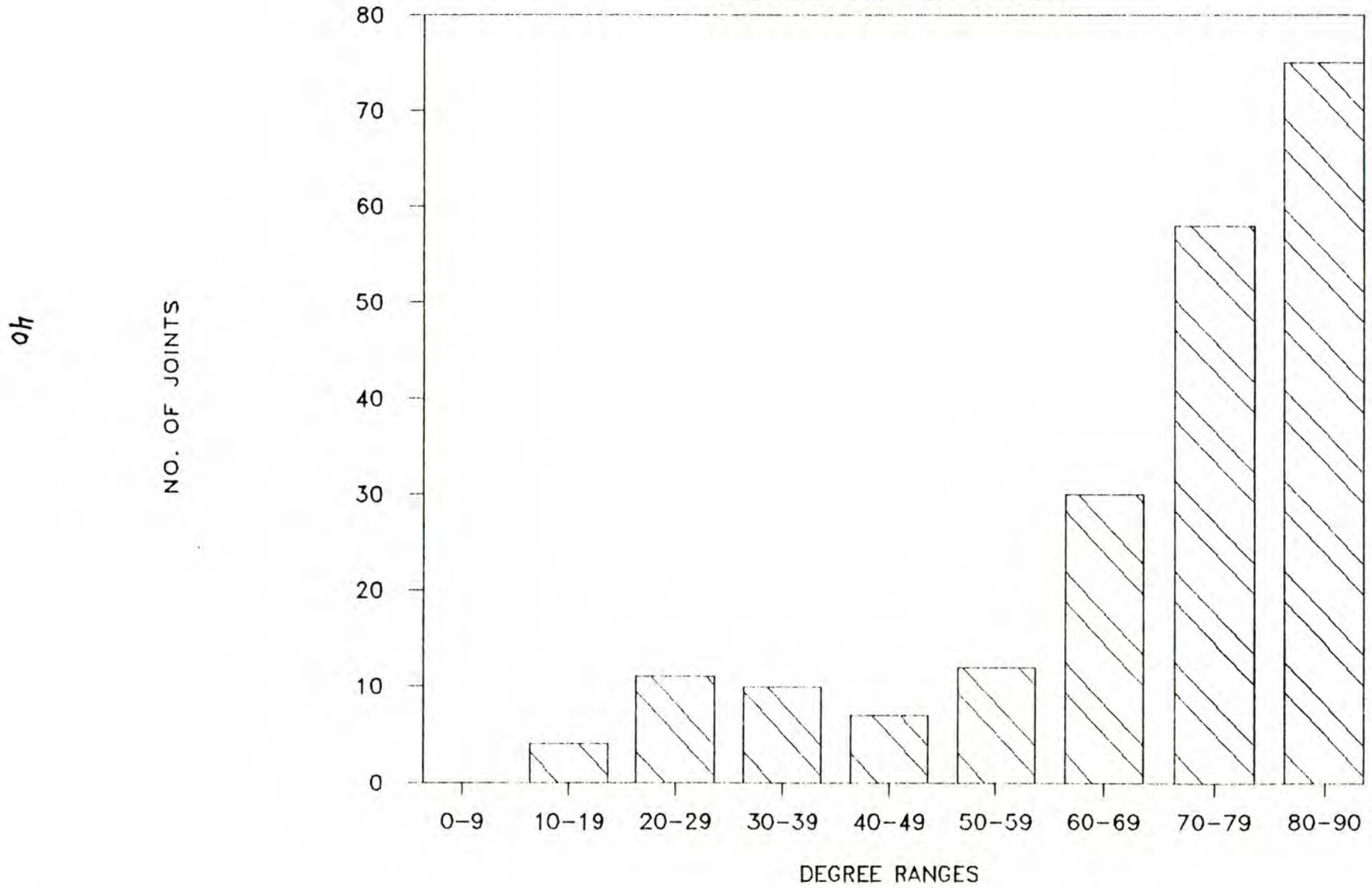
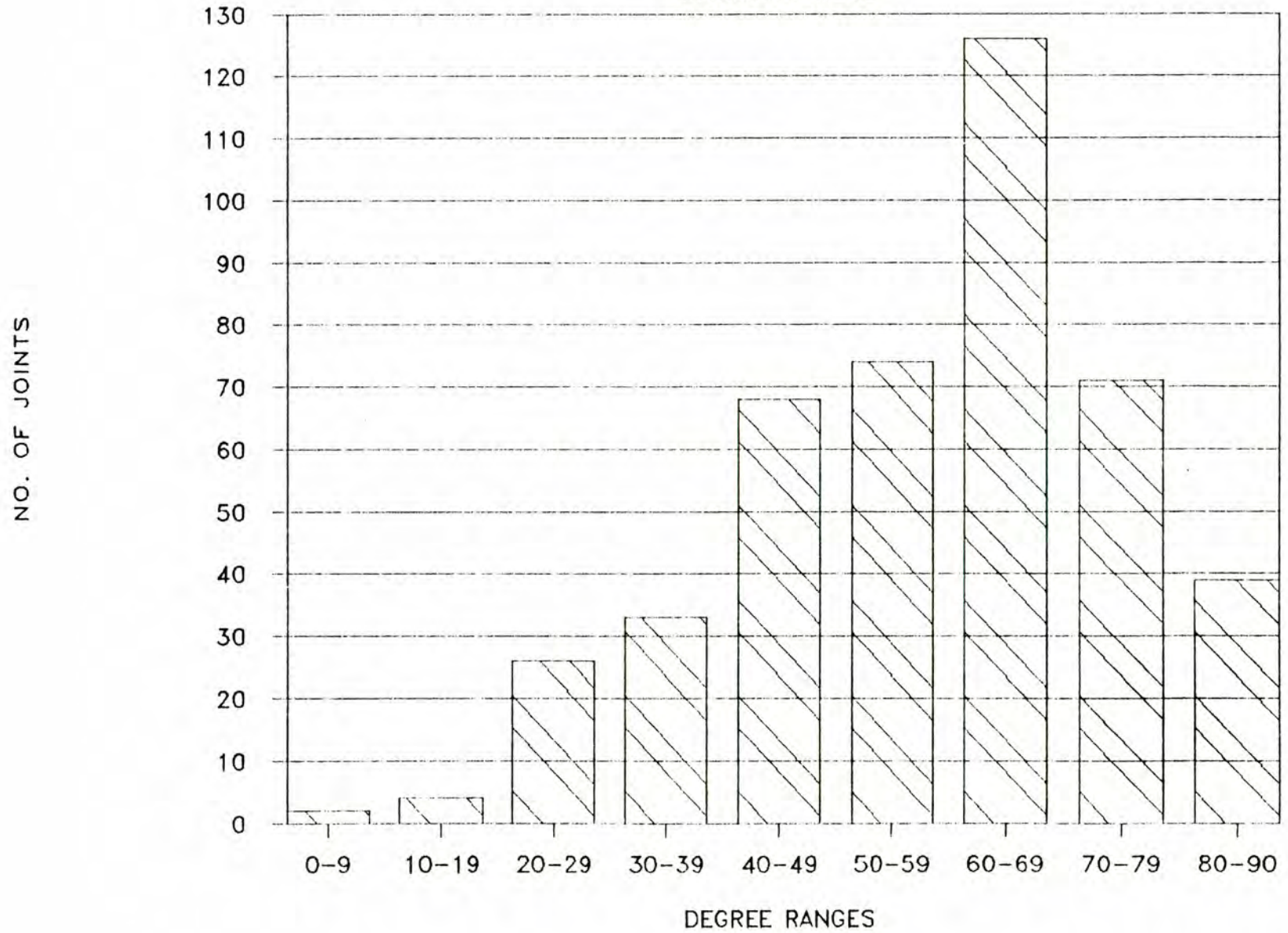


Figure 17 - JOINT DISTRIBUTION BY DEGREES

DRILLHOLE MD05



4.4.2.2. Results of Geological Reconnaissance

The general and ring-specific geologic setting of the Maricopa site was discussed in the site proposal (State of Arizona 1987) and will not be duplicated here. The following represents only new information collected since the submittal of the site proposals. This new information was intended primarily to illuminate the stratigraphic relationships in the ring sectors crossing from the quartz diorite terrane to the east, through the volcanic terrane to the southeast, south, and southwest, and out into the fanglomerate to the west.

Tertiary units are found mainly in the southeastern portion of the Maricopa site, and to a lesser extent in the southwestern portion in the foothills of the Sand Tank Mountains. Stratigraphic relationships in both areas are similar, but rock units vary widely in composition and thickness.

Southeastern Sector of Ring Alignment: approximately Ring Mile 21 to 25.

The surface projection of the ring alignment encounters a shallowly-southwest-dipping sequence of Tertiary rocks at approximately 21.75. Granitic rocks crop out less than 1000 ft northwest of the ring alignment at 21.25 and alluvium covers the Tertiary sequence at approximately 24.25. The granite/Tertiary contact is not exposed on the alignment, but to the northwest, friable, strongly jointed granite grades into a depositional (?) unit made up of randomly-oriented granitic cobbles and boulders (up to several feet in diameter) in a matrix of coarse granitic detritus. This is overlain by a basalt unit, <100 ft thick, which in turn is overlain by a poly lithologic conglomerate dominated by cobble-sized fragments of Pinal Schist and granite. This lower conglomerate is the first Tertiary unit cut by the ring alignment. At 21.8 the "ring" again encounters basalt and seems to remain in this unit until approximately 22.25 where it enters the middle conglomerate. At 22.45 the "ring" enters welded tuff and exits a rough projection of the tuff somewhere in alluvial cover northeast of ring mile 25. No outcrops of the tuff were noted in this area and thin (?) alluvial cover obscures relationships from ring mile 24.25 on to the southwest. Thin (?) alluvium covers the "ring" at 24.25.

Lower Conglomerate - This unit is a slope-former and has no apparent jointing. With the exception of a basalt separating the distinct granitic-clast basal unit from the poly lithologic unit it does not appear to be strongly lithified. Cobbles are the most abundant size fraction, and principal lithologies are Proterozoic basement rocks. The basalt unit is strongly jointed, between 20 and 80 ft thick and forms an outcrop of rounded boulders, 8-18 in. in diameter.

Basalt - A basalt unit appears to separate the middle and lower conglomerates. Preliminary cross sections indicate a thickness of 400 ft to 500 ft depending on slight variations in dip. Surface expression can vary widely, but is principally dependent on joint intensity. Sheeted jointing and intensely jointed material are commonly visible in washes but are generally covered. Their presence may in places only be inferred by abundant

basaltic float. The intense jointing is usually strongly developed in one or two nearly orthogonal directions, but the strike of such joints may change by as much as 30 degrees or 40 degrees in a few feet.

Strongly jointed basalt crops out as piles of spheroidal boulders ranging from 8 in. to 3-4 ft in diameter. Joints are scarce, but usually are well-developed and fairly consistent in strike and dip. Outcrops suggest a well-developed set of near-vertical joints.

Middle Conglomerate - A poorly-lithified poly lithologic conglomerate overlies the middle basalt. This unit is made up of clasts of granite, schist, quartzite, arkose, and limestone of dominantly pebble to cobble size. It forms slopes of low relief and has no jointing. Basalt flows occurring within this unit make thickness very difficult to estimate. A vesicular basalt of unknown thickness overlies the unit in most locations and another basalt occurs at depths varying from 40 to 120 ft stratigraphically below the top of the unit. Both of these basalts are strongly jointed and form strong to intermittent outcrops of spheroidal boulders.

Welded Tuff - The welded tuff unit is typically a reddish-brown massive-to-flaggy unit displaying eutaxitic texture and local vesicles. It varies widely in thickness, from 1-2 ft to more than 20 ft and generally shows well-developed, steeply-dipping widely-spaced joints. Shallowly-dipping joints parallel to the flow-banding are common in the unit. The welded tuff generally overlies a highly-vesicular basalt of undetermined thickness.

Upper Conglomerate - Although three conglomerate units separated by significant thicknesses of basalt were intersected in drillhole MD1R, all three lie beneath the welded tuff unit. The Upper Conglomerate was not definitely identified on the surface during detailed reconnaissance.

Southwestern Section of Ring Alignment: South of alignment from Mile 29 through Mile 35.

The Tertiary section in the southwestern area of the ring alignment differs somewhat from the units identified to the northeast. Both schist and granite are present and are overlain by a relatively thick (200 feet?) section of basal conglomerate containing abundant large clasts of schist, some 6 to 8 ft in length. The conglomerate is overlain by 50-70 ft of interbedded basalts and lahars which form prominent cap rocks on several of the foothills of the Sand Tank mountains.

The granite is distinctly two-phase in this area, with a weakly foliated to mylonitic porphyritic granite intruded (?) irregularly by an equigranular biotite granite. The equigranular granite weathers more rapidly, but both of the granites are strongly jointed, and aplite and pegmatite dikes (E-W) are more numerous than in the granite on the northwestern part of the ring. The schist and possible zones of the granite (??) are strongly foliated. The schist identified in one outcrop has strong N-S-striking foliation, which is parallel to foliation in granite (??) nearby; however, foliation in other more distant (1 to 2 miles) granitic areas did not appear to have any consistent strike direction. It should be noted that the granite exposed roughly one mile south and west of Ring Mile 29 shows

considerable quartz veining and a high degree of propylitic alteration, with in-place rock consisting of essentially red potassium feldspar, chlorite, and quartz. Although this area is geologically complex, weathering affects the basement rocks in a very similar manner. This observation coupled with the fact that all dikes and veins seen were generally thin (<2 feet thick), and greater than 20 feet apart, suggests that tunnelling characteristics (provided that the tunnel even intersects the rock) should be relatively uniform.

Conglomerate in this area is a slope forming unit, exhibiting very poor lithification on the surface and with no apparent jointing. As noted above, clasts are generally much larger than in the equivalent unit north of Freeman Interchange on I-8, with fragments in the 1 ft to 3 ft range being common.

A highly-jointed, intercalated basalt flow was noted near the top of the conglomerate.

4.4.2.3. Discontinuity Orientations

Data from the survey were plotted as normals to planes on lower hemisphere equal-area projections. Collected data were then contoured to give orientation density distributions expressed as percentage values per 1% of area. This allows rapid identification of joint and discontinuity sets.

Data are plotted and contoured and are shown on Figure 3 (in pocket). Accurate locations of these data sources are given on Figure 1 (in pocket).

The general conclusions are:

- (1) Espanto Mountains traverse and scanlines are compared to show that each technique identifies the same major joint sets.
- (2) In the granites, traverse data identified certain fracture trends that are widespread, but locally, different sets can predominate.
- (3) In general, the intrusive rocks (granite and quartz diorites) are well-fractured. Granite fracturing intensity is high in discrete zones, with lower fracturing intensity between. The quartz diorite is fractured with about the same intensity everywhere, although there is some variation. Intensities of fracturing were discussed in 4.4.2.
- (4) Conglomerates in the volcanic assemblage are very sparsely fractured to not at all.
- (5) Welded tuff and basalt fracturing are more intense at the surface than in core, probably a weathering phenomenon. In core, most basalt fractures are curved to wavy

and probably represent cooling cracks that will detract little from rock mass strength.

- (6) Surface mapping agrees qualitatively with core fracturing data and aids in conceptualizing the suite of fracturing to be expected in a horizontal tunnel, which will differ from fracturing expressed in a vertical borehole. The ability to map densely-fractured zones at the surface is limited by the low exposure of these zones.
- (7) Fracture zones align with washes. Topographic highs will be less fractured (most of tunnel). Increased fracturing and weathering will occur mostly beneath washes.
- (8) Faulting is mylonitic, crushed rock filling more than wide shear zones filled with gouge. No wide gouge zones have been found to date, hence, faulting should on a project-wide scale be weak and exceptions will be few. Only one significant fault was found in all traverses to date.

4.4.3. Distribution of Rock Mass Strength

In order to evaluate variability in rock mass strength, the following steps were followed.

- (1) Perform laboratory confined compressive strength testing for various rock types and weathering states. It was not possible to test all rock types in all holes, so methods of extrapolating strength to untested regions were developed as part of the rock mass strength evaluation.
- (2) Reduce the confined strength data by developing failure envelopes over the stress regions of interest, and then construct an equivalent unconfined strength by fitting circles to the developed envelopes with confining stress = 0. This will define a strength value for the shear mode of unconfined failure (an unconfined compressive strength in shear, or, in this report, "UCSS"). For present purposes, linear Mohr-Coulomb envelopes were deemed acceptable.
- (3) Relate the derived UCSS values to the point load indices from the immediate vicinity (0-3 ft core distance). Perform linear regression analysis to help develop conversion factors and correlation coefficients, by which UCSS can be estimated where only point load indices exist.

- (4) Assess the variation in rock substance strength along and between drillholes by developing ranges of correlated UCS values, using the point load indices, for locations not covered by laboratory strength testing. Of most significance is the ability to assess strength of weaker weathered rock that would not withstand preparation for laboratory testing, but for which a point load index could be measured. For very weak rocks, the point load index was estimated if a meaningful test could not be conducted. Estimated values are clearly indicated on the downhole parameter logs on 4.4.1. and were not used in the analysis.
- (5) Using fracture spacing concepts developed from surface mapping, combined with spacing characteristics noted in drill core, develop ranges of rock spacings and strengths corresponding to characteristic weathering intensities and rock types, and generate ranges of rock mass classifications (RMR values) accordingly.
- (6) Use the Hoek and Brown (1980) method to estimate rock mass strength according to the derived compressive strength (UCS), and an assumed range of confining pressures. Since in-place tests are not available to develop site-specific m and s parameters needed for the method, use the rock mass classes (RMR values) from step 5 to estimate m and s from empirical criteria.
- (7) According to down-hole distributions of rock classes as associated with rock mass strengths, examine bedrock seismic velocities at areas where surface seismic geophysics and cored holes coincide.
- (8) Using the benchmarked seismic signatures from step 7, infer the potential bedrock conditions at seismic line locations between boreholes to address the overall continuity of conditions along the tunnel.

The latter two steps are taken up in 4.4.4.

Laboratory tests were run in the confined mode whenever feasible because it was of most interest to provide correlations that could be related to a shear failure mode and to a confining stress. Test results are given on Table 3. Some lithologies were not intercepted in boreholes or did not appear in testable dimensions: welded tuff, leucocratic granite, and Pinal Schist. Highly weathered granite or quartz diorite, and conglomerate, are weaker and difficult to sample. Conglomerate was tested, in unconfined compression in a soil testing machine, to avoid the rigors of jacketing the weak rock.

Processed laboratory test results are summarized in Table 4. Processing consisted of drawing Mohr circles for all the data given. Separate Mohr-Coulomb envelopes were drawn for pairs or triplets of samples with nearby point load tests, and single samples were fitted with Mohr-Coulomb

Table 3 - Laboratory Compression Tests on Core Samples -- Maricopa

Rock Type	Depth (ft)	Confining Pressure (psi)	Axial Strength (psi)	Density (#/cu.ft)
<u>DIAMOND DRILL HOLE MD1R</u>				
Basalt	323-324	250	12207	159
Basalt	342.5-343.5	500	12560	158
Basalt	364	750	16077	161
Conglomerate	95.1-95.7	0	657	135
Conglomerate	215.2-215.8	0	1690	151
Conglomerate	215.2-215.8	0	1795	152
Conglomerate	224.4-225	0	1646	151
Conglomerate	250.3-250.9	0	275	138
Conglomerate	253.1-253.5	0	575	136
Conglomerate	253.5-254	0	630	135
Conglomerate	254.6-255	0	167	140
<u>DIAMOND DRILL HOLE MD3R</u>				
Quartz Diorite	36.9-37.5	250	30360	169
Quartz Diorite	55-55.7	500	33622	169
Quartz Diorite	119.5-120	750	18820*	750
<u>DIAMOND DRILL HOLE MD5</u>				
Granite	431.4-422	500	25199	169
C.Gr.Granite	444-444.7	1000	18005	168
C.Gr.Granite	445.445.4	1500	20395	167
<u>DIAMOND DRILL HOLE MD10</u>				
Diabase	401.8-402.8	300	6737	185
Diabase	401.8-402.8	700	8021	187
C.Gr.Granite	62.7-63.4	250	16170	167
C.Gr. Granite	61.8	1000	21560	166
C.Gr. Granite	77.0	600	20946	167
C.Gr. Granite	84.5-85.0	250	10790	166
C.Gr. Granite	372.0-373.0	250	22371	169
C.Gr. Granite	372	600	27351	169
C.Gr. Granite	370-370.5	1000	34992	168
C.Gr. Granite	230.3-230.9	0	24724	168
C.Gr. Granite	235.6-236.0	250	36779	163
(silicified)				
C.Gr. Granite	232.2-232.7	1000	23418	167
<u>DIAMOND DRILLHOLE MD11</u>				
C.Gr.Granite	62.0-62.8	600	25770	165

* Fracture-controlled failure resulting in an abnormally-low strength.

Table 4 - Summary of Maricopa Rock Properties

	C	UCSS	Kp	ϕ
	<u>psi</u>	<u>psi</u>		
Basalt	1,200	7,800	9.5	57
Granodiorite	5,100	28,500	6.4	47
Fresh Granite	3,400	17,800	5.8	45
Mod.Wthrd.Gran	2,800	12,000	6.1	46
Conglomerate (lower density)	-	450	-	-
Conglomerate (higher density)	-	1,700	-	-

Kp is the triaxial stress factor = $\frac{1 + \sin \phi}{1 - \sin \phi}$

envelopes that paralleled those drawn for pairs and triplets. The cohesion and friction angles resulting from pairs and triplets were combined to yield the data summarized.

In addition, a suite of five geomechanics tests was run on surface grab samples from the Maricopa area. Some of the rocks tested were later found to not fall on the final ring alignment. Tested samples were re-cored in the lab prior to being subjected to small-scale shear, point load, uniaxial, Brazilian, and triaxial testing. A gneiss giving 8 psi cohesion and 23 degrees friction angle was the only valid result for the small scale shear test on the metamorphic rocks. Uniaxial compressive strengths ranged from 6,089 to 16,880 psi and Brazilian tensile strengths from 741 psi to 1,228 psi. Triaxial tests gave varying strengths from 21,601 psi (at 500 psi confinement) to 10,908 at 880 psi confinement. Differences in weathering and degree of foliation are responsible for the scattered strength data in the metamorphic rocks. Igneous intrusive rocks yielded values from 0.1 psi cohesion at 26 degrees friction angle to 16.5 psi cohesion at 21 degrees friction angle for small scale shear tests. Unconfined compressive strengths ranged from 71,160 to 4,737 psi, and Brazilian tensile strengths from 663 psi to 2,901 psi. Triaxial tests yielded values from 71,160 psi at 100 psi confinement to 17,814 psi at 1000 psi confinement.

The above data are reported for completeness. They were not used in the analyses, since they represent uncontrolled sampling, weathering, and lithological effects.

Following the basic processing referred to above, each individual Mohr-Coulomb envelope was fitted with a circle corresponding to unconfined conditions, and then the normal stress intercept was picked off the graph. Each value thus obtained corresponds to a "derived" unconfined strength-in-shear (UCSS) value that could be related to adjacent point-load tests.

Table 5 shows UCSS value and point load index for various rock types. A linear regression analysis was run on the data with the result that the UCSS, in MPA, was found to be predicted very well by multiplying the average point load index for the adjacent core by 17. (Note that conversion factors reported elsewhere in the literature, which range as high as 29, are correlated to unconfined compression test data which will contain data points corresponding to axial splitting, cataclasis, and crushing, which are modes of failure in which rock is typically stronger.) An appreciation of the rock substance strength variation can now be gained by examining the point load parameter logs in 4.4.1 for each borehole.

Rock fracturing and rock substance strength combine to effect rock mass strength. The parameter logs show these relationships for the rock masses at the Maricopa site, by allowing comparison of RQD, a measure of rock fracturing, and measured or estimated point load strength, a measure of rock material strength. The field estimates of rock mass strength were found to respond in general to these parameters. However, it was desired to rationalize the field rock mass strength estimates to numerical values. Accordingly, Rock Mass Rating (RMR) values (Bieniawski, 1973) were obtained for rocks corresponding to subjective strength categories. The groupings used are listed in Table 6.

Table 5 - UCSS and Point Load Index for Various Core Intervals

<u>Hole No.</u>	<u>Rock Type</u>	<u>Depth</u>	<u>Point Load</u>	<u>UCSS</u>
MD10	fresh coarse-grained granite	370-370.5	10.6	17,770
MD10	fine-grained granite	235.6-236.0	14.	35,000
MD10	diabase	401.8-402.8	3.4	4,500
MD10	sl. weathered coarse-grained granite	230.3-230.9 232.2-232.7	8.1	17,700
MD10	mod. weathered coarse-grained granite	62.7-63.4	5.5	14,800
MD10	mod. weathered coarse-grained granite	84.5-85.0 77.	3.2 6.7	9,100 14,800
MD5	sl. weathered coarse-grained granite	444-444.7 421.4-422.	9.2 7.5	13,800 22,000
MD3R	quartz diorite	36.9-37.5	12.1	28,500
MD1R	massive basalt	363.-365.	3.1	7,800
MD1R	lower-density conglomerate	95.1-95.7 250.3-250.9	0.2?	461
MD1R	higher-density conglomerate	215.2-215.8 224.4-225.	1.0?	1,710

Table 6 - Assignment of Rock Mass Ratings to Strength Categories

Strength Category	Rock Mass Description						RMR (Value) Range
	UCSS	RQD	Fracturing			Water	
			Spacing	Condition	Orientation		
8-9	18,000	90	3	fresh rough	fair	dry	(86) 80-100
5-8	12,000	70	1.5	sl. weath trace clay	fair	dry	(73) 60-80
3-5	8,000	50	0.8	mod. weath. trace clay	fair	dry	(54) 40-60
2-3	5,000	25	0.4	mod.-str. weathering common slicks clay 0.05 in.	fair	damp	(30) 20-40
0-2	2,000	<25	<0.4	very soft clay >0.05 in. common slicks	fair	damp	(16) 0-20

Note: Above parameters are primarily for the intrusive assemblage. Values for other site material types were assigned separately. See text.

Rock mass ratings for basalt and welded tuff used separate classification input values that are specific to those rock masses. Basalt was found to have an expected RMR of 69, and was therefore assigned to strength category 5-6. Welded tuff was assigned strength category 4-5 on the basis of data from very limited core intercepts coupled with field mapping. Conglomerate and fanglomerate, which are intermediate between "rock" and "soil" for purposes of forecasting engineering behavior, are not amenable to rating according to rock classifications. Because of the paucity of fracturing, the ratings are unrealistically high (67 in the case of the conglomerate). Therefore, the strength ratings assigned in the field were reconsidered where appropriate in view of the laboratory strength data and the geophysical signatures, in order to develop rock mass strength concepts for assessing tunnel construction performance in these materials.

Since there were no back-analyses of excavations or in situ tests available, numerical rock mass strength was estimated according to the criterion of Hoek and Brown (1980, p. 137) and using the modified m and s parameters proposed by McCreath (1984) related to rock mass quality. The relationship provides a means to predict a failure stress for the rock mass at different levels of confinement. For the straight-line portion of the Mohr-Coulomb failure envelope, which is considered a reasonable criterion for most of the brittle rocks and/or shallow depths of construction at the Maricopa site, the values given in Table 7 were obtained.

Inspection of the subjective strength parameter logs with these correlated strength properties in mind will also reveal that problematically weak components of the Maricopa site rock masses are scarce at ring depths. For example, at the maximum 1,400 ft depth of the ring at the site, which occurs in granite, the vertical assumed stress would be $1.1 \times (1,400) = 1,540$ psi, and the expected horizontal stress would be roughly a third of this, or 510 psi. Under such a stress field, the maximum tangential stress around a circular tunnel in isotropic, homogeneous rock would be approximately 2.7 times the vertical stress or about 4,000 psi, and would occur at the springline rock surface. Rock masses with subjective strength ratings greater than about 5 would remain elastic under these conditions. At the more-typical tunnel depth of 300 ft, rock masses with subjective strengths greater than about 3 would remain elastic. Rock masses remaining in the elastic range would require little, if any, systematic support.

Examination of the core logs and the seismic data show that, for the granite and granodiorite at least, the lowest strength categories are associated with weathering that is a near-surface effect where depths, and therefore required rock strengths, are not high. Lower strengths are also associated with intermittent but widely-spaced zones of heightened fracturing intensity that have been found as deep as 600 ft. However, fracturing this deep is thought to be mostly associated with relatively rare, major structural trends.

The volcanic rocks and fanglomerates present special cases. The basalts are of moderately high (3-6) strength factors and will be nearly self-supporting wherever they are found at the expected tunnel depths. The conglomerates are expected to be weak and may require a systematic lining for depths in excess of the open-cut cutoff. However, weak conglomerate sections will behave like the fanlomerate sections of tunnels (see Section

Table 7 - Rock Mass Properties Corresponding to Strength Category

<u>Strength Category</u>	<u>Rock Mass Friction Angle, (degrees)</u>	<u>Rock Mass Cohesion (psi)</u>	<u>Rock Mass UCS (psi)</u>
8-9	52	2,350	13,600
5-8	48	1,250	6,200
3-5	35	400	1,600
2-3	30	75	290
0-2	18	30	90

6) in that they will offer very rapid advance rates. The conglomerates may upon further investigation prove to be stronger in place than was apparent in recovered core, as is suggested by seismic velocities in the neighborhood of 9,000 ft/sec.

4.4.4 Seismic Refraction Interpretation

4.4.4.1. Distribution of Detected Seismic Velocities

Figure 18 plots the depth to the lower contacts of each stratum indicated in the seismic data against the interpreted seismic velocity. These are aggregated data for the entire site and include lines sited over conglomerates derived from many different source areas and lines from areas known to have shallow bedrock. Nonetheless, several groupings are immediately apparent. There are reasonably-distinct groups of seismic velocities in the data that probably represent zones of distinct geotechnical behavior. Most of the data fall into the ranges 400-1,000, 1,000-2,000, 2,000-4,500, 4,500-6,800, 6,800-8,000, 8,000-11,000, 11,000-15,000 and more than 15,000 ft/sec.

There appears to be a group of materials with velocities ranging from 6,800 to about 8,000 ft/sec that generally was not detected shallower than 250 ft. This probably represents a rock-like deep valley conglomerate. Materials with velocities greater than about 8,000 ft/sec were found at depths ranging from 40 to 520 ft. Because of the widely-ranging but generally-high velocities, the variation in top surface depth, and the fact that lower limits to these bodies were not detected, it is suggested that at least some, if not all, of these velocities represent bedrock of various lithologies and weathering intensities. Velocities in excess of 12,000 ft/sec probably represent hard igneous rock.

Although Figure 18 indicates the depth of near-surface low-velocity sediments, it does not indicate the possible presence of deeper low-velocity sediments, since the seismic refraction method used here does not detect low-velocity zones at depth. The good agreement between the seismic interpretation and well logs from nearby borings indicates that significant low-velocity zones are probably rare.

A discussion in Section 7 will cover the ring-specific seismic signatures and show how they relate to information from drilling and testing.

Time-distance profiles from the seismic data exhibited some evidence of gradual velocity changes with increasing depth, notably where a transition to an inferred bedrock refractor was being crossed. The evidence consists of slight curvature in the straight-line portions of many of the time-distance profiles, making the assignment of layer thicknesses and the associated velocities less well-determined. These seismic lines used a uniform 120 ft geophone spacing.

To check whether potential weathered transition zones or thin layers were being suggested but not fully resolved by some of the longer lines, a survey was run with shorter geophone spacing (50 ft) at a location where a

SEISMIC VELOCITIES VS DEPTH

ALL LINES

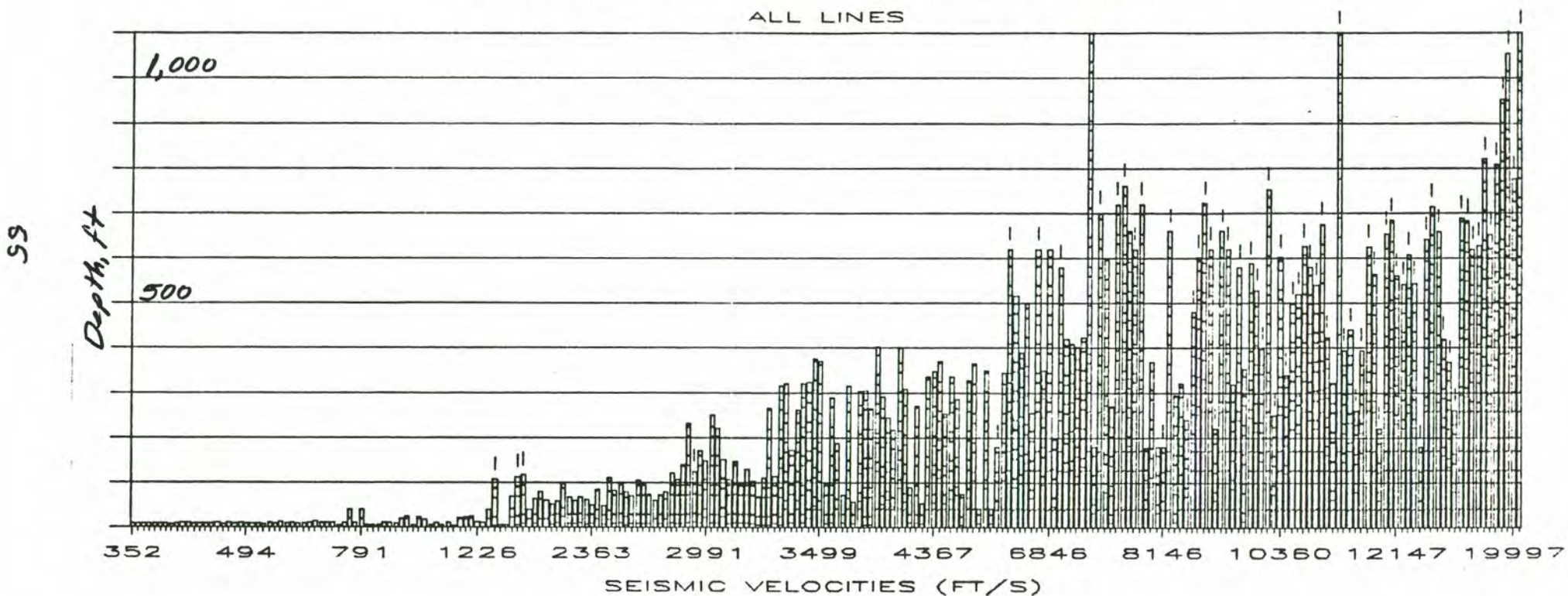


Figure 18. Site-Wide Distribution of Seismic Velocities Versus Depth
The double-hatched zones are the depth intercepts.
Where the survey did not identify a lower boundary,
a vertical slash is shown.

transition from weathered to fresh bedrock was found to exist near tunnel depth (MD11 drill site). Comparison of Figure 19 with the core log and with the rock mass quality measures depicted in Figure 8, shows that the weathered and fractured near-surface layers are visible in the seismic response. The correlation between borehole geology and the interpreted seismic profile is excellent. The surface unconsolidated layer and a moderately-consolidated near-surface layer are clearly indicated. An 80-ft thick zone of weathered, fractured granite with clay-filled joints was found in the core and fits the seismic interpretation closely. The deepest seismic layer corresponds to intact moderately-fractured and slightly weathered granitic bedrock, such as would be expected below a weathered zone. The apparent difference in measured velocity of this deepest refractor between the east and west line may be partly the result of a potential local, buried bedrock high, whose presence is suggested by a substantial knoll just to the northwest of the line and by the dip suggested in the interpreted profiles. Considering the relatively high level of fracturing found in the weathered core, it is possible that an increased level of fracturing to the west of MD11 (between it and the southward projection of the knoll) could also account for the reduced velocity in the bedrock.

The significance of this profile is to show that a zone of weathered rock should be expected atop interpreted bedrock refractors and that the wider geophone spacings necessary for some of the longer lines designed to "see deeper" may incompletely determine such zones or mask them completely. It should be emphasized that zones of weathered material atop intact bedrock have been found in all the drillholes in intrusive rocks to date. Seismic velocity data for these zones would characterize them as being in the 4,000 to 8,000 ft/sec range, which should provide a suitably-gradual transition into the harder portions of the intrusive rock masses for the tunnel boring machines.

4.4.4.2. Correlation with Strength and Modulus

Seismic profiles indicate that within the assemblages of materials to be crossed by the ring, the velocities of discrete, recognizable zones (surficial alluvium, cemented alluvium or conglomerate, weathered zones, and bedrock) fall within consistent ranges. Thus it should be possible to draw correlations with strength and thereby modulus. Correlation factors with bedrock strength were assessed before and after modifying laboratory strengths for core taken from nearby boreholes, as described in 4.4.3. of this report, to account for fracturing in the rock mass that could affect the seismic data. For conglomerate and alluvium whose in-place behavior is not significantly affected by fracturing, the correlation is established with strength values from laboratory tests, in situ shear testing, and dilatometer testing.

The Young's modulus (E) can be estimated from the theory of elasticity:

$$E = C \frac{2}{p} \frac{(1 + \nu)(1 - 2\nu)}{(1 - \nu)} \frac{\gamma}{g}$$

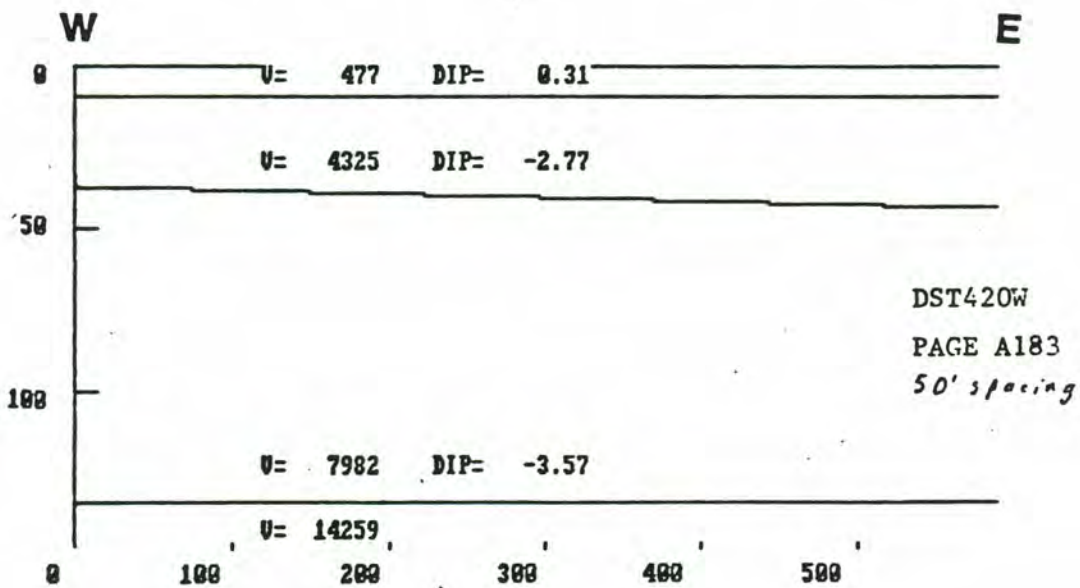
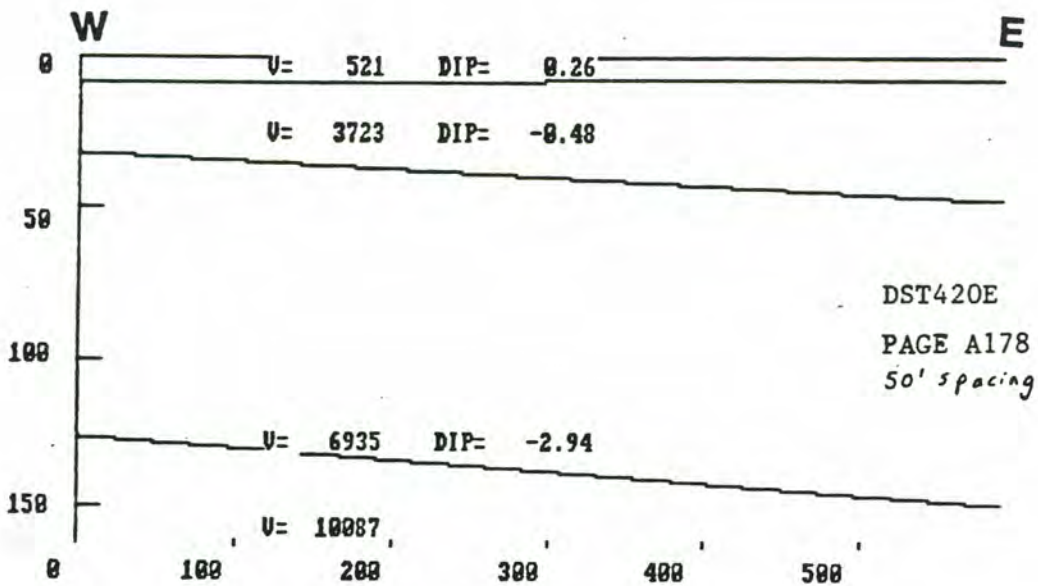


Figure 19. Velocity Profiles for Line DST420. These lines were directly over the MD11 drillhole site. Layer thicknesses compare very favorably with the drillhole data (see Figure 8).

where ν is Poisson's ratio, ρ is density and g is acceleration due to gravity. This is reasonable provided the magnitude of C_p is high enough to indicate a dense material, that could be expected to behave elastically.

There are also relationships between modulus and strength. Hobbs (1974) shows such data, based on a large sample of weak sedimentary rock. For Bunter sandstone and arenaceous sediments that are similar in overall character to weakly-consolidated sandy fanglomerate, Hobbs (1974) suggests that the modulus ranges from 50 to 200 times the compressive strength.

Relations between compressive strength and P-wave velocity based on laboratory tests carried out at U.S. Bureau of Mines laboratories were analyzed by Judd and Huber (1961) and Farmer (1968). Their data are illustrated in Figure 20 and show that the p-wave velocity is generally proportional to the square of the unconfined compressive strength at failure. Of the curves for three groups of rocks, that for the upper bound is quite close to the theoretical/empirical model proposed above.

Also included in Figure 20 are data on sonic velocity collected by Sternberg and others (1988) in various geophysical surveys of the Maricopa site. These are compared with strength data from diamond drill cores. The sonic velocities cover quite broad ranges and may not truly represent the average layer velocity. The rock strengths are averages for the borehole length coinciding with the sonic velocity range. The weaker rocks may not strictly satisfy the elasticity criterion mentioned above. Nonetheless, there is an apparent correlation between field data and laboratory data. Two basic trends can be observed:

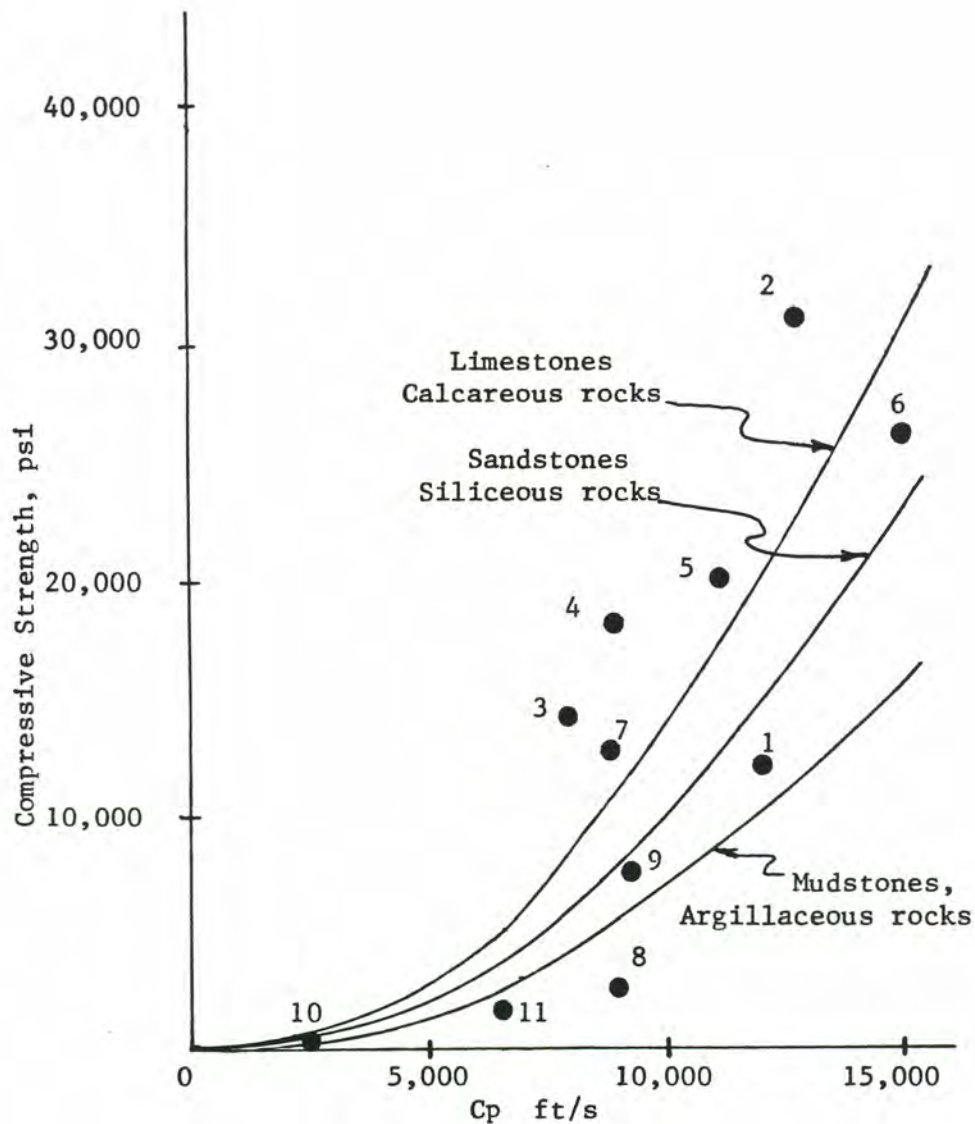
- (a) For porphyritic granite, the data follows a curve steeper than for laboratory data.
- (b) For fanglomerates the curve is less steep than for laboratory data.

Weathering and fracturing also affect the passage of seismic waves, however, and the laboratory strength data do not include these features. Since the fanglomerates and conglomerates are essentially unfractured, this effect may not be as important for these as for the intrusive and harder volcanic rocks. If the laboratory strength for the fractured rocks is viewed as an upper bound to rock mass characteristics that must govern the observed velocities, then the correlation apparent in Figure 20 is strengthened.

4.4.5 Forecast of Hard Rock Tunnelling Characteristics

Hard rock units for purposes of this discussion include the granitic intrusive masses, the quartz diorite intrusive masses, and the volcanic assemblage that in turn is comprised of basalts, welded tuff, and conglomerate. These assemblages will display different responses to tunneling. These assemblages are discussed in a somewhat generic sense here.

Tunnel construction progress was assessed on a preliminary basis using the methods suggested by the University of Trondheim (Norwegian Institute of Technology, 1983). This method represents considerable hard rock tunnel



- 1 MD1R Basalt
- 2 MD3R Quartz Diorite
- 3 MD5 Porphyritic Granite (60-190 ft)
- 4 MD5 Porohyritic Granite (>190 ft)
- 5 MD10 Porphyritic Granite (50-100 ft)
- 6 MD10 Porphyritic Granite (>100 ft)
- 7 MD11 Porphyritic Granite (40-100 ft)*
- 8 MD12 Fanglomerate (30-145 ft)*
- 9 MD13 Weathered Diorite (>75 ft)*
- 10 MR1 Fanglomerate (40-70 ft)**
- 11 MR1 Fanglomerate (140 ft)**

Curves from Judd and Huber (1961) and Farmer (1968)

* Strength estimated from point load test data

** In-situ strength from dilatometer test

Figure 20. Comparison of Compressive Strength Obtained from Seismic Velocities and Various Strength Tests

boring data that were used to develop a series of nomographs for assessing TBM performance. Site specific data required by the method include the intensity and orientation of fracturing, the strength of the rock, and the tunnel diameter. The assessments can therefore be carried out for various rock conditions. The method also accounts for all significant sources of TBM downtime. Industry-wide average values are used for most downtime sources but the primary source of downtime (cutter change time per length of tunnel advance) is calculated separately from estimates of rock hardness and abrasiveness. TBM operating performance is corrected for gripper thrust efficiency, RPM, cutter size and distribution, and modification of rock strength due to fracturing.

In considering the Maricopa site conditions, the following parameters were assumed for all TBM sections:

Cutter disc diameter: 14 in.
 Tunnel diameter : 10 ft (3m)
 TBM rotation : 11 RPM
 Cutter spacing : 2 1/2 to 3 1/2 in.
 Number of cutters : 26

Of course, actual TBM design can be expected to differ because more detailed data for each construction unit would be collected before the start of final design. Certainly the TBM design used by prospective contractors could be expected to be optimized according to those data. Since the assessment described herein is for average, not optimized performance, and because the method draws from data dating back several years prior to 1983 (the date of publication), modern optimized TBM performance could be expected to be superior. Other methods of forecasting TBM performance are given by Wang and Ozdemir (1978) and Graham (1976).

In Section 7, the concept of Construction Units, each segment corresponding to a commonality of tunnelling conditions, is introduced, and the assemblages are described more rigorously.

It should be realized that ancillary activities (handling muck, laying track, installing ventilation and lighting, and so on) will need to be designed to keep up with the TBM to prevent underutilization of machine capacity. As will be shown, the TBM daily performance for most of the proposed SSC sites' geologic conditions was considered for each assemblage, as follows:

<u>Rock Conditions</u>	<u>Approximate Strength Conditions</u>	<u>Fractures per Meter of Tunnel</u>
Granites		
strongly weathered	2-3	20
moderately weathered	4-6	10
lightly weathered to fresh	7-8	3
Quartz Diorite		
strongly weathered	2-3	20
lightly weathered to fresh	7-9	5
Basalts	5-6	5
Welded Tuffs	4-5	5
Conglomerates (volcanic)	3-4	0
Fanglomerates	1-2	0

Fanglomerate response to tunneling is discussed more fully in 5.5.7.2.

Rock support recommendations covered as parts of the following discussion are based on experience with similar fractured and weathered rock masses in Arizona, on the results of comparisons of rock mass strength with stress concentrations for various depths (see discussion in 4.4.3), and on the recommendations of the Geomechanics Classification of Bieniawski (1973), as described previously.

4.4.5.1. Intrusive Assemblage

Approximately 19% of the tunnel alignment crosses the granitic assemblage in Construction Units 3, 4, 8 and 9. As described previously, this assemblage consists primarily of Precambrian porphyritic granite, quartz diorite, and local xenoliths of gabbroic intrusive rocks and Pinal Schist. Locally, small diabase dikes or silicic pegmatites may occur in the granite, and a finer-grained phase may also be encountered locally.

The granitic rocks present at the site are among the oldest rocks known in Arizona. Most have experienced multiple episodes of tectonic activity that are evidenced by mineral recrystallization and minor introduction of calcite, quartz, and epidote veinlets; development of weak to moderate foliation; and several different suites of fracturing.

There is a noticeable absence of strong mineralization and alteration. Changes in rock composition and structural fabric that determine the strength and other engineering properties appear to be largely the result of weathering that is chiefly near (100 ft or so) to present or buried bedrock surfaces, but may be encountered deeper in fractured ones. Such weathering is expressed as accumulations of iron oxides on fractures and around ferromagnesian minerals, along with the disruption of inter-grain bonds, tending to weaken rock material strength.

As shown in the preceding subsection, the rock mass strengths in this assemblage vary in response to the occurrence of fracturing and weathering. However, the rock masses are expected to be generally very competent. Boreholes drilled to date in the intrusive rock masses have all been in topographic lows. Fractures analyses introduced in 4.4.2 show a strong coincidence of mountain front embayments with fracture orientations, suggesting that many of these may be structurally controlled. This is very likely the case in the area of MD10 and also probable in the cases of MD5, MD11, and MD13. It needs to be stressed that tunnels will encounter more competent rock beneath topographic highs than would be deduced from core conditions in these boreholes, which preferentially sample the poorer rock.

Considerable site evidence (Section 4.4.2) proves that fracturing and jointing tend to occur in discrete zones. In porphyritic granite core, steeply-dipping joints are commonly found in groups separated by several feet of unfractured rock. The Booth Hills quartz diorite in the injector complex area appears to be more intensely fractured. Both rock types exhibit broad zonation in core quality, with large intervals of core of very good quality separated by intervals of poorer quality core. In drill core, about half the joints logged are rough and relatively clean; most of the

remainder contain clay or calcite, and are fairly smooth. Joints containing calcite may be partly open but all those seen that contain quartz or clay are completely filled. Although the net effect of the fracturing is to lessen the relatively high strength of the plutonic rocks, the quality of the rock is likely to remain good for tunneling at the ring horizon.

Rock stress conditions are unknown. No condition indicative of unusual stress conditions, such as core discing, was noted in drill core. In most cases, the shallow depth of tunneling and the intensity of the fracturing make encountering difficult stress conditions unlikely. Furthermore, major tectonic influences, such as regional thrust faults, that could suggest a potential for high residual stress fields, are unknown in the area.

Rock stress is likely to be less than 20% of the compressive strength and therefore unlikely to introduce or extend fracturing. Rock mass strength calculations were carried out and compared with probable stress gradients corresponding to varying depths of cover. These calculations were described in 4.4.3. Rock masses with strength ratings of 5 or greater should remain elastic even at the maximum tunnel depth of 1400 feet. Since this depth occurs at only one location, the calculations were performed for a more-representative depth of 300 feet. Rock masses with strength categories as low as 3 should remain elastic at these depths. Rock masses that remain elastic should require only localized bolting to prevent block loosening.

Inspection of the borehole parameter logs given in 4.4.1 show a higher percentage of strength category 3 rock than is expected, because the portions of the granitic masses that were drilled probably represent the least-competent components. From the field mapping, it can be expected that about 60% of the tunnel length in this assemblage will encounter category 5 rock or stronger and will therefore require no internal support; 80% will be category 3 or stronger, again requiring no to minimal internal support, and rock weaker than category 3 will mostly occur near bedrock top surfaces where rock stress will be low. Internal support if required at all will be light (most likely mesh-reinforced shotcrete or, in unusual cases, light ribs). Deep (more than 500 feet) occurrences of rock weaker than category 3 could require light steel ribs and reinforced shotcrete for long-term support, but such instances on the whole should be rare enough as to be incidental to overall construction.

In general, the granitic assemblage may be characterized as generally strong but variably fractured, with weathering at tunnel depths tending to be confined to the upper bedrock surfaces and the major mountain-front embayments where structural elements may extend the depths of weathering. Jointing intensity ranges from low to moderate and most fractures are moderately strong. The tunnel should be dry and complications arising from the influence of water should be absent. These rock masses can be classified as "good" to "excellent" and for all practical purposes will be nearly self-supporting.

Exceptionally weak zones, such as wide faults filled with gouge, or wide fault zones of crushed and deaggregated granite, are not expected from the surface exploration and were not indicated in drill core. The true widths of faults and deep weathered zones, as measured in core, were typi-

cally not more than a few inches, and were never found to exceed 0.5 ft. The maximum depth of substantial weathering appears to be less than 100 ft, with weathering below that depth limited to slight discoloration of feldspars and joint in-filling, ordinarily in discrete zones associated with minor faulting or an increase in the density of fracturing. At shallow depths, typically 50 ft below the bedrock surface, weathering can be intense and result in nearly complete disaggregation of the rock. Should such weathered zones occur in surface excavations, they can be easily excavated by surface earthmoving equipment. Underground, the weathered material, should it be encountered, can be adequately restrained by the planned shield support system. Weathered zones at the tops of intrusive rock masses were consistently found in the field investigations. Thus no sharp transitions (mixed faces) corresponding to changes from relatively weak fanglomerate to strong, fresh granite or quartz diorite, are likely.

The calculations described previously show that the intrusive assemblage materials are favorable for machine tunneling, offering high advance rates and requiring very little or no support. For segments in the granitic assemblage constructed by tunneling through harder rock, calculated thrust utilization factors show that sidewalls will permit the high gripper thrusts needed to maintain high advance rates, yet the material strengths are not so high as to indicate low cutter penetrability and high cutter wear rates. For the ten miles of granitic assemblage, tunnel advance rates are expected to be distributed as follows.

<u>Rock Characteristic</u>	<u>Expected Average Daily Corrected Tunnel Advance (ft)</u>
Granite	
strongly weathered (10%)	225
moderately weathered (25%)	178
slightly weathered to fresh (45%)	112
Quartz Diorite	
strongly weathered (10%)	245
slightly weathered to fresh (10%)	108

A weighted average progress rate was computed, using the previously-listed percentages, (taken with respect to all intrusive rocks) expected to be encountered at the tunnel horizon. The weighted average overall progress rate is 153 feet per day. A conservative estimate, deducting 10% for geotechnical contingency and 10% for general and equipment contingency and start-up time, is nonetheless a very good 120 feet per day. This value was used in the preparation of the cost and schedule estimates advanced in the site proposal.

4.4.5.2. Volcanic Assemblage

The volcanic assemblage occurs in the southeastern portion of the ring alignment in Construction Unit 5 and constitutes 14% of the rock to be tunneled. As described earlier, this assemblage consists of thick basalt flows interbedded with thick sequences of conglomerate. Locally, rhyolitic welded tuff might be encountered. These rocks have been carefully studied in drill hole MD1R and in outcrop.

The basalt is strong and has a low fracture frequency. It has a measured laboratory compressive strength of near 8,000 psi. Joints are commonly irregular, rough to wavy, with calcite fillings, and will detract little from rock mass strength. Vesicularity is low to moderate and tends to reduce the material's strength. As represented in core, this thick unit is quite homogeneous. No recognizable flow stratigraphy was noted above tunnel depth, such as flow-top breccia or buried ash, regolith, or cinder layers.

The conglomerates are unjointed. They are probably much stronger in place than they appear to be in recovered core. Detailed logging indicates an average of 40% sandy matrix and 60% lithic fragments, which may range up to six inches in diameter. The matrix is poorly cemented but lithic fragments, which include a wide variety of igneous and metamorphic rock types, are generally quite strong.

There is a possibility that the tunnel will encounter thin layers of rhyolitic welded tuff. Surface exposures and experience with similar rocks elsewhere in Arizona lead to expectations of low to moderate spacings of rough to irregular joints, and rock strengths in the range of 15,000-25,000 psi.

Attempts to measure depth to water table in the volcanic assemblage in MD1R were unsuccessful because the depth to water exceeded the 500 foot reach of the cable. This depth also exceeds the depth of the tunnel by about 150 feet at this location. Thus the volcanic rock units are expected to be damp to dry when tunneled. In particular, the moisture content of the conglomerates should be low, which will enhance their strengths.

The volcanic assemblage will be an excellent medium for tunneling. The contacts between various rock types are clear and should be easily locatable for tunnel design. The basalts should stand without any support except occasional rock bolts. Welded tuffs may require pattern-bolting at places or a light, reinforced shotcrete lining. The conglomerates may require a segmental liner, particularly if the transition to a more competent unit is to be made. The presence of a segmental liner would ensure a smooth transition from conglomerate to basalt with full thrust capacity (reacting off the liner). The conglomerates have low to moderate strengths and will permit excellent tunneling advance rates. The strength of the welded tuff could be high, but it is sufficiently fractured so as to permit rapid tunneling advance rates. The following advance rates were calculated using the methods outlined at the start of this subsection.

<u>Rock Characteristic</u>	<u>Expected Average Daily Tunnel Advance</u>
Basalt (30%)	160
Conglomerate (50%)	164
Welded Tuff (20%)	173

The weighted average progress for the above approximate percentages of the volcanic assemblage comes to 160 feet per day. The volcanic stratigraphy is not yet precisely known, so the encountered proportions of the various strata could differ from those above. Actual advance rates will probably

reach or exceed those calculated, however. This is in part because the nomographs used do not contain basalts or the relatively weak but unfractured conglomerates found in this assemblage in the data base (the closest analogy to the conglomerates is a sandstone) and the "net advance rate" parameter, which has a substantial effect on the calculated adjusted advance rate, is sensitive to fracturing. Observations in core show that separations between clasts and matrix will contribute to the conglomerates' rock mass weakness, but there is no provision in the nomographs for this effect, which would tend to offset penalties for possible abrasiveness. In 5.5.7.2 it will be shown that soft-ground tunneling rates in conglomerate could theoretically exceed 200 feet per day (limited perhaps by the rate at which the lining can be installed) and if this were also the case in the volcanic conglomerates, a theoretical average daily advance rate of 180 feet is conceivable.

The Buckskin Tunnel is an example of a successful Arizona TBM project through a complex volcanic sequence. The Buckskin Tunnel (N.R.C., 1984) was 35,771 ft long with an excavated diameter of 23.5 ft. It was constructed through a thick complex sequence of Tertiary to Quaternary andesitic lava flows and related volcanic deposits with uniaxial compressive strengths ranging from 10-40 ksi. These dense, strong formations comprise the dominant rock type but were associated with subordinate brecciated and vesicular andesite and tuff with agglomerate interbeds. The succession is considerably more extensive and varied than the interbedded volcanics and lava flows in the Maricopa site.

The tunnel was mechanically excavated with a Robbins tunnel boring machine with a two speed domed cutterhead and full length flexible articulated shield to provide full ground support in difficult ground. The tunnel was fully lined with a four piece concrete tongued and grooved segmental ring in 5 ft lengths. The progress record may be summarized:

Maximum advance/8 hr. shift	65 ft.
Maximum 24 hr. advance	150 ft.
Maximum weekly advance	625 ft.
Maximum monthly advance	2,665 ft.
Maximum yearly advance	18,450 ft.
The overall rates for the contract were:	
Average advance/8 hr. shift	16 ft.
Average advance/day	49 ft.
Average advance/week	245 ft.

5.0 CONSTRUCTION SEGMENTS IN ALLUVIUM AND FANGLOMERATE

One of the most advantageous characteristics of the Maricopa SSC site is that much of the facility's subsurface construction can be in cemented alluvium, locally termed fanglomerate. This section will show how the fanglomerates at the SSC site are strong enough to stand unsupported for long periods in deep excavations, yet are easily excavated by conventional earthmoving or mechanized tunneling equipment.

Numerous drillholes in fanglomerate at the site show consistently-high blow counts in standard penetration tests. In-place tests have developed strength and modulus values for the undisturbed material. The results of seismic refraction surveys agree well with their corresponding bore holes. The test data allow for reliable relationships between seismic velocity and strength to be developed, and this extends the data base between bore holes and test sites, to demonstrate that the fanglomerates are consistently favorable in their properties.

Seismic velocities for fanglomerate materials to be encountered at tunnel depth are characteristic of materials that can be readily removed by scraper with or without prior ripping. In tunnels these materials will offer excellent advance rates with few complications. Tunnels and large surface excavations have been constructed in similar material in Arizona, with excellent results.

5.1 Description of Surface Studies

5.1.1. Geophysical Surveys

Seismic refraction geophysics of the type described in 4.1.1 investigated the fanglomeratae overburden as well as the underlying bedrock. Methods for such surveys were described in 4.1.1.

Resistivity surveys (Sternberg, Thomas and Fink, 1987) were carried out to improve knowledge of depth to bedrock in the sections of thicker alluvium. Some additional seismic refraction surveys (Bryan, et.al., 1987) were carried out in the campus area for the same purpose.

Gravity surveys were run to determine thickness of basin fill and gross bedrock configuration in the Rainbow Valley (north of the ring, for hydrogeological purposes) and in the Maricopa Valley (interior of the ring, for geological interpretation and hydrogeology).

5.1.2. In-Place Testing

Field Slope Testing

Much of the basin fill and fanglomerate is lightly to moderately cemented, and it is very difficult to acquire undisturbed specimens from standard field sampling techniques. Disturbed and undisturbed test specimens will exhibit nearly identical internal friction angles, provided that the specimens possess similar void ratios. However, the material's apparent cohesion generally decreases as the degree of sampling-induced disturbance increases. For this reason, laboratory testing may significantly underestimate the shear strength of the material in its natural, undisturbed state.

A novel program of field slope testing was therefore conducted in the campus area to identify the shear strength of the fanglomerate in its natural state. A 10-ft-deep, 35-ft-long benched trench was dug in the material with a steam shovel, and several separate slope failures were then induced by applying a surface loading at the crest of the newly-created vertical slope.

A one-inch thick, square steel plate, 8 in. or 15 in. in length, was placed near the crest of the slope, as shown in Figure 21. A uniform load of increasing intensity was then applied to the plate by means of a 50-ton hydraulic jack. The rear end of the steam shovel provided the reaction support for the hydraulic jack. The surface surcharge was gradually increased until the slope failed, and the failure load and slip surface geometry were then recorded. Ten separate tests were performed -- five on the upper slope and five more on the lower slope. The shear strength parameters of the undisturbed basin fill were then back-calculated by means of an accepted analytical procedure (described in detail in 5.5.2).

5.1.3. Examination of Nearby Exposures

Information on the long-term and construction behavior of typical fanglomerates was obtained from first-hand examination of standing exposures in two nearby copper mines, Sacaton (ASARCO) and Ajo (Phelps Dodge). Sacaton is approximately 20-30 miles west of the Maricopa site and the New Cornelia Mine at Ajo is about 42 miles to the southwest.

The fanglomerate exposed in the upper benches of Sacaton is approximately middle-to-late Miocene in age, somewhere between 18-20 ma (personal communication ASARCO staff, 1988). It consists of a tan to light-brown, very-poorly sorted, matrix-supported fanglomerate, with variable caliche cement. It is poorly- to moderately-lithified, and has been stable in essentially vertical bench cuts, for more than 15 years. These cuts were examined during a site visit by Earth Technology personnel in conjunction with the State of Arizona SSC personnel. Figures 22, 23, and 24 will illustrate the competence of this fanglomerate.

At the New Cornelia Mine at Ajo, the Locomotive Fanglomerate is exposed on the southwest wall of the pit and in outcrops southwest of the mine. Interbedded volcanics within the unit have been tentatively dated at 26 ma

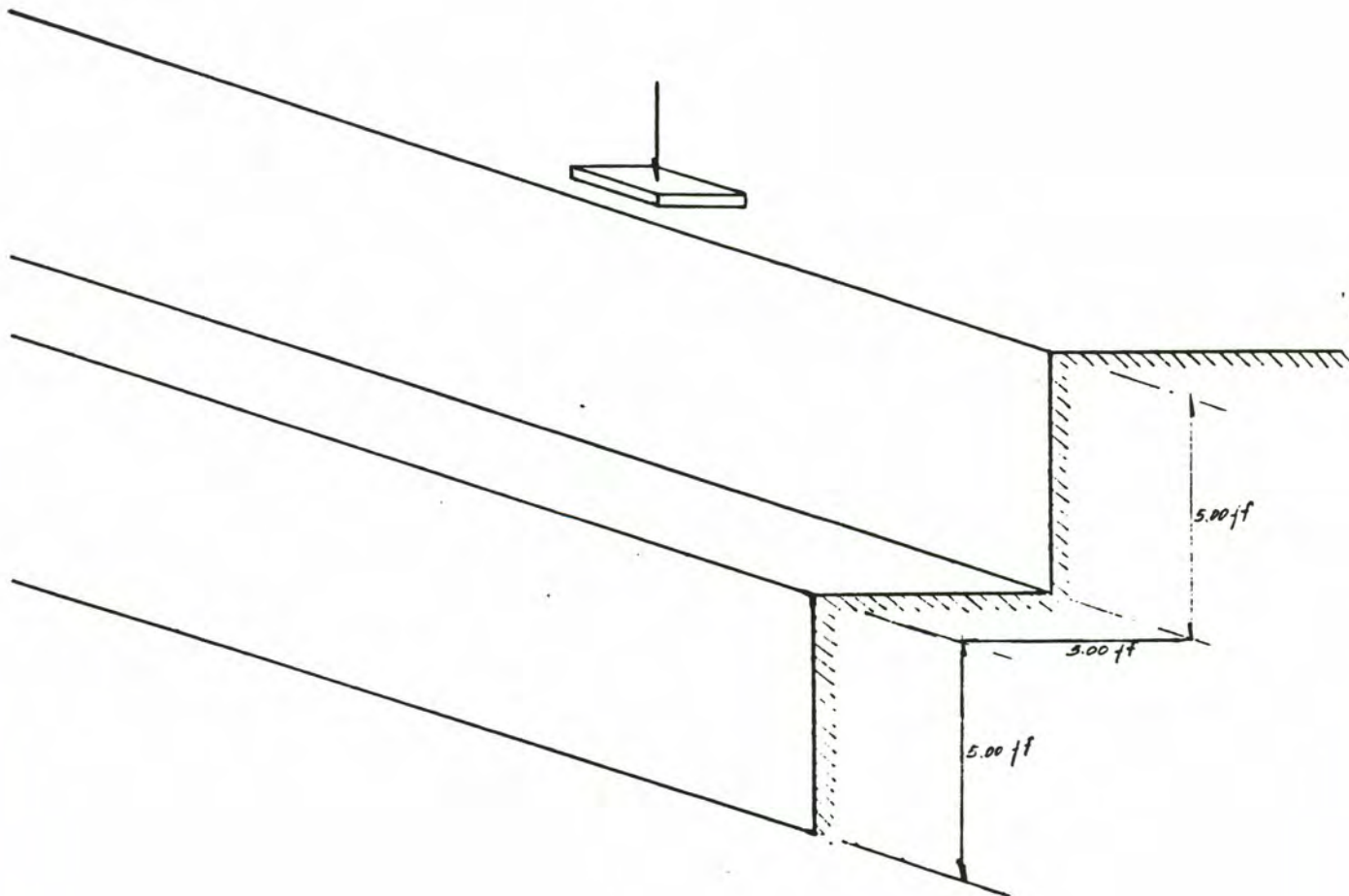


Figure 21.

Sketch of Field Slope Testing Set-up, Maricopa Site



Figure 22. View Looking South in Sacaton Pit. Grey unit approximately 6 ft thick separates younger fanglomerate (horizontal bedding) from older crossbedded fanglomerate (dipping to north). Benches are approximately 50 ft high. Note nearly vertical walls after 15 years since mining began.

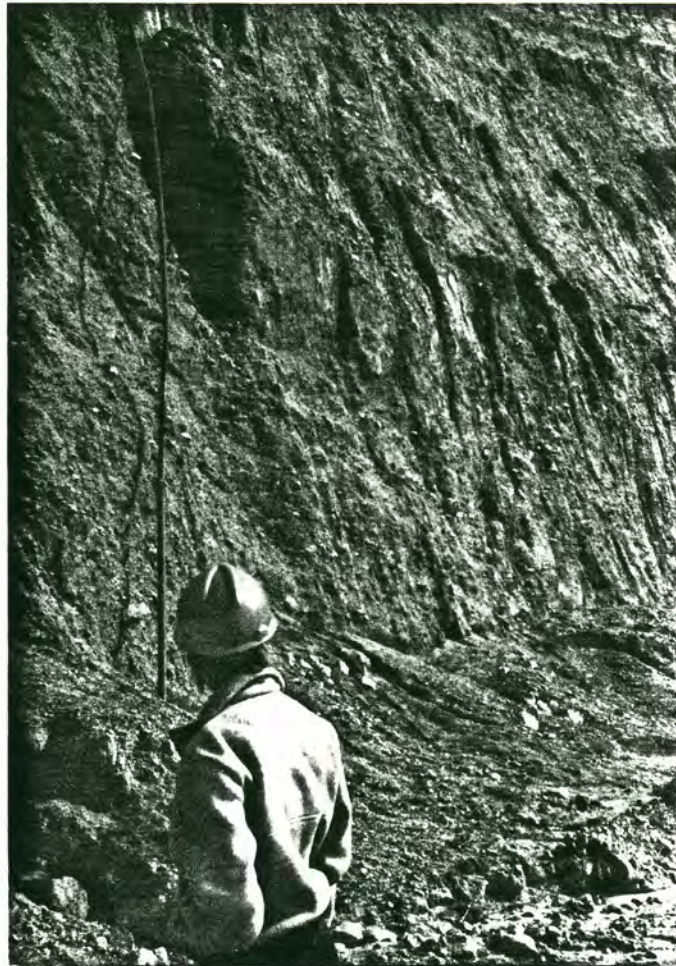


Figure 23. Iron-Stained Fanglomerate at Sacaton pit. View looking northeast. Note very poor sorting characteristic of fanglomerate. Bench is approximately 20 feet high.

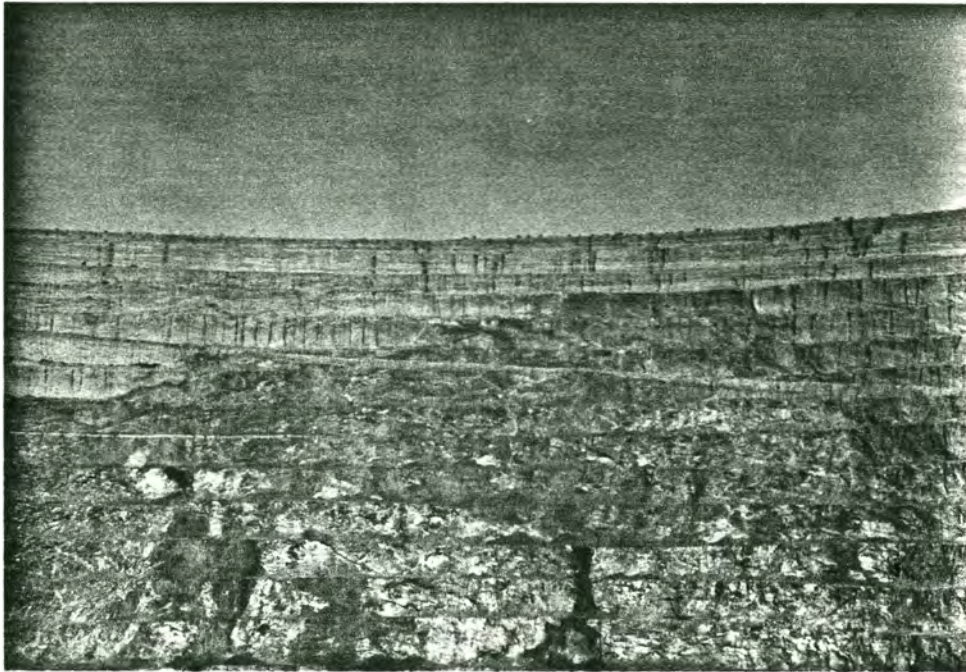


Figure 24. View Looking at West Side of Sacaton Pit. Reddish material is oxidized volcanic and intrusive rock of the Sacaton orebody. The two top benches are mostly younger fanglomerate, while the lower tan material is cross-bedded older fanglomerate. Bench height is approximately 25 feet and bench faces are nearly vertical.

(personal communication, USGS, 1988), making it substantially older than the fanglomerates expected to be encountered at the Maricopa site. The fanglomerate is dark reddish, very-poorly-sorted, and dominantly matrix supported. The Locomotive Fanglomerate is very well lithified and has been standing as irregular monoliths in outcrop, and on 1/2:1 and steeper slopes, for at least five years. The Locomotive fanglomerate is an example of how strong these types of materials can become.

5.2. Subsurface Studies

5.2.1. Drilling

Thirteen auger holes and rotary drill holes were drilled at the Maricopa site. The auger and rotary holes are described in Table 8.

The following data were collected:

- o The auger borings were completed utilizing a CME-75 drill rig and hollow stem auger (HSA). These borings penetrated the unconsolidated basin alluvium (younger fanglomerates) underlying the Maricopa Site injector complex, main campus, and isolated locations around the collider ring surface trace. Standard penetration testing was performed in all the HSA borings at depth intervals of five feet or less. Selected soil units were sampled utilizing a three-inch O.D., 2.42-inch I.D., tube sampler with brass inserts or a CME soil core sampler which receives a relatively undisturbed sample in cemented soil conditions. All soils were classified utilizing the Unified Soil Classification System, with drilling operation supervision and field lithologic logging performed by Sergeant, Hauskins, and Beckwith of Phoenix, Arizona.
- o The 42-inch large-diameter auger borings were drilled using a Texoma 900 foundation drill rig. After the holes were excavated, steel casing with twelve-inch square windows at five-foot vertical spacing was placed into the hole. Personnel were then lowered into the holes with a special harness and cage to inspect the soils, and to obtain photographs of the soils exposed at the windows. MA2 was also utilized to assess the vibration impact of passing railroad trains at collider ring depths. All soils were classified utilizing the Unified Soil Classification System, with drilling operation supervision and field lithologic logging performed by Sergeant, Hauskins, and Beckwith of Phoenix, Arizona.
- o Two reverse circulation dual-tube air-rotary borings (MD6 and MD7) provided cutting samples and subjective material descriptions. This method provides excellent

Table 8 - Fanglomerate Drilling Program, Maricopa Site

<u>Type</u>	<u>Hole No.</u>	<u>Location</u>	<u>Depth</u>	<u>Diameter</u>
Auger	MA1	On ring; mile 15.5	76 ft	6 5/8 in
Auger	MA2	On ring; mile 8.5	70 ft	42 in
Auger	MA3	On ring; mile 4.5	60 ft	6 5/8 in
Auger	MA4	On ring; mile 42	100 ft	6 5/8 in
Auger	MA5	On ring; mile 38 [?]	70 ft	42 in
Auger	MA10	Injector Complex	150 ft	6 5/8 in
Auger	MA11	Injector Complex	74 ft	6 5/8 in
Auger	MA12	Injector Complex	74 ft	6 5/8 in
Auger	MA13	Campus Area	75 ft	6 5/8 in
Reverse Circulation Rotary	MD6	1 mi no of mi 30	258 ft	5 1/8 in
Reverse Circulation Rotary	MD7	1 mi no of mi 2	655 ft	5 1/8 in
Direct Circulation Air Rotary	MR2	Injector Complex	206 ft	5 3/4 in
Standard Circulation Air Rotary	MR2	On ring; mi 8.5	100 ft	5 3/4 in

sample recovery which is not contaminated by spalling from the bore hole walls above the bottom of the holes. All soils were classified utilizing the Unified Soil Classification System, with drilling operation supervision and field lithologic logging performed by Sergeant, Hauskins, and Beckwith of Phoenix, Arizona. Down-the-hole geophysical surveys were performed by Geo-Hydro-Data and included self-potential resistivity, gamma, and caliper.

- o Two borings (MR1 and MR2) were advanced utilizing direct-circulation air rotary techniques and a 5-3/4-inch diameter bit. One of these borings was located along the campus area - injector complex boundary, and one was located at the eastern intersection of the collider ring surface trace and the Southern Pacific Railroad right-of-way. The primary purpose for advancing the rotary borings was for the installation of bore hole instrumentation. In the case of MR1, bore hole dilatometer test equipment was temporarily installed. Boring MR2 received vibration monitoring equipment to measure vibrations from passing train traffic. In both borings all soils were classified utilizing the Unified Soil Classification System, with drilling operation supervision and field lithologic logging performed by Sergeant, Hauskins, and Beckwith of Phoenix, Arizona.

5.2.2. In-Place Testing

Dilatometer Testing

As a check on seismic refraction signatures and to develop a strength relationship for seismic response and the SPT data, borehole dilatometer tests were run in the campus area. An experimental dilatometer developed by Ian Farmer and Associates, Ltd. (1987) in the U.K. was used to determine fanglomerate strength and deformation in borehole MR1. The dilatometer comprises a 125 mm TAM packer inflatable to 70 MPa. The overall packer length is 1.2 m and the inflatable length 0.91 m. The packer has been modified to contain 4 LVDTs with a working range of 35 mm to measure diametral deformation in the plane of the borehole at the center of the packer. Data can be reduced to measure deformation, strength and in-situ stress.

The dilatometer was lowered into the borehole using a wireline log. Data were reduced on site using a color monitor, micro-processor and analog/digital converter. Some difficulties were experienced because of the uneven nature of the hole (see Figure 25), which required modification of the packer. Malfunction of the LVDTs limited the usefulness of the in-situ stress interpretation. Typically the data obtained were the ultimate pressure and the associated diametral displacement of the hole.

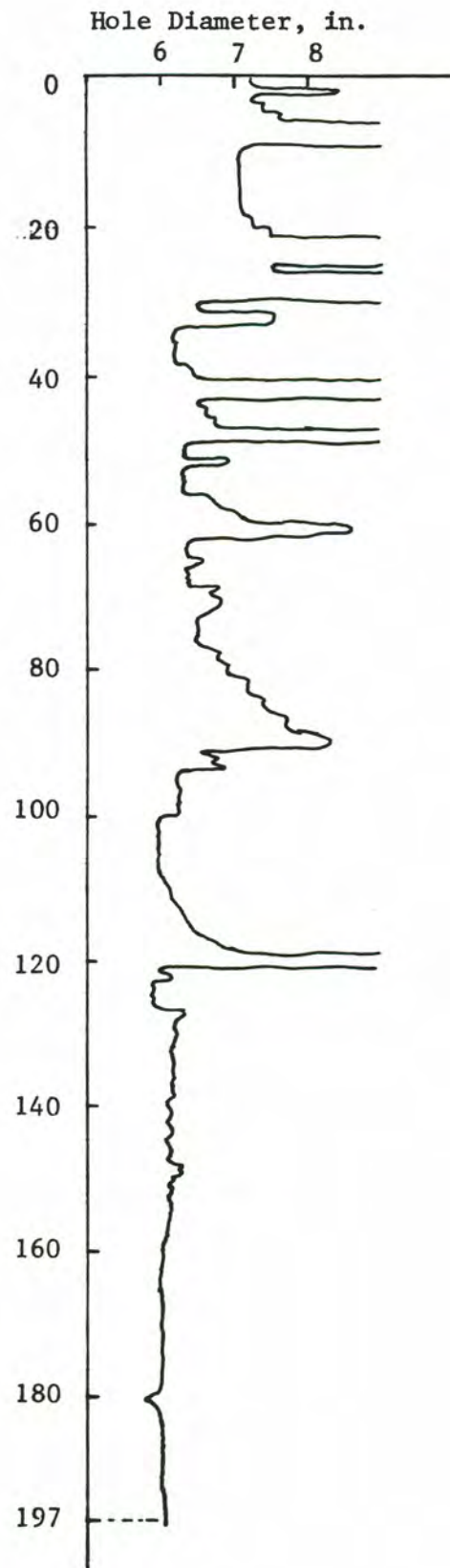


Figure 25. Caliper Log, MR-1

Pressuremeter Testing

During the completion of the HSA borings, a total of seven pressuremeter tests was performed in the cemented alluvial profile. The testing involved the drilling of a 2-7/8-inch-diameter boring in advance of the hollow stem auger, followed by the introduction of a Menard Type G-Am pressuremeter. Volumetric change was measured at 30- to 60-second intervals as pressures ranging from 0.25 to 55 bars were applied to the borehole wall.

The pressuremeter testing field data and calculated test results are presented in Appendix B to Sergeant, Hauskins and Beckwith (1988).

5.3. Laboratory Testing

Tests were carried out on deaggregated samples obtained from various depths in boreholes MR1, MR2, MA2, MA5, MA6, MA7, MA10, MA11, and MA12 as well as split-tube core retrieved from MD12. Tests included the standard suite of soil index and strength tests, and special tests for collapse potential and swelling. Details may be found in reports by Nowatzki, et.al. (1988), and Sergeant, Hauskins, and Beckwith (1988).

5.3.1 Sieve Analyses

Sieve analyses were performed on samples acquired from different depths within the various boreholes. All analyses were conducted in accordance with ASTM D421 and D422 standards for sample preparation and testing. A sample weighing between 100 and 500 grams was oven-dried and then placed in a sieve stack consisting of #20, #40, #60, #140, and #200 sieves. The stack was vibrated in a mechanical sieve shaker for about ten minutes, and the percentage (by weight) of material passing each sieve was recorded. The sample's grain size distribution curve was constructed from the five data points obtained by means of the sieve analysis. The in situ moisture content of each sample was also measured.

5.3.2. Atterberg Limits Analyses

Atterberg Limits analyses were performed on remolded samples acquired from different depths within the various boreholes. All analyses were conducted in accordance with ASTM 4318 standards.

5.3.3. Soil Classifications

The borehole samples were classified according to the Unified Soil Classification System (USCS) using the standard ASTM D2487 procedure. The results of the sieve analyses and Atterberg Limits testing provided the necessary numerical data relating to grain size and plasticity.

5.3.4. Direct Shear Testing

Direct shear testing was performed on intact CME and diamond drill core

samples from boreholes MA12 and MD12. All testing was conducted in accordance with ASTM D3080 standards. Tests were run at several different normal (vertical) stresses, and continuous measurement was made of both shear stress and shear deformation. Vertical displacement during shear was not recorded.

5.3.5. Triaxial Testing

Unconsolidated drained (UU) triaxial testing was performed on intact diamond drill core samples from borehole MD12, in accordance with ASTM D2850 standards. Each 2-inch (50 mm) diameter, 4.5-inch (114 mm) high cylindrical sample was tested at its natural moisture content. The testing was all strain-controlled, with an axial deformation rate of 0.40 in/hr (10 mm/hr). Each test was carried beyond the point of peak deviator stress and to an axial strain of at least 5%.

5.3.6. Analysis of Collapse Potential

The procedure followed in determining the collapse potential of near-surface soils at the Maricopa Site is described in detail by Nowatzki (1980) and is referred to as the "one-dimensional pseudo-consolidation test." The test is called a pseudo-consolidation test because the sample in the oedometer is not saturated prior to load application, as is the case in a conventional consolidation test. Instead, a series of tests is performed in which undisturbed samples, approximately two inches in diameter and one inch thick, are placed at in-situ moisture content in an oedometer. Following application of a 200 psf seating load, each sample is loaded in a sequence of vertical stress increments until a predetermined maximum stress is reached. The applied stress increments generally double the magnitude of the existing stress.

Following application of a given stress increment, displacement readings are taken periodically (usually 15 minutes apart for the first hour and then once every hour) until the difference between two successive readings is less than 0.001 inches. When the vertical stress on the sample has been incremented to a level approximately equal to the anticipated allowable foundation pressure, the sample is saturated while still under load, and displacement readings are taken in the same manner as described above. The anticipated allowable foundation pressure is predetermined on the basis of design loads, the foundation soil's strength properties, and the type and size of foundation system that is most economical.

In general, the pseudo-consolidation test as described above can be completed within 24 hours. The results are usually reported in terms of total applied stress and percent compression (strain). Since anticipated foundation pressures were not known at the time of testing, the following general loading sequences were used in this study:

1. 200 psf, 1200 psf, saturation
2. 200 psf, 2400 psf, saturation
3. 200 psf, 1200 psf, 2400 psf, saturation
4. 200 psf, 12100 psf, 2400 psf, 4800 psf, saturation

5. 500 psf, 1000 psf, 2000 psf, 4000 psf, 16000 psf
32000 psf, 4000 psf, 32000 psf, saturation

5.4 Hydrology

The Maricopa Site touches portions of the Vekol Valley, Waterman Wash, and Bosque geohydrological basins. These are structural depressions surrounded by mountains that are composed of intrusive rocks, mostly granite, with small areas of metamorphic and sedimentary rocks. Dense, impermeable bedrock forms the mountains that bound the valley floors. Pediment areas, in which the bedrock is at a shallow depth, extend valleyward for varying distances from the base of the mountains. The central portions of the valley are underlain by great thicknesses of basin-fill sediments. The basins are filled with alluvial fan and alluvial plain deposits consisting of lenticular beds of poorly sorted gravel, sand, silt, and clay. These deposits generally exhibit some degree of calcium carbonate cementation.

Hydrologically, the most important aspect of the geologic setting around the site is the distribution of the bedrock and other impermeable materials and the more permeable basin-fill sediments. No interaction is expected between the construction of the SSC and the water table. In general, the site is underlain by unconfined aquifer systems. Permeabilities in the alluvial aquifers, as is expected in alluvial fan materials, are very site-specific.

Because of the lack of prior development in the area of the site, ground water elevation data are sparse along and within the tunnel alignment. As a result, the ground water table has been estimated over much of the site by using linear interpolation and extrapolation techniques combined with geologic and hydrologic knowledge of the area. The site's simple geology combined with experience from similar basins and the available data suggest that the aquifers have a predictable and consistent water-table gradient in areas of little or no pumping. High confidence in the estimated values along with the site's overall great depth to water in relation to the tunnel elevation strengthens the statement that no part of the tunnel will be in saturated material. The depth to water appears to be 300 feet or greater around the entire site.

One reason the Maricopa Site is an excellent site for the SSC is that water-related construction problems are extremely unlikely. Water-table elevations are expected to be well below the proposed tunnel elevations. The only potential for inflows, therefore, is from perched water or from temporary seasonal pulses of recharge from the normally dry stream channels. Perched water has not been found nor is it expected to be found in the site area. The proposed Maricopa tunnel alignment intersects only two large watercourses, Bender Wash (twice) and the West Prong of Waterman Wash. At these locations the depth of the tunnel suggests that no problems will be encountered.

5.5. Findings

5.5.1. Results of Drilling

Thirteen new test borings were conducted as part of the most recent geotechnical investigations. The actual field boring logs are contained, for reference, in Appendix A of the report by Nowatzki et.al., (1988). The borings were taken to a depth of up to 200 feet. A wide range of materials was encountered, ranging from boulders and cobbles, to clayey gravels (GC soils, according to the Unified Soil Classification System), to well- and poorly-graded sands, silty sands, and clayey sands (SW, SP, SM, and SC soils), to silts, sandy silts, clays, and sandy clays of low plasticity (ML and CL soils). No silts or clays of high plasticity were encountered. In all, standard penetration testing was done at boreholes MA1, MA3, MA3A, MA4, MA6, MA10, MA11, MA12, and MA13 and all blow count information is contained on the respective boring logs.

Variation in density of soils, as revealed through SPT blow counts (N), is summarized in Table 9 for drilling done during the summer of 1987. The empirical relations of Gibbs and Holtz (1957) are used to relate N to relative density (DR). Peck, et.al. (1953) give relationships between N and the coefficient of friction. For unsaturated, arid-region alluvial soils, particularly where gravel or cobbles may be present, these relationships should be used with caution.

Nonetheless, the data in Table 9 can be used with confidence to conclude that the alluvial soils and fanglomerates in the areas where boreholes were drilled are generally of high strength, and that some zones may be stronger than others.

These conclusions are supported in the literature. Beckwith and Hansen (1982) use SPT blow count as a guide to the classification of calcareous soils such as fanglomerates. They found that a blow count of 60 to 200 indicates a very strongly cemented material with essentially the properties of a soft rock. A blow count greater than 200 indicates a moderately hard rock.

In the field, SPTs were terminated if more than 50 blows were needed to penetrate 6 inches. Effectively this means that blow counts in excess of 100 were not specifically monitored. The blow count data in Table 4 have been normalized to a 1-ft basis. It can be seen that, with few exceptions, the blow counts in the deeper portions of the holes will be significantly in excess of 200 per foot.

Beckwith and Hansen (1982) relate N values to deformation modulus based on pressuremeter tests, and show that a blow count of 200 blows/ft is equivalent to a deformation modulus of at least 4,000 ksf or 30 ksi. In the previous section it was shown that seismic velocities of fanglomerates having high blow counts of this type are at least 3,000 ft/sec.

Table 9 - Summary of SPT Blow Count Data, Stage I Drilling (1987)

Depth (ft)	MA1		MA3		MA4		MA6	
	Pen. (in)	B/ft	Pen. (in)	B/ft	Pen. (in)	B/ft	Pen. (in)	B/ft
0	12	7	12	13	12	6	12	11
5	12	23	12	49	12	11	5	120
10	12	74	12	82	5	26-65-120	4	150
15	5	55-120	12	93	5	120	6	100
20	12	88	4	138-150	5	74-101-120	3	200
25	12	78	12	54	5	12	1 1/2	400
30	4	129-150	12	62	5	120	5	120
35	6	100	4	126-150	4	150	4	150
40	4	135-150	5 1/2	109	4	93-150	5	120
45	4	150	5 1/2	109	4	99-150	3	200
50	2	222-300	5 1/2	109	4	150	5	120
55	2 1/2	240	5	120	12	62	5	120
60	5	120	5	120	5	29-70-120	5	120
65	3	200	3	200	5	38-62-120	5 1/2	109
70	3	200			4	75-150	5	120
75	3	200			5 1/2	52-109		
80					5 1/2	109		
85					5	120		
90					5	84-120		
95					5	120		
100					6	100		

*P - Total penetration achieved

B - Equivalent number of blows required to penetrate 1 ft.

5.5.2. In-Place Testing Results

Field Slope Testing

Disturbed and undisturbed test specimens exhibit nearly identical internal friction angles, provided that the specimens possess similar void ratios. Hence, the friction angle of the basin fill in its natural state may be fixed at $\phi = 32$ -- the value that was measured by direct shear laboratory testing on intact samples extracted from borehole MA12 (Nowatzki, et. al., 1988).

A slope failure is associated with a safety factor of $F = 1$. Since the applied surface surcharge, failure surface geometry, and in situ unit weight were measured for each of the ten individual field slope tests, the cohesive component of shear strength becomes the only relevant unknown. Stability analyses of the slopes may therefore be used to back-calculate the basin fill's undisturbed cohesion c . The relatively small loaded surface area led to the development of a roughly wedge-shaped slip surface (Figure 26). Conventional two-dimensional plane strain slope stability procedures, such as Bishop's Modified Method (Bishop, 1955), Janbu's Method (Janbu, 1973), or the Morgenstern-Price Method (Morgenstern and Price, 1965), would overestimate the cohesion associated with a given safety factor. The method of Hovland (1977), on the other hand, accounts for the "end-effects" associated with a truly three-dimensional failure surface, and this procedure was therefore used to analyze the field test data.

The cohesion c is calculated from the equation (Hovland, 1977):

$$C = \left[\frac{\gamma b' \sin i}{3B} \right] \left[F3 - \frac{\tan \phi}{B \tan i} \right]$$

where:

$$B = \left[\left[\frac{2b' \sin i}{w} \right]^2 + 1 \right]^{1/2}$$

ϕ = internal friction angle = 32°

i = angle of inclination of the slip surface (measured)

b' = maximum depth of the failure surface perpendicular to the crest of the slope (measured)

w = maximum length of the failure surface parallel to the crest of the slope (measured)

γ = equivalent unit weight (which accounts for the unit weight of the soil plus the applied surface surcharge)

$F3$ = the three-dimensional safety factor = 1 (at failure)

A complete record of the field slope testing is included in Appendix B of Nowatzki, et. al., (1988). An example of the back-calculation procedure is also provided there. The cohesion values associated with the various tests are presented in Table 10. As may be observed, the cohesion values for the uppermost five feet of soil (Tests #1-#5) are significantly lower

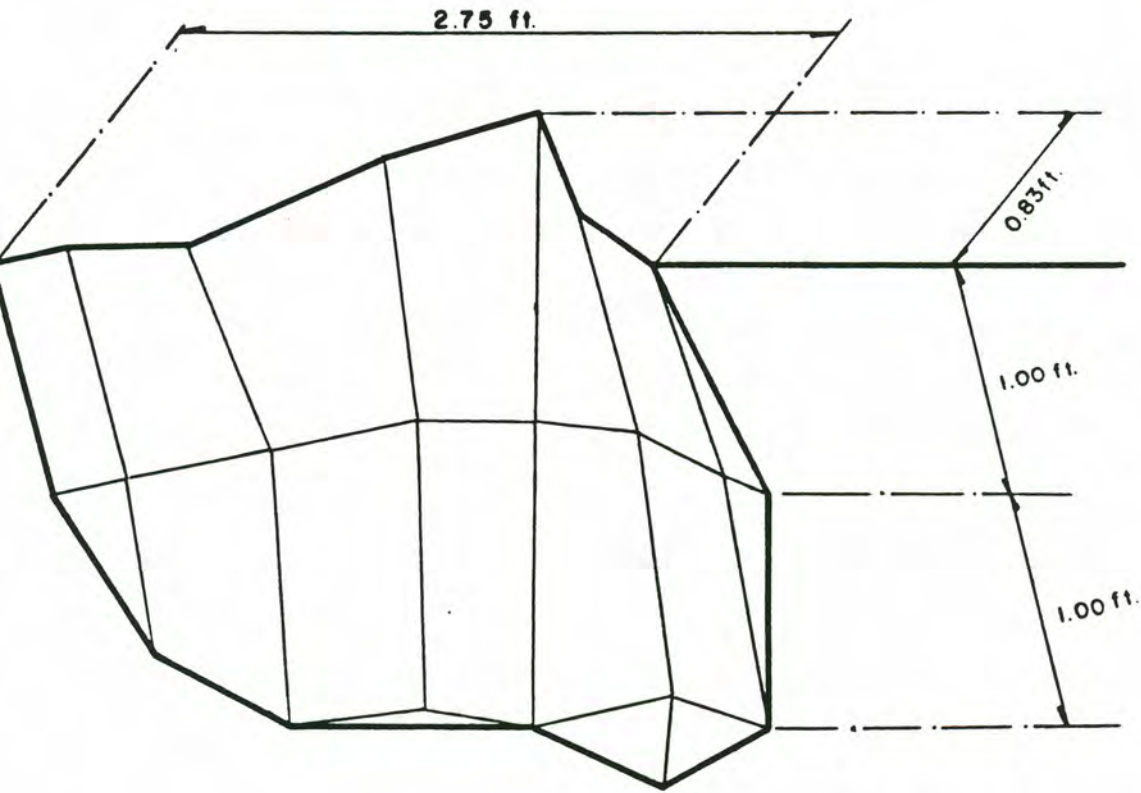


Figure 26.
A Typical Field Slope Failure Surface Geometry

Table 10 - Values of Cohesion as Back-Calculated
from Field Slope Testing

<u>Test #</u>	<u>Bench</u>	<u>Cohesion (in psf)</u>
1	Upper	--
2	Upper	1393
3	Upper	1203
4	Upper	738
5	Upper	469
6	Lower	--
7	Lower	2619
8	Lower	2657
9	Lower	--
10	Lower	2007
Average Cohesion For Upper-Bench Failures		950
Average Cohesion For Lower-Bench Failures		2430

than the values corresponding to failure surfaces within the five-to ten-foot depth range (Tests #6-#10). These results should be expected, since normal exposure and weathering reduces the cohesive particle bonding in the uppermost few feet of material. The value of $c = 2430$ psf, which is the average value for the lower-bench failures (Tests #6-#10), may therefore be regarded as a conservative lower estimate of the undisturbed cohesion of the basin fill material.

Pressuremeter Testing

Detailed data on pressuremeter testing may be found in Sergent, Hauskins, and Beckwith, 1988, in Appendix B. Figure 27 shows the strength values obtained from pressuremeter tests.

Dilatometer Testing

Useful data were obtained in MR1 at four depths: 15 ft, 48 ft, 77 ft, and 140 ft. All these positions are above the water table. A typical data printout is given in Figure 28. This shows a steep curve, terminating in a yield pressure, followed by fracture and continued expansion at an increasing rate. Data can be calculated using the following equations developed by Menard (1975) and others (See Hunt, 1984):

$$C_u = \frac{PL - P_0}{2K_b}$$

$$E_c = K \frac{dP}{dL}$$

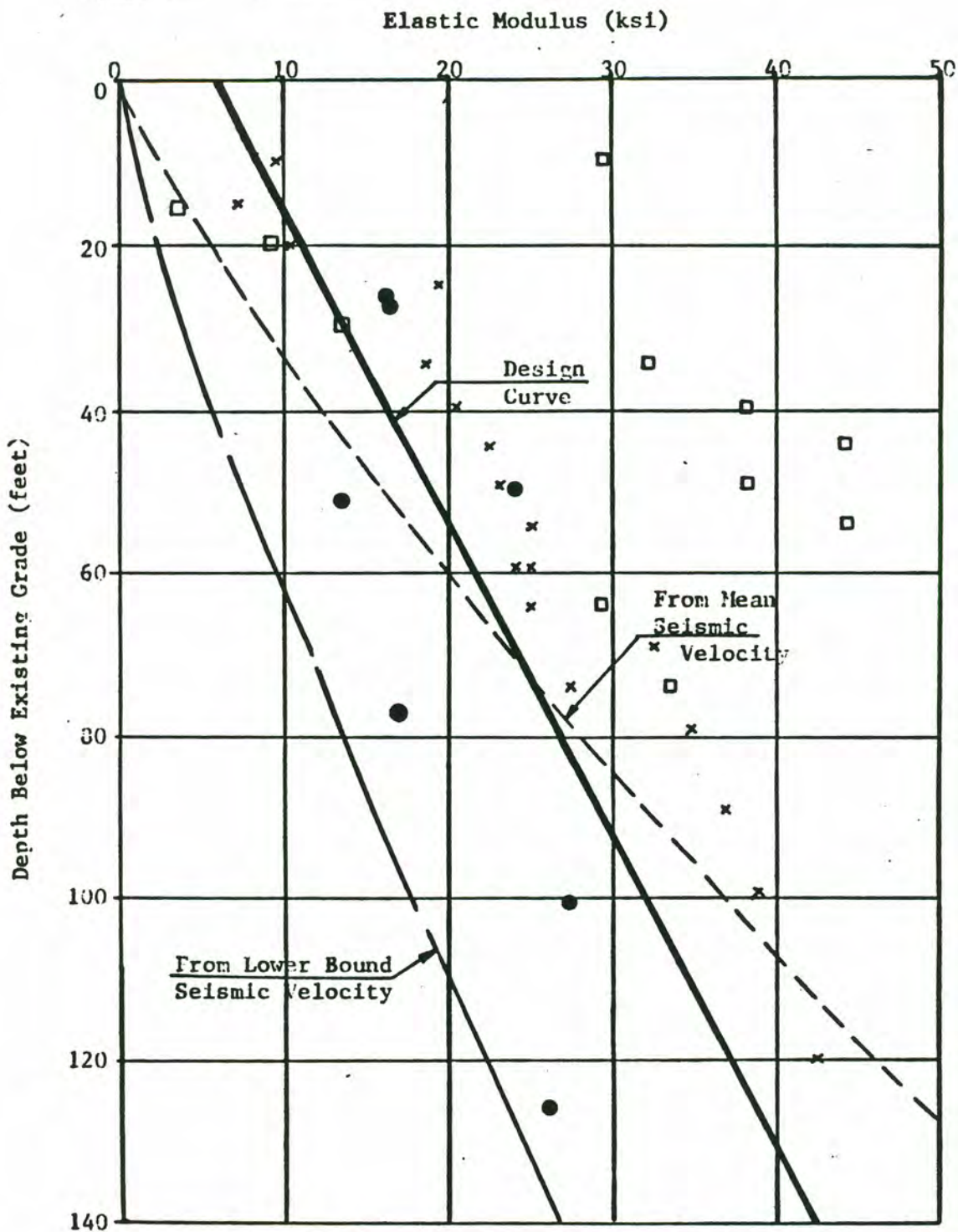
where:

- E_c, C_u = compression modulus and undrained cohesion
- dP/dL = slope of the pre-failure curve
- $K = 2(1 + \nu)Db$ is a constant relating Poisson's ratio and expanded borehole diameter
- PL, P_0 = the yield and initial borehole pressure
- K_b = is a constant varying with E_c/PL and typically equal to 5.5

Calculated values of C_u, E_c are given in Table 11, together with values of σ_{cf} (compressive strength) estimated at $2C_u$.

5.5.3. Laboratory Testing Results

Some unconfined compression tests on specimens obtained from the CME rig yielded strengths of $q_u = 2520$ psf and $q_u = 2180$ psf. Such anomalously low values are attributed to sample disturbance and the probable creation of microfractures within the specimens. These values yield a conservative value of cohesion $c = 1200$ psf (DeNatale et. al., 1987). Later discussions will describe how these data have been improved.



- - Pressuremeter Tests
- × - SPT-N Values Conversion (Seed and Others, 1984)
- - SPT-N Values (Beckwith and Hansen, 1981)

Figure 27. Results of Pressuremeter Testing (from Sergent, Hauskins, and Beckwith, 1988, Appendix B)

DILATOMETER TESTING — S.S.C. PROJECT

MARICOPA SITE BH=MR1 DEPTH=77ft

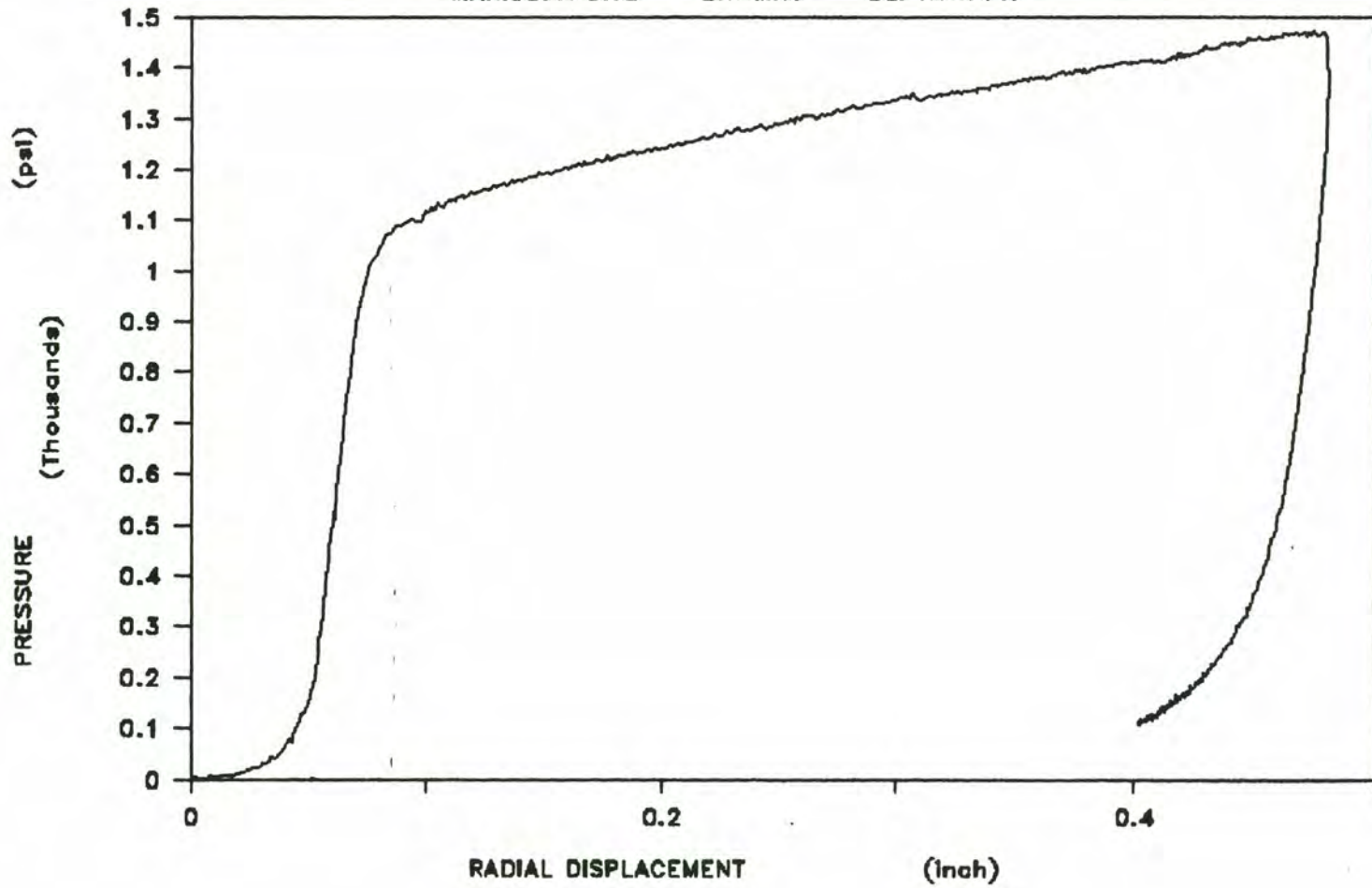


Figure 28. Typical Pressure-Displacement Curve for Dilatometer Testing

Table 11 - Fanglomerate Material Properties from Dilatometer Testing

Depth	Yield Pressure	Shear Strength psi	Comp Strength psi
15 ft	625	55.7	11
48 ft	610	51.7	103
77 ft	870	73.0	146
140 ft	4740	420.0	840

The data obtained from the laboratory sieve and Atterberg Limits analyses, and the direct shear, triaxial, and consolidation testing may be found in Appendix C of Nowatzki, et.al. (1988). The results of the sieve and Atterberg Limits analyses are summarized in Table 12, and the results of the strength testing program are summarized in Table 13.

The results of the pseudo-consolidation tests are summarized in Table 14 and shown graphically in Figure 29. Jennings and Knight (1975) regard the strain occurring at a saturation stress of 4000 psf as an index of collapse called the "Collapse Potential". They define the following critical values for the Collapse Potential (CP):

<u>CP %</u>	<u>Severity</u>
0-1	No problems
1-5	Moderate problems
5-10	Problems
10-20	Severe problems
>20	Very severe problems

As can be seen from Table 14 and Figure 29, the data obtained from pseudo-consolidation tests performed on soils from the Maricopa Site suggest a Collapse Potential of approximately 9%. This indicates that there is a potential for settlement problems as a result of collapse. However, the field samples were not retrieved directly into oedometer rings, as is usually the case. Thus, pseudo-consolidation test specimens had to be prepared in the laboratory by extruding them from the field sampler into the oedometer rings. This dual handling procedure undoubtedly resulted in sample disturbances which caused the specimens to have greater values of CP than conventional "undisturbed" samples would have had. For this reason, the severity of the collapse problem is expected to be less than that suggested by the laboratory test data.

This interpretation is consistent with the evaluation of collapse susceptibility made on the basis of the Gibbs criterion as shown in Figure 30. Therefore, methods typically recommended by geotechnical engineering consultants in Arizona for stabilizing such soils (e.g. excavation and recompaction under controlled conditions) are expected to be effective for collapse susceptible soils at the Maricopa site.

The pseudo-consolidation tests in this study were performed on samples retrieved from depths of from 30 to 60 feet. Ali (1987) has shown that the probability of encountering collapse susceptible soils decreases with depth. Therefore, soils exhibiting a high degree of collapse potential are not expected to occur below a depth of about 30 feet, and probably more shallow. Since the potential for collapse settlement is such an important consideration in the design of foundations for surface structures, and since the results of laboratory pseudo-consolidation tests are susceptible to sample disturbance, full scale field tests should be performed at the site of the main campus to verify the existence of collapse-susceptible soils and determine their severity with depth.

Table 12 - Results of Laboratory Sieve and Atterberg Limits Analysis

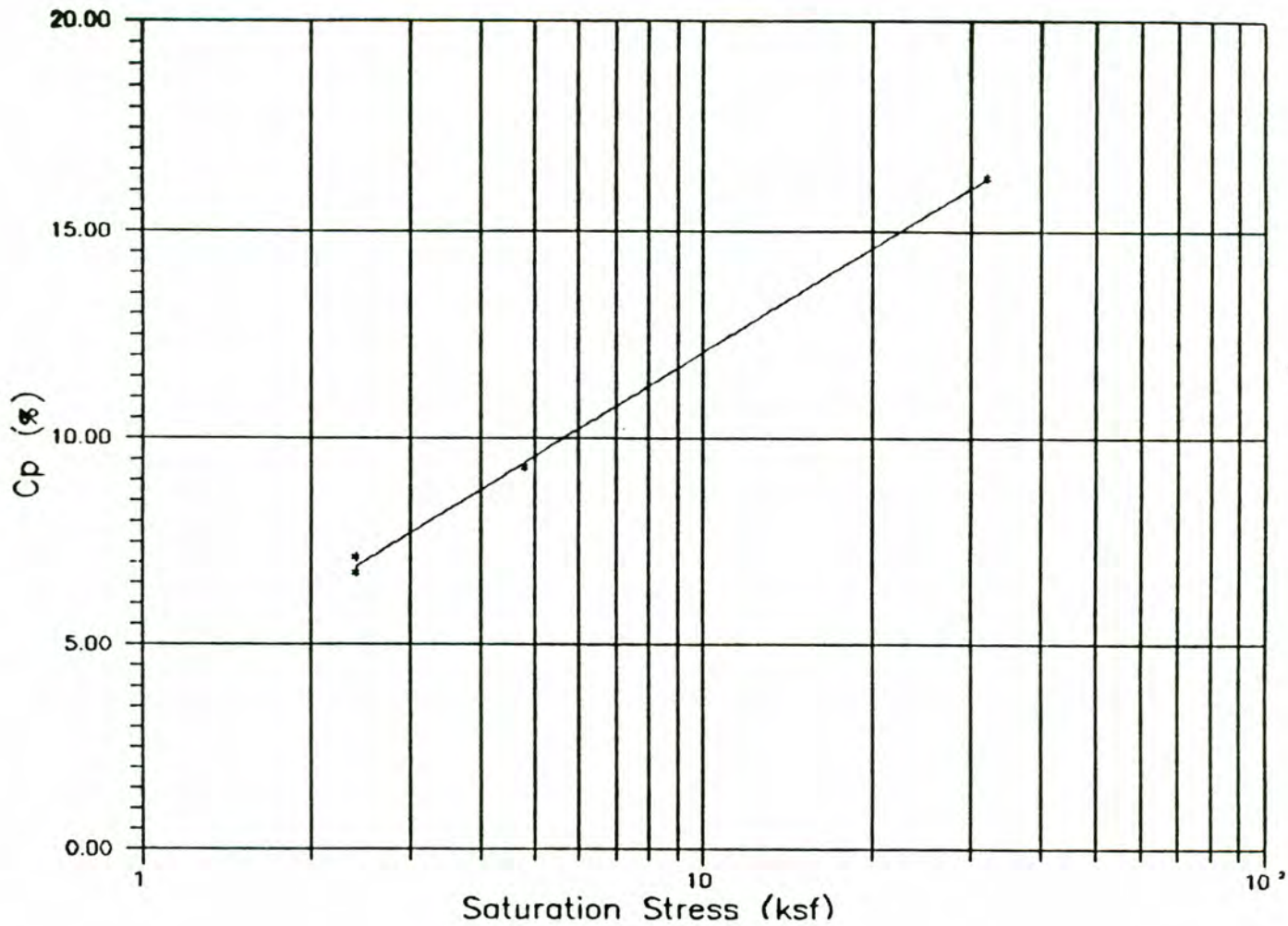
<u>Borehole</u>	<u>Depth (ft)</u>	<u>% < #200 Sieve</u>	<u>Moisture Content</u>	<u>Atterberg Limits</u>		
				<u>LL</u>	<u>PL</u>	<u>PI</u>
MA10	0.5 - 2.0	29	3.4			
	3.5 - 5.0	26		21	20	1
	8.5 - 9.0	14	4.3			
	13.5 - 13.9	17				
	19.5 - 23.5	24				
	30.0 - 30.5	13		23	19	4
	40.0 - 40.3	19				
	55.0 - 55.4	22				
	60.0 - 60.5		5.7			
	65.0 - 65.4	30				
	68.5 - 73.0	7				
	80.0 - 80.2	35				
	85.0 - 85.4		7.0			
90.0 - 90.4	37					
MA11	0.5 - 2.0	31	3.8			
	10.0 - 10.4	14	6.7			
	20.0 - 20.3	35	6.2			
	30.0 - 31.5	14	4.2	19	18	1
	40.0 - 40.3	23	5.5			
	55.0 - 55.2	21	6.4			
	65.0 - 65.5	19	3.4			
	73.5 - 73.8	11	6.3			
MD12	0.5 - 2.0	12	2.0	22	9	13
	15.0 - 15.7	22	7.1			
	25.0 - 25.8	38	7.6			
	30.0 - 32.8			38		
	33.5 - 34.9	16	3.7			
	48.5 - 48.9	41	7.4			
	53.5 - 54.2	34	8.0			
	61.0 - 62.0	27	7.1	37		
	68.5 - 69.1	38	12.6			
	73.5 - 73.9	28	9.2			
MR1	5 - 10	10	2.4	28	19	9
	15 - 20	13	7.4	44	22	22
	25 - 30	22	2.4	26	22	4
	35 - 40	14	4.3	31	17	14
	45 - 50	14	3.1			
	55 - 60	5	4.0			
	65 - 70	6	4.9			
	75 - 80	11	4.8			
MR2	5 - 10	11	6.2	54	50	4
	15 - 20	21	4.3	32	22	10
	25 - 30	4	2.9	35	27	8
	35 - 40	17	3.6	37	20	17
	45 - 50	17	0.9			
	55 - 60	19	2.5			
	65 - 70	19	3.6			
	75 - 80	13	2.8			

Table 13 - Results of Laboratory Strength Testing

<u>Source of Specimens</u>	<u>Type of Material</u>	<u>Laboratory Test</u>	<u>Cohesion c (psf)</u>	<u>Friction Angle ϕ</u>
MA12	Basin Fill	Direct Shear	2160	32
MD12	Fanglomerate	Direct Shear	9000	27
MD12	Fanglomerate	Triaxial	11400	26
MD12	Fanglomerate	Triaxial	2000	39

Table 14 - Results of Pseudo-Consolidation Testing for MA12

<u>Sample Depth</u>	<u>Applied Stress (psf)</u>	<u>Strain (%)</u>
30'3" - 32'9"	1200	2.38
	1200 S	11.59
		Cp = 9.21
30'3" - 32'9"	2400	5.87
	2400 S	Cp = 7.14
30'3" - 32'9"	1200	1.85
	2400	4.70
	2400 S	11.45
		Cp = 6.75
30'3" - 32'9"	1200	1.78
	2400	4.38
	4800	7.36
	4800 S	16.68
		Cp = 9.32
61'0" - 63'6"	500	0.50
	1000	1.42
	2000	2.61
	4000	3.49
	8000	4.91
	16000	6.89
	32000	8.44
	4000	7.20
	32000	8.68
	32000 S	25.00
		Cp = 16.32



Collapse Strain (%) versus Saturation Stress (ksf)
 Maricopa SSC Site - Borehole MA-12
 Collapse Potential = Collapse Strain at Saturation
 Stress = 4 ksf (Jennings & Knight, 1979)

Figure 29. Collapse Potential, MA12

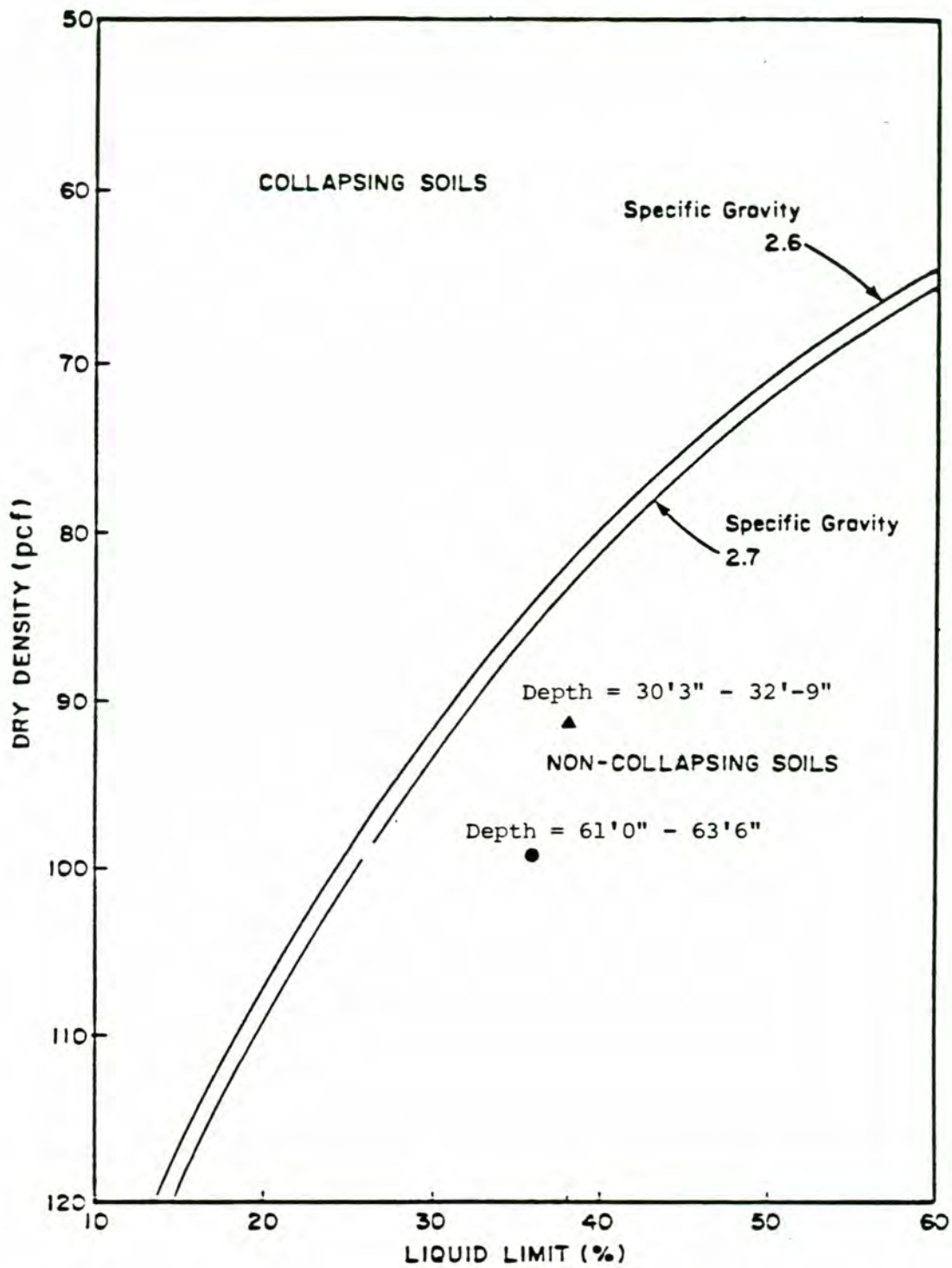


Figure 30.

Collapse-Susceptibility Diagram (After Gibbs, 1961)
 Maricopa SSC Site - Borehole MA-12

5.5.4. Comparability of Fanglomerate Strength Data

Lab Data Versus Field Slope Data

Direct shear testing was performed on intact specimens of basin fill material extracted from borehole MA12 at depths of 30 to 65 feet. As mentioned previously in Section 5.3., this direct shear testing yielded minimum shear strength parameters of $\phi = 32$ and $c = 2160$ psf. By comparison, the field slope testing on the unweathered lower bench (involving material at depths of 5 to 10 feet) yielded an average cohesion of $c = 2430$ psf. As a consequence of sampling-induced disturbance, the laboratory specimens should be expected to have a cohesion which is lower than that for the material in its natural (undisturbed) state. Samples at greater depth should, in principle, be stronger. Therefore it appears as though the process of sampling reduces the material's cohesion by at least 10%.

The results of the laboratory and field testing are broadly consistent, however, and minimum strength parameters of $\phi = 32$ and $c = 2430$ psf may be assigned, with confidence, to the cemented basin fill material. From Mohr circle geometry, one can derive an unconfined compressive strength of near 60 psi for these cohesion and friction angle values. These may be considered to represent values within the range of those for the younger fanglomerate.

By contrast, cohesions from confined compression tests on intact core (MD12) probably representing an older fanglomerate than that above were in excess of 11,000 psf, with a friction angle of 26 degrees. This would be equivalent to an unconfined strength of around 250 psi.

Lab Data Versus Dilatometer Data

The dilatometer testing indicated compressive strengths (Table 11) ranging from 11 to 840 psi, with strength increasing steadily with depth. These values bracket the laboratory strength data given above. There are no blow counts or other data that can be used to develop a laboratory strength profile for MR1 to develop a more exact comparison.

5.5.5. Seismic Refraction Interpretation

Figure 18 in Section 4.4.4, and the accompanying discussion, provide a site-wide interpretation of the refraction data focusing on the hard rock responses. Figure 18 also plots the depth to the lower contacts of each fanglomerate stratum indicated in the seismic data against the interpreted seismic velocity.

Material with a seismic velocity of less than 2,000 ft/sec was typically found in near-surface layers (thicknesses of 10 ft). A subset with velocities less than 1,000 ft/sec represents a veneer of loose material. Velocities less than 2,000 ft/sec were not found at depths of greater than 40 ft. This represents poorly-consolidated to lightly-consolidated, surficial alluvium. Also cropping out at the surface at places, or occur-

ring under a shallowly-buried upper surface at other places, is a group of lightly-cemented, indurated alluvial deposits or fanglomerates with a nearly-continuous spectrum of seismic velocities in the range of 2,000 to 4,500 ft/sec. In addition to being much more competent than most of the near-surface material with lower velocities, this younger fanglomerate also tends to be thicker and extend deeper than the near-surface material. Material in this range with velocities less than about 3,000 ft/sec is much less common below 100 ft depth, than is the material greater than about 3,000 ft/sec.

At a few places, seismic profiling revealed layers with velocities in the 4,500 to 6,800 ft/sec range. These tend to be buried and to be underlain by higher-velocity materials, suggesting that they represent either weathered variants of the stronger rock beneath, or dense, rock-like fanglomerate (older fanglomerate) that has not been transported very far.

In general, the resistivity data confirmed the seismic interpretation. At the sites in Section 32 (approximately 3 miles northeast of Estrella), however, the interpreted depths to boundaries based on the resistivity data are 50 percent too high. The discrepancy is most likely due to vertical anisotropy, arising from large amounts of clay that were reported during drilling in the area. At all other sites there is good agreement between the resistivity and seismic interpretations.

The gravity data are discussed in detail in Sternberg and Sutter (1988). The plots of gravity data around the ring in that report indicate the location and relative depth of the alluvium. Some of the data from that report were modelled to provide quantitative estimates for thickness of alluvium and the results are reported in Bryan, et. al., (1987). The reader is referred to these two reports for detailed plots showing interpreted changes in thickness of alluvium.

5.5.6. Comparison of Fanglomerate Strength and Seismic Response

SPT Blow-Count Data Versus Seismic Survey Data

A comparison is made between elastic moduli determined from SPT blow counts obtained from boreholes on or near the ring alignment with modulus values computed from velocity data obtained from seismic surveys performed at or in the vicinity of the borehole locations. The seismic data were correlated to modulus by the elastic relationship introduced in 4.4.4.2. For the materials at the Maricopa site the following values of the material parameters were found to be appropriate:

$$\begin{aligned}\nu &= 0.33 \\ \gamma &= 125 \text{ pcf}\end{aligned}$$

These values were used with $g = 32.2\text{ft/sec/sec}$ along with seismic layer velocities to estimate the modulus.

relationship developed for sands and gravels by Wrench and Nowatzki (1987):
0.888

$$E(\text{tsf}) = 22.2 N$$

Table 15 shows that, although the moduli do not appear to correlate very well numerically at shallow depths, there is consistency between the results regarding an increase in modulus with depth. Both sets of data suggest that the material within approximately 20 ft of the surface has a much lower modulus than the alluvial fanglomerate below that depth. At shallow depths the modulus is generally less than 1,000 tsf, whereas at depths greater than approximately 20 ft the modulus is generally greater than 3,000 tsf and in some locations greater than 7,000 tsf. This agrees with results reported elsewhere (see, for example, DeNatale, et. al., 1987, and Sergent, Hauskins, and Beckwith, 1988).

It should be noted that seismic data give an integrated value for velocity and modulus over a range of depths, whereas blow counts are taken at specific depths. With the seismic data, discrete changes in strata density are recorded by discrete changes in compression wave velocity. SPT blow counts, on the other hand, are non-integrative and pertain only to the depth from which they are taken. It is probable that local variations in strata competence affect blow count data differently than they do the seismic response. It would not be correct to average blow counts over a range of depths and use the average value as representative of the stratum.

In addition, for this study, the blow counts were recorded for three 6-in. increments with the reported N-value being the sum of the blows over the last two 6-in. increments. If the full 6-in. penetration was not reached after 50 hammer blows in any one increment, the test was discontinued, and the count was recorded as 50 blows for the actual penetration that was achieved. In these cases, the blow count was increased linearly to the full 6-in. penetration, so that a blow count value could be computed for use in the equation above. This extrapolation can significantly underestimate the penetration that would have occurred had the test been continued. Therefore, the moduli reported in Table 15 for depths greater than 10-20 ft represent lower limits of the in situ moduli that can be expected.

In all cases, data were used from the seismic survey closest to the borehole from which SPT data were obtained.

Dilatometer Data Versus Seismic Strength Prediction

In the first part of Section 5.5.4, Figure 20 is introduced, which contains a comparison of seismic velocity and strength as determined by the dilatometer. The results suggest a parabolic relationship, as would be expected. Although there is too much uncertainty in the method to define a numerical correlation, it is clear that seismic velocity does respond systematically to measurable variations in in situ strength.

5.5.7. Forecast of Fanglomerate Tunnelling Characteristics

Table 15- COMPARISON OF ELASTIC MODULI OBTAINED FROM SPT BLOW COUNTS
 WITH MODULI OBTAINED FROM SEISMIC SURVEYS.
 From Nowatzki, et. al., (1988)

<u>Boring</u>	<u>SPT Blow Count Data</u>		<u>Seismic Survey Data</u>	
	<u>Depth (ft)</u>	<u>Maximum Modulus (tsf)</u>	<u>Depth (ft)</u>	<u>Modulus (tsf)</u>
MA-1	0 - 11 11 - 75	< 500 >4000	0 - 57	5694
MA-3	0 - 11 11 - 60	<1000 >4000	0 - 6 6 -300	838 20522
MA-4	0 - 11 11 -100	< 500 >3000	0 - 5 5 - 36 36 -509	1500 23784 78357
MA-6	0 - 5 5 - 70	< 500 >5000	0 - 15 15 -260	2046 24481
MA-10	0 - 9 9 - 65 65 -150	< 500 >3000 >7000	0 - 44 44 -106 106 -319	5909 16379 56202
MA-11	0 - 20	<1000	0 - 8	258
MA-11	20 - 40 40 - 74	>3000 >7000	8 - 29 29 -221	7470 14798
MA-12	0 - 10	< 500	0 - 9	247
MA-12	10 - 74	>4000	9 -130	10926
MA-13	0 - 22 22 - 75	<2000 >5000	0 - 97 97 -161	327 16583

5.5.7.1. Open Cut Construction - Stability Analyses For 90 Degree, 60 Degree, and 45 Degree Slopes

The primary component of the SSC project is the 52-mile long collider ring that will be housed in a 10-foot diameter concrete tunnel placed 30 feet or more below the ground surface. The most economical way to construct an underground tunnel of this type in Arizona is by the cut-and-cover method. In this approach, a tunnel is formed by excavating downward from the ground surface. Precast cylindrical concrete tunnel segments are placed in the open trench with cranes, and the trench is then backfilled with the excavated soil. At the Maricopa site, about half of the underground accelerator ring can be placed by the cut-and-cover method. Since the amount of material to be excavated decreases as the sides of the excavation become more steep, the cut-and-cover method becomes most economical when an unsupported vertical excavation profile can be used.

Table 16 presents a summary of safety factors for heights of up to 100 feet and slope angles of 45, 60, and 90 degrees. It should be pointed out that vertical slope faces are actually preferable to inclined ones, since vertical faces are less susceptible to weakening due to water infiltration in the event that precipitation occurs before the excavation has been backfilled.

Cut-and-fill will be used extensively at the Maricopa site. The geotechnical properties of the fanglomerate and the great depth to ground water permit safe and efficient uses of this technique. The flexibility to use cut-and-fill methods guarantees low cost, high advance rates, and reliable construction.

Cut-and-fill is the best construction method for CUs 2 and 7, and the injector complex, in cuts less than 80 ft deep. Stacking the injector components can further reduce the depth of cut and improve construction efficiency. The LINAC would be constructed at the surface.

The tunnel itself would use either precast cylindrical concrete tunnel segments or cast-in-place segments. The cut-and-fill method becomes more cost-effective as sideslopes become steeper because smaller volumes of material are handled. The feasible depth for cut-and-fill depends on equipment performance, material handling costs, and safety. Recent improvements in equipment, coupled with the strength and stability of the fanglomerate, suggest that excavation depths up to 80 ft are practical and safe.

A conservative depth cut-off of 60 ft with a 60 degree average slope angle was used for all cost and schedule estimates. Additional reductions in time and costs, using a cut-off depth of 80 feet, are possible. Approximately twelve miles of the ring alignment is amenable to construction by this method, using a 60-foot cut-off and 60 degree slope angle.

Several mass excavation systems are available for digging a trench in the fanglomerate, as follows.

Scrapers. The mining industry has long used large volume scrapers for excavation in open-pit operations. Scrapers were used to remove the

Table 16 - Safety Factors as a Function of Slope Height and Slope Angle

Slope Height (feet)	-----Safety Factor Values-----		
	Slope Angle of 45 degrees	Slope Angle of 60 degrees	Slope Angle of 90 degrees
40	4.05	3.35	2.17
50	3.47	2.87	1.81
60	3.08	2.53	1.57
70	2.80	2.28	1.40
80	2.59	2.09	1.27
90	2.41	1.94	1.17
100	2.29	1.82	1.09

fanglomerate from the Twin Buttes and Sacaton Mines, and were also used on the CAP canal. Major portions of all three projects were excavated in fanglomerate that had geotechnical properties similar to those present at the Maricopa Site.

Holland Loader The Holland Loader is essentially a modified scraper. For example, the Holland 700 Loader used on the Red Rock section of the CAP northwest of Tucson consisted of a bottom-cutting loader propelled by two large Caterpillar D10 tractors placed in tandem. A large diesel engine mounted on the loader frame drove a belt conveyor which was also supported by the frame. For the 45 degree side slopes of the CAP canal, a bridge conveyor was suspended between the rear tractor and a third tractor at the top of the excavation. When weathered or fractured rock was encountered, a ripper tooth, mounted on the front tractor, allowed the Holland Loader to excavate materials that would have been impossible for conventional scrapers to handle. (Production levels using this system reached 3,400 tons/hour in fanglomerate similar to that found at the Maricopa Site.) The modified Holland Loader used on the Red Rock section of the CAP proved so effective that the most recent section of the CAP was bid and won on the basis of projected production rates of 7,800 tons/hour (Cockran, 1987).

For steeper cuts the top of the bridge conveyor could be supported over the open cut at the end of a short stacker conveyor. With this system even vertical cuts could be made by adapting conventional conveyor systems to the Holland Loader. Another adaptation that has been proposed for steeper cuts in open-pit mines is to use the loader's feeder belt to load a sandwich belt high-angle conveyor system. Such systems allow shorter conveyor length and permit muck removal from excavations having steeper slopes, both of which result in construction savings. This system seems ideally suited for the 60 degree slopes proposed for the Maricopa SSC cut-and-fill construction segments.

The Arizona SSC Project prepared a contractor's estimate to document the cost and scheduling benefits that could be realized by using the Holland Loader for cut-and-fill sections of the ring (State of Arizona, 1987). It was assumed that a Holland Loader would make successive passes along the trench line and dig a 20-foot wide trench graded to an angle of 60 degrees. Muck spoils will be conveyed to one side of the excavation over the rear loader. Tunnel sections will be cast in place, and liner construction will proceed at a rate of 300 feet per day.

A small rotary separator will sort the excavated materials for select backfill that will be tamped into place around the tunnel sections with a sheepsfoot roller at 2,000 cu yd/hr. The Holland Loader will replace regular backfill at a rate of 6,000 cu yd/hr. Leftover materials will be spread over the disturbed area, contoured by a grader, and reclaimed by hydroseeding.

The State of Arizona's site proposal also describes a continuously-excavating, cast-in-place pipe laying system that was demonstrated in Arizona for a Defense Department project (State of Arizona, 1987, vol. 3, p. 75). This system placed nearly 700 ft of 14.3-ft (i.d.) pipe (wall thickness 8 in.) in eight hours.

5.5.7.2. Soft-Ground Tunnelling

Construction Units to be crossed by tunnels in fanglomerate at greater depth than the assumed cutoff are designated as soft-ground TBM segments.

There is ample field evidence for assuming that the TBM technique is well suited for tunnelling in fanglomerate. Seismic velocities indicate substantial strength, especially in the older fanglomerates, which should behave as a lightly-cemented but unfractured sandstone. The strength of the older fanglomerate material, when compared with elastic stress concentrations based on depth, is sufficient to be self-supporting (shotcrete may be needed for weathering protection) for significant sections of some construction units. The Lakeshore Mine, near Casa Grande, has large utility drifts in a fanglomerate that is of comparable strength and character to the older fanglomerate at the Maricopa site. These drifts have been stable with minimal maintenance for years -- despite the presence of a large, active, caving area (mining method) nearby.

For protection from rock fall, these drifts are provided with mesh or chain link affixed from springline to springline with short split set bolts.

Weaker (younger) fanglomerate may not be as well-consolidated, but will nonetheless constitute a very good tunnelling medium. As the discussion in 4.4.4. and the accompanying Figure 18 show, younger alluvium and fanglomerate have not been found at excessive depths. Most of it may not require support. In order to be conservative until this point is further evaluated, and to allow for a potentially needed source of thrust, the sections of tunnel through younger alluvium have been costed as if they were to require a segmental liner.

The Papago tunnel project is an example of a successful Arizona tunnel project through weak alluvium. The Papago Tunnel (Whyte, J.P., 1987) comprised three lengths -- the North tunnel, 6,554 ft long with an excavated diameter of 17 ft, the East tunnel, 13,551 ft long with an excavated diameter of 25 ft, and the West tunnel, 13,968 ft long with an excavated diameter of 25 ft. All were constructed in relatively shallow alluvium with low strength. The alluvium was weaker than that to be expected at the Maricopa SSC site and the tunnels were larger. The tunnels were constructed using a Hitachi shield and digger thrusting against four piece concrete segmental linings each 4 ft long.

Advance rates were:

North tunnel:	Average advance/day	71 ft
	Maximum advance/day	140 ft
East tunnel:	Average advance/day	101 ft
	Maximum advance/day	180 ft
West tunnel:	Average advance/day	117 ft
	Maximum advance/day	220 ft

The North tunnel was the first to be driven and this encountered severe ground support problems initially in an area of unusually loose alluvium close to the shaft. This was overcome by extending the machine shield and

subsequently very high average and maximum daily advances were obtained: 117 ft per day increasing to the maximum of 220 ft per day.

The SSC site conditions offer the advantages of a smaller tunnel, a more-competent medium, a greater length in which to optimize operations, and less likelihood of interferences that are common in an urbanized environment, such as utility relocations, handling of muck, concern for surface construction, and so on. On the other hand, muck tramping distances, being higher than they were in the Papago tunnels, could affect progress if possible maintenance and scheduling problems are not avoided.

Computation using site-specific strength data according to the methods outlined in Section 4.4.5 for hard rock give an average predicted daily rate of progress of very nearly 200 ft. For this analysis, the fanglomerate was treated as if it were a moderately-abrasive, weak sandstone with very few to no fractures. No credit was taken for the absence of fractures in enhancing gripper thrust and it was assumed that minimum necessary thrust could be consistently obtained from the lining.

Site data appear to be very supportive of these assumptions, and although the method used has its limitations, the result is reasonable in view of the Papago Tunnel's data. For this reason values close to 200 ft per day were used in the cost analysis.

Construction units involving fanglomerate that may also involve some hard rock sections are 3,4,5 and 8. The transitions from fanglomerate to rock should, according to field evidence, involve a progressive rather than abrupt change in competence. The intrusive assemblage members seem consistently to be bounded by weathered zones whose strength mimics that of the adjacent fanglomerate. Older fanglomerate will typically be found between bedrock and younger fanglomerate in each construction unit. Thus mixed-face concerns such as inability to develop sufficient thrust entering a harder zone, steering problems, excessive chattering, and so on, should be fairly rare. The TBM should of course be designed against likely changes in conditions.

6.0. CONSTRUCTION OF OTHER FEATURES

Major components of the SSC project besides the ring itself are the shafts, access roads, injection complex and experimental chambers, the central campus, and the Area S and T Cluster Interaction Regions.

The campus area, injection complex, and interaction areas were studied geotechnically by Sergeant, Hauskins, and Beckwith (1988). Shaft construction aspects were considered in the site proposal.

6.1 Shafts

Key information on the Maricopa Site shafts is provided in Table 17. Included are the location of each shaft by mile number, the construction unit in which it is located, the type of shaft, the depth of the shaft, and the major rock type to be encountered. Three of the shafts (Mile 5, 13.3 and 36.5) are to be box-trenched for tunneling purposes. Drifts would be driven, probably by hand, from the shaft breakout to the main tunnel (ring) or vice-versa.

The shafts are 20 or 30 feet in inside diameter, with depths projected to range from 50 to 810 feet. An impact breaker mounted on a tractor base is recommended for the shafts collared in fanglomerate. The drill-and-blast method is recommended for excavating hard rock shafts.

The method of mucking out is an individual choice and will depend on the equipment already owned by the contractor. The estimated costs in the site proposal were based on using a front end loader for mucking the 30-foot-diameter shafts and an Eimco 630 for the 20-foot-diameter shafts.

For the five shafts in fanglomerate less than 120 feet deep, an auger drilling method may be a less-costly alternative. Since the water table is several hundred feet deep in these areas, it will not hinder the application of the technique. In Arizona, this method was effectively used to construct Titan II missile silos in fanglomerate similar to that present at the Maricopa Site. If the method is cost-effective, large-diameter auger drilling methods would greatly increase safety when sinking these shafts. There may be as many as three shafts that will pass through significant thicknesses of both fanglomerate and bedrock.

A type of finish used in mines is considered suitable for the shafts and drifts. The recommended method is lining with welded wire mesh, rock bolts and shotcrete.

Successfully-constructed shafts in Arizona have overcome far more severe groundwater and rock conditions than are likely at the Maricopa site. This experience further demonstrates that Maricopa Site shaft depths will not restrict or add costs to the operation and maintenance at the sector service areas or exit shafts.

Table 17 - Maricopa Shafts

<u>Mile</u>	<u>Construction Unit</u>	<u>Type(1)</u>	<u>Hoist Method</u>	<u>Costed Depth(2)</u>	<u>Actual Depth(2)</u>	<u>Rock Assemblage</u>
0.0	1	E 3	Crane	250	260	Fanglomerate
2.5	1	F 2	Crane	100	120	Fanglomerate
5.0	1	E 2	Crane	80	80	Fanglomerate
7.5	2	F 1	Crane	60	55	Fanglomerate
10.0	2	E 1	Crane	60	50	Fanglomerate
13.3	3	F 10	Crane	240	110	Granitic
16.5	4	E 10	Crane	180	150	Granitic
18.9	4	F 9	Crane	210	185	Fanglomerate
21.45	5	E 9	Crane	330	300	Volcanic
24.0	5	F 8	Headframe	380	340	Volcanic
26.5	5	E 8	Headframe	350	335	Fanglomerate
29.0	6	F 7	Headframe	400	380	Fanglomerate
31.5	7	E 7	Crane	270	250	Fanglomerate
34.1	7	F 6	Crane	160	150	Fanglomerate
36.5	7	E 6	Crane	110	115	Fanglomerate
39.7	8	F 5	Crane	70	80	Fanglomerate
42.8	9	E 5	Crane	120	145	Fanglomerate
45.2	9	F 4	Headframe	370	460	Granitic
47.8	9	E 4	Headframe	800	810	Granitic
50.3	9	F 3	Headframe	470	480	Granitic

(1) E shafts are 20 feet in diameter. F shafts are 30 feet in diameter.

(2) Costed depth is the depth used to estimate the cost of construction. An adjustment to the ring tilt changed the shaft depths to the listed actual depth.

No shafts are in Construction Unit 10.

6.2 Campus Area, Injector Complex, and Experimental Halls

Construction requirements for the injector complex, experimental chambers, and campus building area, as well as general analyses for foundation bearing capacity, settlement, and swell/collapse potential are discussed in detail by Beckwith et al (1988).

6.2.1. Physical Layout and Description

Principal facilities in the Injection Complex will be the following:

- o A Linear Accelerator (Linac), which will be a square tunnel with 12-ft inside dimensions, 494 ft in length.
- o A Low Energy Booster (LEB) in a circular tunnel 820 ft in circumference with a 12-ft-square inside dimension.
- o A Medium Energy Booster (MEB) ring 6,236 ft in circumference. The circular tunnel cross section will be 10 ft inside diameter.
- o A High Energy Booster (HEB) Ring 3.7 miles in circumference. This circular tunnel will also have a 10-ft inside diameter.
- o Test Beam Facility consisting of a square tunnel of 8-ft inside dimensions tangent to the HEB tunnel, underground enclosures for dipole magnets, and a Test Beam Hall.

Most of these facilities will be at or near the grade of the main collider ring tunnel or about 70 to 90 ft below existing grade.

The Injection Facility will include various access shafts and control and support buildings at the surface.

The HEB will be connected to the main collider ring by injection line tunnels. The radio beam accelerator systems building at the surface, and the beam dump abort systems housed in concrete vaults will be located in this vicinity.

The principal facilities in the two Cluster Interaction Regions (S and T) in the east cluster are the Type A Collision Halls, connecting access halls and assembly areas. The Collision Halls will extend 30 ft below the main collider tunnel and house the 50,000-ton detectors which rest on rectangular foundations about 70 ft in width and 75 ft in length. The bottom of the Collision Halls will be about 160 ft below existing grade at locations S and T.

Two similar facilities will be constructed in the west cluster at locations Y and Z. The detectors in the Type B halls will rest on square foundations of about 50-ft width. The bottom of the collision halls will be about 120 feet below existing grade at locations Y and Z.

The Central Campus will be at or somewhat above existing grade. The facilities will include a four-story central laboratory building; six-story steel frame heavy works building with high-bay work areas; three single-story steel frame shop buildings; and various ancillary buildings of one-story steel frame construction. Water and sewage treatment plants will be a part of the facilities.

6.2.2. General Soil Conditions

The moderately- to very-strongly-cemented alluvial soils will provide excellent support for foundations in the Main Campus and Injector Complex. These soils are very stiff to hard and their geotechnical properties are not significantly affected by moisture increases.

For the Main Campus structures and other facilities at or near existing grade, the thin surface layer of moisture-sensitive alluvium should be removed and the site brought up to subgrade elevation with structural fill. With this treatment, spread-type or mat-type foundations designed at moderate bearing pressures can be used. For the depressed structures where the sub-grade will rest on the moderately to very-strongly cemented alluvium, high bearing pressures can be used in the design of spread-type and mat-type foundations.

It appears the Collision Halls at S and T in the east cluster will bear on sound Booth Hills quartz diorite rock. Settlements of a mat foundation on rock for support of the detectors would be very slight. The rock could be stiffened by grouting and rock bolting to further reduce settlements.

The Collision Halls in the West Cluster at Z seem to be underlain by older fanglomerate, while cemented alluvium (younger fanglomerate) underlies the Collision Hall at Y. Settlements of mat foundations at these locations would be relatively low, but they could be reduced to very small values with the use of stiff pier supported mats.

It is envisioned that the "at grade" facilities will be raised a few feet above existing grade for drainage proposed or the sites will be prepared with shallow cuts and fills with drainage channels being provided to handle storm runoff.

6.2.3 Estimated Settlements and Recommended Provisions for Construction

Methods of analysis of soil conditions, and their implications to construction considerations, are the same as discussed in Section 5.2.3.

As mentioned previously, near-surface weakly-cemented alluvium may have substantial collapse potential and should be replaced with properly-compacted structural fill. Both the overexcavated surface soils and the soils from deep excavations will be suitable for structural fill. After compaction, the more calcareous soils tend to recement and become as stiff as the older cemented alluvium in-place (Crossley and Beckwith, 1978).

The use of straight, machine-cleaned, drilled, cast-in-place pier foundations provides an alternative to shallow foundations and may be most economical for some structures, both in the "at grade" and depressed areas. Relatively high bearing capacities are afforded by the cemented desert alluvium. Drilled piers can be constructed very rapidly in comparison to shallow footings. The placement of horizontal reinforcement, forming, and backfilling procedures involved in the construction of shallow foundations

are avoided with the use of drilled piers. Drilled piers will be particularly efficient for support of the steel frame building in the Main Campus area where most foundation loads will be imposed by columns.

Drilled piers can be excavated in the soils involved with only minimal caving or overbreakage. Bits and techniques are available that allow proper cleaning of the bottom of drilled pier excavations by mechanical means.

The cemented alluvium can be efficiently excavated with conventional equipment, but because of its high strength and the absence of fissures and other weakening discontinuities, can be safely cut at steep slopes.

Several innovative approaches to deep, below-grade walls have been increasingly employed in the Phoenix and Tucson areas in the past several years in similar cemented alluvium. These have included soldier pile systems with soil anchors and precast or cast-in-place concrete facing, soil nailing, reinforced earth, and tangent walls formed with a row of cast-in-place concrete piers. It appears that economy of design can be achieved for some of the below-grade structures by using one or more of these approaches. These are discussed in detail in Sergeant, Hauskins, and Beckwith (1988).

The safe soil bearing pressure of about 10,000 psf should not be exceeded in the design of spread-type and mat-type foundations. By limiting the bearing pressure to 10,000 psf, a factor of safety of 3 or more will be provided.

In many cases, design bearing pressures will be controlled by settlements. Estimated settlements versus width for 4-ft-deep square and continuous footings, respectively, were made using elastic methods given by Bowles (1987). Settlements are expected to occur almost instantaneously with the application of load, as has been demonstrated by full-scale load tests in similar cemented alluvium (Beckwith and Bedenkop, 1973).

Drilled pier foundations could provide factors of safety of about 3. For concentrated loads up to 1,000 kips, it is estimated that settlements will be no more than 1/4 in. Settlements are expected to be essentially elastic and complete within a few minutes after application of load.

Bearing capacity calculations were made using the general geostatic approach presented by Kulhawy and others (1983) and special techniques developed for local calcareous soils described by Beckwith and Bedenkop (1973) and Quiros and Reese (1977). Load tests in calcareous soils recently reported by Tucker (1987) provide further validation of these techniques.

Several options are available to calculate lateral soil-pier interaction, lateral deflections, and moments. Computer Program COM 624G (Reese and others, 1984) has been calibrated to local lateral load tests in cemented alluvium (Newlin, 1968; GAI Consultants Inc., 1982; 1982b). CUFAD (Troutman and Kulhawy, 1987) includes a recent modification of the Electric Power Research Institute lateral soil-pier interaction program described by GAI Consultants, Inc. (1982a, 1982b). This is an alternative approach which has been calibrated to local cemented alluvium. This program is believed to provide a somewhat better model than COM 624G for very short, stiff piers.

It is anticipated that the structures in the Injector Complex will extend about 70 to 90 ft below existing grade. Preliminary recommendations given earlier apply specifically to this case. However, they are also probably applicable to the elements of the Collider Ring Facilities and Interaction Region that penetrate the moderately- to strongly-cemented alluvium.

For shallow foundations, a safe soil bearing pressure of 25 ksf should not be exceeded in the design of spread-type or mat-type foundations, except for very wide mats. This limitation will provide a factor of safety of 3 or more.

For drilled piers, it is estimated that settlements of isolated piers supporting column loads up to 1,500 kips would not exceed 1/4 in. and would be almost ideally elastic in nature.

Net pressures imposed on rectangular mat foundations for the detectors would be about 19 ksf and 40 ksf for Type A and Type B Collision Halls, respectively. Dimensions of the mat areas will be about 70 ft by 75 ft for Type A and 50-ft-square for Type B. The detectors are assumed to weigh 100,000 kips.

Geotechnical conditions for all Collision Halls are such that initial settlements of the detectors can be limited to very small amounts. Moreover, it is feasible to limit load-unload movements when detector components are removed and reinstalled to very small magnitudes so that realigning and calibration of the equipment will be simplified. Settlements for all of the cases discussed below are expected to be essentially elastic in nature. The detector foundations at S and T will probably rest on quartz diorite bedrock. Based on rock descriptions and correlations given in this report, and using methodology presented by Kulhawy and Goodman (1987), settlements in the range of 0.02 to 0.10 in. are estimated for rigid mat foundations supporting the detectors. Settlements could probably be limited to or below the lower value by stabilizing the more highly-stressed zone of rock with prestressed rock bolts or tendons and grouting.

The Collision Hall at location Y appears to be underlain by cemented alluvium similar to that of the Main Campus and Injector Complex with bedrock at about 100 ft below the base. Settlement analysis was made using the E_s versus depth relationship for below grade structures on Figure___. Using the method of Bowles (1987), a settlement of 0.6 in. was estimated for a rigid mat foundation.

As an alternative approach, settlements of a stiff pier-supported mat 6 ft thick were evaluated using methods of Poulos and Davis (1974, 1980). This analysis indicates it is feasible to limit initial settlements to less than 0.1 in. and load-unload deformations involved during maintenance to a few hundredths of an inch even if piers are not extended to rock.

As indicated previously, the Type B detector foundation at Location Z may rest on fanglomerate. Based on the measured compression wave velocity of 8,000 ft per second and previous projects involving similar formations, E_r is estimated to be in the range of 500 to 1,000 ksi. Mat settlements in the range of 0.15 to 0.30 in. were estimated for a 50-ft-square mat suppor-

ting the 100,000 kip detector with this range of E_r , using methodology given by Kulhawy and Goodman (1987). Settlements could be reduced to well below 0.1 inch with the use of a pier-supported mat. Although drilling is difficult, rock auger and core bits are available locally that would allow drilling of large diameter rock-socket piers into the conglomerate.

Excavation methods including those applicable for the open cuts which will be involved for the below grade facilities in the Injector Complex are addressed in 5.5.7.1 of this report. As in the open-cut portions of the ring tunnel, the Injector Complex excavations can be made efficiently with conventional scrapers or Holland loader systems and temporary cut slopes of 60 degrees or steeper can be made safely in the older cemented alluvial soils. It was also confirmed that excavations for drilled piers and shafts can be made in the cemented alluvium with conventional, large truck-mounted and crane-mounted auger rigs available in Arizona.

Restrained, essentially rigid, reinforced concrete retaining walls such as basement walls braced by floor systems should be designed to resist "at-rest" earth pressures of 50 psf per ft of depth. Reinforced concrete cantilever retaining walls should be designed to resist "active" earth pressures of 30 psf per ft of depth.

General practice in Arizona has been to backfill walls largely with the cemented alluvial soils providing a degree of drainage with small zones of clean, granular material to allow for small amounts of seepage due to irrigation or broken conduits. Geomatrix drains (Koerner, 1986) have recently provided an efficient means of providing drainage.

Economy of design may well be effected for certain elements of the SSC facilities by using the following kinds of earth support systems successfully employed on recent Arizona projects.

A. Using a row of concrete soldier piles at 10- to 12-ft centers (often reinforced with H-beams) and small diameter soil anchors as the basic structural system. The cemented soils span between the soldier piles without caving. The perimeter wall surface is constructed with reinforced shotcrete or precast concrete elements.

B. Reinforced earth walls using cast-in-place concrete facings. A metal strip reinforcement system and various designs with geosynthetic reinforcement (Jones, 1985) have been used.

C. Soil nailing with reinforced shotcrete facings (Gastler and Gudhaus, 1981; Bruce and Jewell, 1986).

D. Reinforced concrete tangent or secant walls formed with a row of drilled piers and supported by soil anchors.

The cemented alluvial soils and fills constructed from these soils will provide relatively stiff support for compressors, fans and other vibrating machinery involved for the SSC.

6.2.4. Seismic Design Provision

The site is in one of the most tectonically stable areas in North America and has extremely low seismic hazard. As documented by Chapter 3 of the State of Arizona proposal (Arizona Department of Commerce, 1987), the effective peak horizontal ground acceleration (Aa) from the maximum earthquake (MCE) is about 0.09 g.

The most likely event to affect the site, a distant earthquake on the San Andreas Fault System in the Imperial Valley of California or the Gulf of California would produce an Aa of less than 0.05 g. Thus, structural designs by Zone 2 requirements of the Uniform Building Code, ATC-3 (Applied Technology Council, 1978), or the American National Standards Institute (1982) criteria would probably not be damaged by the MCE. If conservative designs are nonetheless desired, they can be achieved for machinery, piping, detectors and other sensitive electronic equipment, superconducting magnets, the electrical and communications systems, etc. by special dynamic design methods such as those described by McBean and others (1983). The effects of the MCE at the site are well below the threshold of damage for tunnels determined by Dowding (1979) of $Aa = 0.2$ g.

6.3 Temporary Portals and Access Ramps

Construction of some of the tunnelled portions of the ring itself may be most expeditiously done via ramp access from the surface. Construction Unit 2 is projected to be entirely cut-and-fill, and practically all in fanglomerate with a potential short section of weathered granite in the cut towards the north end. This cut could provide ramp access for portalling the deep tunnel projected for Construction Unit 3, a hard-rock TBM segment through mostly Booth Hills quartz diorite, and Construction Unit 1, presently expected to be a weak rock (soft-ground) TBM segment. Construction Units 4 and 5 will probably both have to be supported through one or more of the shafts that would be provided in any event around the ring. Construction Unit 6, a soft-ground TBM segment, may be accessible via ramp since it is adjacent to Construction Unit 7, which is a cut-and-fill segment. Construction Unit 8 may be ramp-accessible for the same reason. Construction Unit 9, however, would have to be supported through shafts, as would Construction Unit 10, which does not intercept any near-surface construction units.

Temporary ramps and portals could be constructed along with the open-cut segments, and using similar methods. Slopes and access would need to be modified in the local area of the portal. To achieve longer-term stability, slopes may need to be flattened in the portal area or special protection provided. Steeper slopes would be less-susceptible to erosion than flatter slopes, which may need to be covered with a geotextile or shotcrete if erodability is high. These slopes would need to remain open with a high assurance of stability for 1-2 years, whereas the slopes for the cut-and-fill sections would need to stand open for only weeks before the trench, with the tunnel in place, would be backfilled.

7.0 CONCLUSIONS

7.1 Ring Geology by Construction Units

Table 18 presents the summarized interpretations of the investigation data in terms of the types of materials expected to be encountered as the ring is constructed. For purposes of estimating construction time and cost, the construction operations are expected to be carried out in segments, with construction procedures to be roughly consistent within each segment. Thus a construction segment, or Construction Unit (CU), would not ideally be composed half of fanglomerate cut-and-cover tunnelling and half of deep hard rock tunnelling through fresh granite. The lengths of construction segments within these guidelines were assigned so as to provide large-dollar-value contracts but were restricted so that adequate competition would exist for all construction segments.

Accompanying each of the following CU geologic descriptions is a graph showing the distributions of measured seismic velocities with depth within the CU. These figures are intended to show the overall distribution of the seismically-determined stratigraphy and particularly the measured depth limits of occurrence of the layers. A special designation on each figure indicates if the lower bound of the layer was not detected by the survey, as is commonly the case where fanglomerate accumulations are very thick away from the mountain fronts or where bedrock of great thickness extent underlies the seismic profile at detectable depth.

Construction Units 1 and 2 (Mile 52.2 to 5; Mile 5 to 12.80)

The ring passes through fanglomerate in most of these two CUs. Seismic refraction profiles along this length indicate that the upper 655 ft of fanglomerate consists of a two-layer system with the upper 250-300 ft consisting of indurated, fine, sandy or locally clay-rich silts with compressional wave velocities commonly between 2,800-4,000 ft/s. The lower unit consists of indurated, poorly sorted, sandy gravel with compressional wave velocities between 6,900 and 11,000 ft/s. Figure 31 for CU 1 and Figure 32 for CU 2 show that, with two exceptions, seismic velocities lower than about 3,000 ft/s will probably not be encountered deeper than 150 ft and velocities lower than about 1,500 ft/s are strictly near-surface deposits and should not occur deep enough to cause difficulties. The two measured exceptions, where a lower boundary for materials in the 1,000-1,500 ft/s range was not detected deeper than 100 ft in CU 1, are weathering shots (Sternberg, 1988) and not well-suited to detecting deeper layers. In addition, Figures 31 and 32 show that materials with velocities higher than about 6,000 ft/s are unlikely to occur above 100 ft in CU 2, that materials with velocities higher than about 6,000 ft/s are unlikely above 300 ft in CU 1, and that most velocities experienced between 100 ft and 300 ft in CU 1 will be in the range of 3,000 to 6,000 ft/s.

Table 18 - Summary of Maricopa Site Construction Units

CONSTRUCTION UNIT	GEOLOGY*	CONSTRUCTION METHOD**
1 (Mile 52.2 to 5.0)	Fanglomerate	TBM
2 (Mile 5.0 to 12.8)	Fanglomerate	Cut-and-Fill
3 (Mile 12.8 to 15.3)	Granite and Fanglomerate	TBM
4 (Mile 15.3 to 21.3)	Granite and Fanglomerate	TBM
5 (Mile 21.3 to 28.2)	Volcanic and Sedimentary Rocks	TBM
6 (Mile 28.3 to 37.4)	Fanglomerate	TBM
7 (Mile 37.4 to 41.5)	Fanglomerate	Cut-and-Fill
8 (Mile 41.5 to 45.0)	Granite and Fanglomerate	TBM
9 (Mile 45.0 to 62.2)	Granite	TBM
10 (Mile 35.5 to 43.5)	Fanglomerate	TBM

* Geologic descriptions are qualitative only, detailed descriptions are provided in Section 2.

** Construction methods are described further in Sections 4.4.5 and 5.5.7.

TBM = tunnel-boring machine

SEISMIC VELOCITIES VS DEPTH

CONSTRUCTION UNIT 1

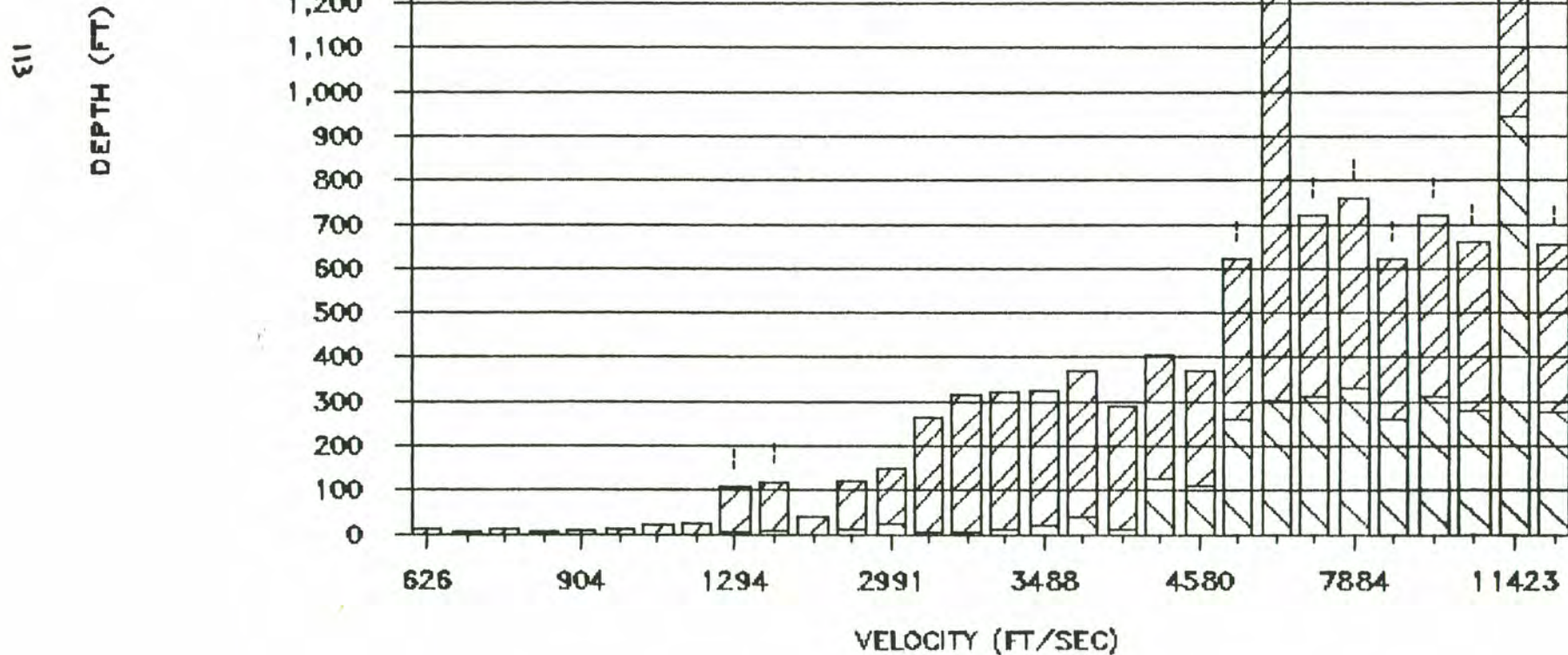


Figure 31. Seismic Velocities Versus Depth, Construction Unit 1

SEISMIC VELOCITIES VS DEPTH

CONSTRUCTION UNIT 2

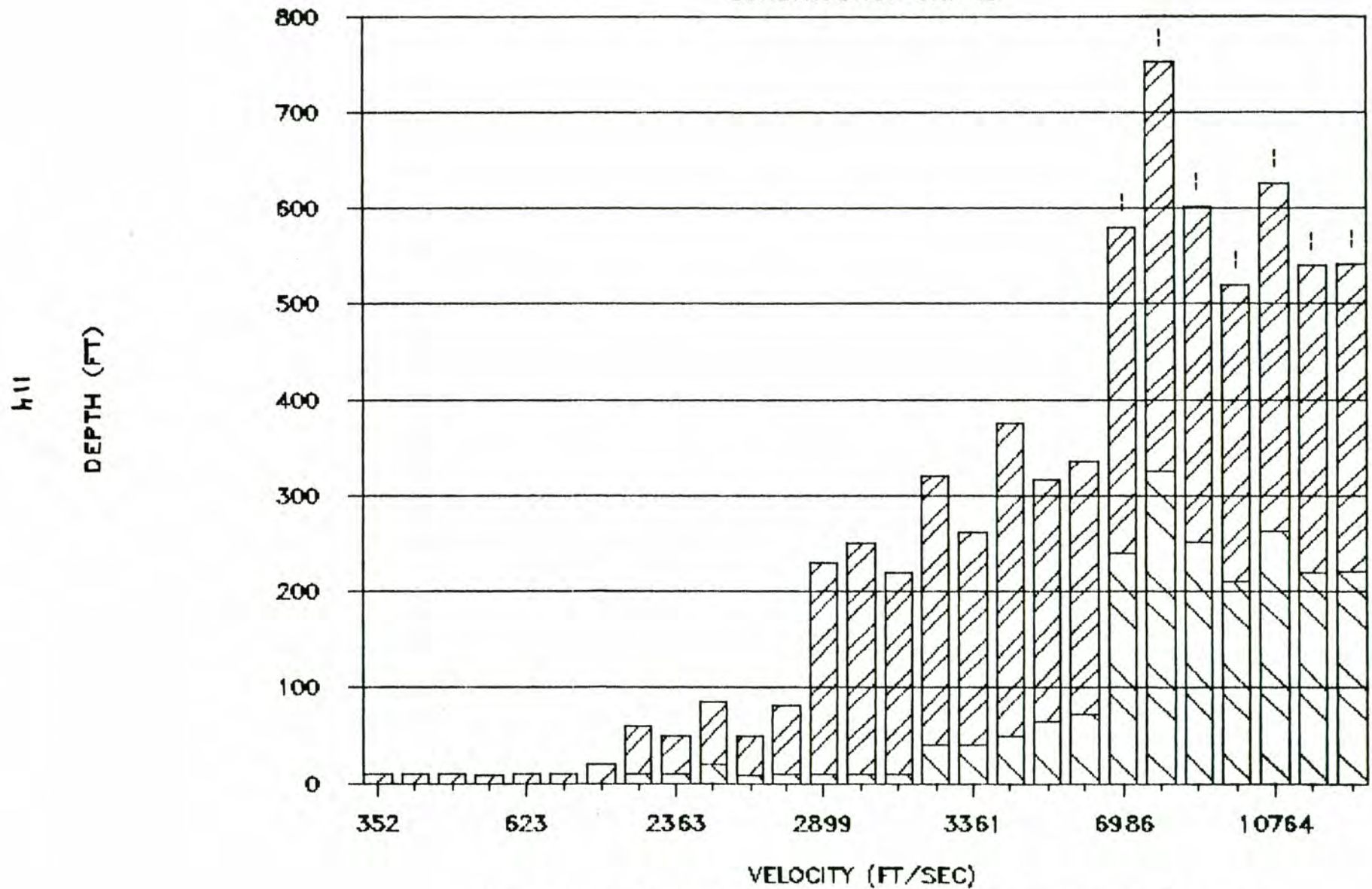


Figure 32. Seismic Velocities Versus Depth, Construction Unit 2

This stratigraphy is generally desirable for the types of construction expected. The depth of the ring varies from about 300 ft to about 100 ft in CU 1 and from 100 ft to 50 ft or so in CU 2. The seismic data therefore indicate that nearly-all TBM tunnelling in CU 1 will occur in reasonably-competent 3,000-6,000 ft/s materials and that the thicknesses of weaker materials detected overhead at some places will be essentially irrelevant. The seismic data also indicate that substantial thicknesses of material with velocity less than about 2,000 ft/s should not occur in the walls of the open cut, and that undesirably-high-strength materials (greater than 10,000 ft/sec) that could slow excavation with conventional earthmoving equipment are unlikely in the open cut. The bottom of the cut will most likely occur in 3,000-6,000 ft/sec material, which should provide stable side slopes.

Near mile 4.5, a 6.5-in hollow stem auger hole was drilled to sample the upper silts. The hole, borehole MS3, was drilled to a depth of 32 ft, where it bottomed in cobbles or a boulder. Therefore, borehole MS3A was drilled to a depth of 60 ft, 300 ft or so to the southwest of MS3. The composite section derived from logs of both holes shows the profile to consist of 12% silty clay, 5% sandy silt, and 83% clayey to gravelly sand (visual classification). The predominance of sandy lithologies and the nearly-ubiquitous presence of fine gravel suggest that MA3 and MA3A are not greatly distant from bedrock. Thin interbedding and textural characteristics of the sediment suggest an alluvial fan.

At mile 8.25 a 42-in large-diameter auger hole, MA2, was drilled to a depth of 70 ft. Visually-classified sediments consist of 9% clay, 34% silt, 43% silty sand and 14% sand. The generally finer-grained-character of this sediment as compared to that encountered in boreholes MA3 and MA3A, the presence of abundant mica, and the paucity of gravel, suggest a lower-energy deposition overall and greater distance from bedrock. General fining of sediments basinward has been observed in many basins throughout Arizona (Scarborough and Peirce, 1978). These sediments probably represent distal alluvial fan and intermittent stream overbank deposits.

Near mile 6 the ring passes 500 feet south of a Proterozoic porphyritic granite ridge. It has not been proven that the granite intersects the ring alignment in this area. Gravity and seismic data from elsewhere on the ring suggest that subhorizontal pediment surfaces beneath alluvium are rare, and it is therefore considered unlikely that a granite intercept would occur. The granite is a gray to brownish-tan, medium- to very-coarse-grained porphyritic biotite granite. Potassium feldspar phenocrysts in the coarsest phases average one to two inches in length. The granite ranges from undeformed to well-foliated although the vast majority of outcrop exposures are weakly- to moderately-foliated. Foliation is commonly best developed along zones where the porphyritic granite is intruded by a younger leucocratic muscovite-biotite granite. A mylonitic fabric is locally well developed.

Construction Unit 3 (Mile 12.8 to 15.3).

At mile 12.8 the ring alignment passes into the Booth Hills which

SEISMIC VELOCITIES VS DEPTH

CONSTRUCTION UNIT 3

911

DEPTH (FT)

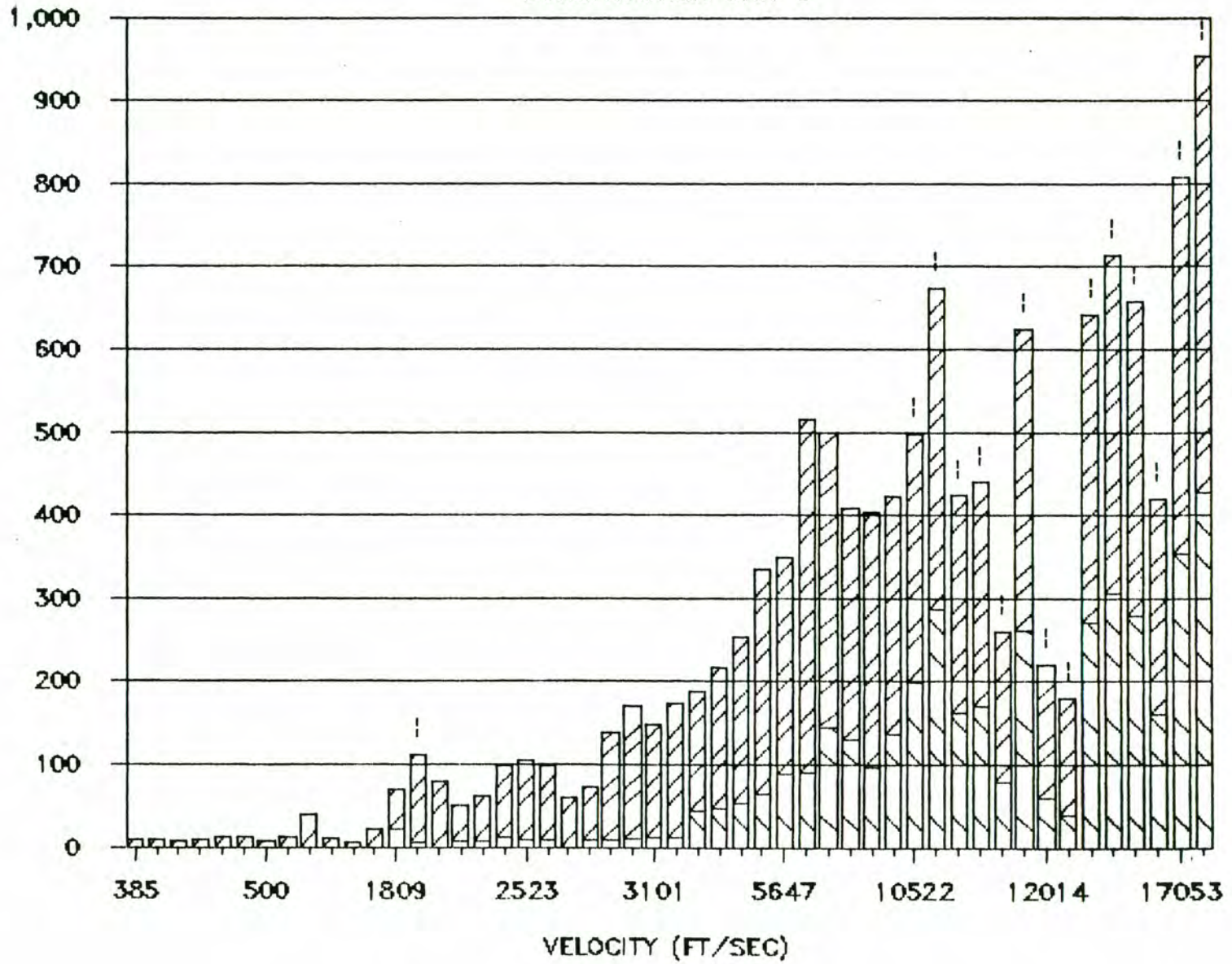


Figure 33. Seismic Velocities Versus Depth, Construction Unit 3

consist of mesocratic, fine- to medium-grained, biotite-hornblende quartz diorite. Locally, epidote is present along fractures and replaces biotite and hornblende. Conspicuous 0.5- to 0.75-inch quartz eyes are characteristic of this unit. Figure 33 shows the variation of seismic velocities with depth. There were no seismic lines run on bedrock outcrop, although some apparent bedrock velocities (more than 10,000 ft/sec) at depths shallower than 100 ft were obtained.

At mile 14.2 the ring leaves the Booth Hills and enters a zone of fanglomerate and shallow bedrock. The bedrock is expected to be a subsurface projection of the Booth Hills quartz diorite. This was verified by Borehole MD3R which was diamond-drilled through 120 feet of homogeneous Booth Hills quartz diorite near mile 14. The fanglomerate consists of cemented sands, silts and gravels.

Seismic refraction surveys indicate compressional wave velocities of 2,000-3,000 ft/s. The tunnel in this CU is nowhere shallower than 100 ft and nowhere deeper than about 200 ft. Figure 33 shows that nowhere have materials with velocities slower than 2,000 ft/s been detected deeper than 100 ft. In fact, most fanglomerate penetrated at tunnel depth should be in the 3,000-5,000 ft/s range. Figure 33 shows that some high (more than 12,000 ft/s) bedrock velocities have been detected in this CU but also that these materials are normally found below tunnel depth. Bedrock seismic expression at tunnel depth is more commonly in the 8,000-12,000 ft/s range, providing regular transitions from fanglomerate into bedrock and vice versa. The fact that materials with velocities greater than 12,000 ft/s were detected at less than 100 ft in only two cases indicates that this zone of weathering can be expected to be the normal but now exclusive circumstance in this CU.

In order to obtain data on the stratigraphy of the fanglomerate adjacent to bedrock outcrops, a 6.5-in hollow-stem auger hole, MA1, was drilled near mile 15 to a depth of 76 ft. Refusal was encountered in cemented gravel or cobbles. Visual classification of the sediments show that they consist of 34% sandy clay, and 66% clayey or silty sand. Interbedded clayey sands and sandy clays, with few silty units, suggest the possibility of a succession of buried paleosols. This type of sequence is what might be expected in relatively-thin, pediment-mantling deposits where a long stable period of basin-fill is represented by only a few feet of sediment. Thicknesses above the pediment range from 150 to 0 ft, and probably vary abruptly over buried topographic features developed on the pediment.

Construction Unit 4 (Mile 15.3 to 21.3)

The ring continues to traverse fanglomerate, probably shallowly flooded by Booth Hills quartz diorite until mile 16.3. At mile 16.3 to it enters Booth Hills quartz diorite and leaves it again at 16.9. To mile 20.5 the ring probably passes largely through fanglomerate. Depth to bedrock is poorly defined for this segment of the ring path, however, and the ring could pass into bedrock. Basement in this area may be Pinal Schist, porphyritic granite, or Booth Hills quartz diorite. The fanglomerate here consists of cemented sand and silts derived from eroded porphyritic granite, Booth Hills quartz diorite, and Pinal Schist. At mile 20.5 the ring enters

porphyritic granite and remains in granite until the end of the CU.

Figure 34 shows the velocity-depth distribution for this CU. It is apparent that there is little chance of encountering material of less than 2,000 ft/s velocity deeper than 50 ft; tunnel depth varies from about 125 ft to over 300 ft. From Figure 34, it is seen that the weakest material likely to occur in the tunnel would have a velocity of over 3,500 ft/s but that materials with velocities of near 15,000 ft/s could also be encountered. The several scattered instances of material between 9,000 and 12,000 ft/s with the range of tunnel depths suggests a reasonably-widespread distribution of older fanglomerate or weathered bedrock that will mitigate the potential for mixed-face conditions.

Porphyritic granite, Booth Hills quartz diorite, and Pinal Schist were described in Section 2.

Construction Unit 5 (Mile 21.3 to 28.8).

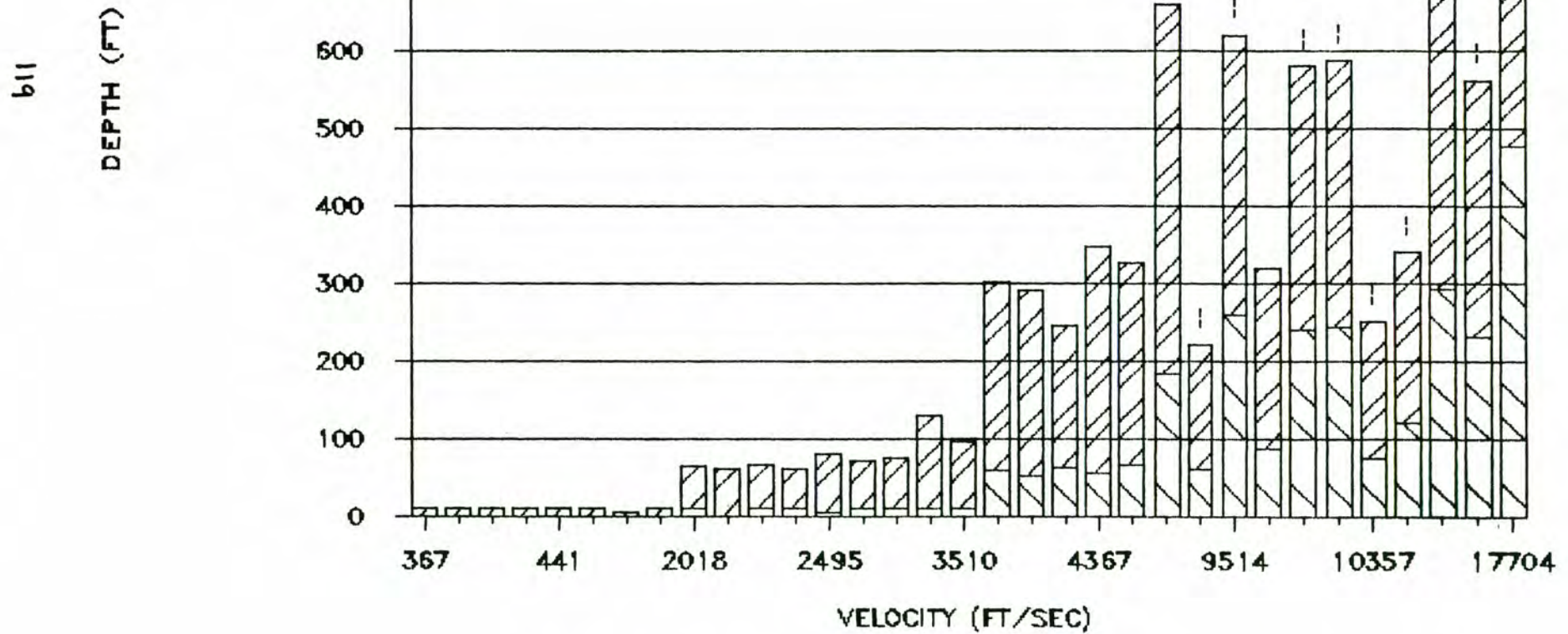
The ring passes from the porphyritic granite of CU 4 into a Tertiary sequence of volcanic and sedimentary rocks.

The overall geologic character of this assemblage has been pieced together from observations of a wide area in the southeast portion of the ring. The assemblage itself is quite thick, and its stratigraphic constituents are generally thick as well. (Borehole MD1R bottomed in a consistent conglomerate that it had been in for hundreds of feet, despite the shallowness of the stratigraphic dip at that location.) Thus the variation in overall makeup of this assemblage expressed in this report does not imply frequent changes in tunnelling conditions along the tunnel alignment. Along the tunnel, such changes will occur on scales of thousands of feet to miles. Once such a change has been crossed by the tunnel, tunnelling conditions beyond will be quite consistent.

The tunnel will first enter into a poorly sorted granite-clast conglomerate. This unit lies depositionally upon basement and varies laterally in thickness. Clasts are typically one inch in diameter, but in rare instances they can reach dimensions of three feet. Engineering properties of the conglomerate would be similar to those of the older fanglomerate. Clasts are subangular to subrounded, and cemented by a dark red, locally arkosic, quartzose cement. Tuffaceous sandstone subunits occur locally within the lower sections of the basal conglomerate. Lying depositionally above the basal conglomerate is a thick sequence of dense to moderately vesicular black to medium-gray olivine basalts. Flow foliation is common in the basalts. Above the basalt is the middle conglomerate unit which is predominantly composed of clasts of all Precambrian basement lithologies in a quartzose cement. Within the middle conglomerate are intercalated basalt flows and a thin, very fine-grained, thinly laminated, lacustrine(?) limestone. The middle conglomerate is unconformably overlain by a reddish-gray massive welded tuff that is horizontally and vertically fractured. Above the welded tuff is the upper conglomerate that is poly lithologic and also contains subunits of basalt flows and tuffaceous sandstone. Clasts in the upper conglomerate are generally two to five inches in diameter with a few clasts up to 20 inches. The clasts are matrix-supported in a dark red

SEISMIC VELOCITIES VS DEPTH

CONSTRUCTION UNIT 4



quartzose to calcareous cement.

Core from diamond drillhole MD1R, one mile southeast of mile 23.5, reflects the thickness and facies variations that may occur within the Tertiary rock sequence. This hole penetrated 1,250 ft of volcanic and sedimentary rocks and did not reach basement. According to drillhole information, the upper conglomerate is at least 250 ft thick and underlain by 350 ft of basalt flows. Two hundred fifty feet of middle conglomerate lie beneath the basalts. Separating the middle and basal (?) conglomerates is 200 ft of basalt. Drilling ceased after 200 ft of basal (?) conglomerate was sampled.

The entire Tertiary sequence strikes approximately N 45 degrees W and dips gently to the southwest. The Tertiary basin is an asymmetric trough that plunges gently to the southeast. No faults are known to occur within the Tertiary section, but the basin is known at locations away from the ring to be in fault contact with the Pinal Schist to the west.

At mile 25.5 the ring passes from the Tertiary rock sequence into the conglomerates of the Bosque Valley. The conglomerate there is composed primarily of eroded granite and is expected to consist of cemented sands, silts, and fine-grained conglomerates.

The depth of the tunnel in the CU ranges from a little more than 450 ft to slightly more than 300 ft. Figure 35 shows that materials of less than 8,000 ft/s velocity are very unlikely at tunnel elevation within the CU, and that some very competent material may be encountered. The downstation end of the CU, which ends in conglomerate, is near diamond corehole MD12. A seismic line centered over MD12 showed a 10,000-plus ft/s velocity beginning at around 10 ft depth, and drill core corroborates the strength and uniformity of the material. Some high velocities (20,000 ft/s) in this CU probably represent massive, fresh granite bedrock near the upstation end of the CU.

Construction units 6 and 7 (Mile 28.2 to 37.4; Mile 37.4 to 41.5)

For the entire length of CUs 6 and 7 the ring passes through conglomerates of the Bosque Valley. Seismic refraction profiles along this length indicate that the conglomerate has compressional wave velocities varying from 3,700 to 8,500 ft/s. Figure 36 shows seismic refraction thickness and velocity information applicable to CU 6. Although the data are fewer than other CUs, they indicate great thicknesses of conglomerate whose velocities and distributions are consistent with those of other, more-heavily-surveyed, construction units. Figure 3 (in pocket) shows CUs 6 and 7 to both be distant from the mountain front and the conglomerate velocities represented in both Figures are entirely consistent with this expectation.

CU 6, a TBM segment, begins at a depth of about 300 ft and becomes shallower (to 125 ft or so) downstation to where CU 7, a cut-and-fill segment, begins and maintains a consistent depth in the range of 80 to 100 ft. Figure 36 for CU 6 shows that the TBM face could be expected to consistently be in fairly strong conglomerate of velocity at least 4,000 ft/s. Correlations developed in Section 5 indicate this conglomerate should be basically self-supporting at these depths.

SEISMIC VELOCITIES VS DEPTH

CONSTRUCTION UNIT 5

121
DEPTH (FT)

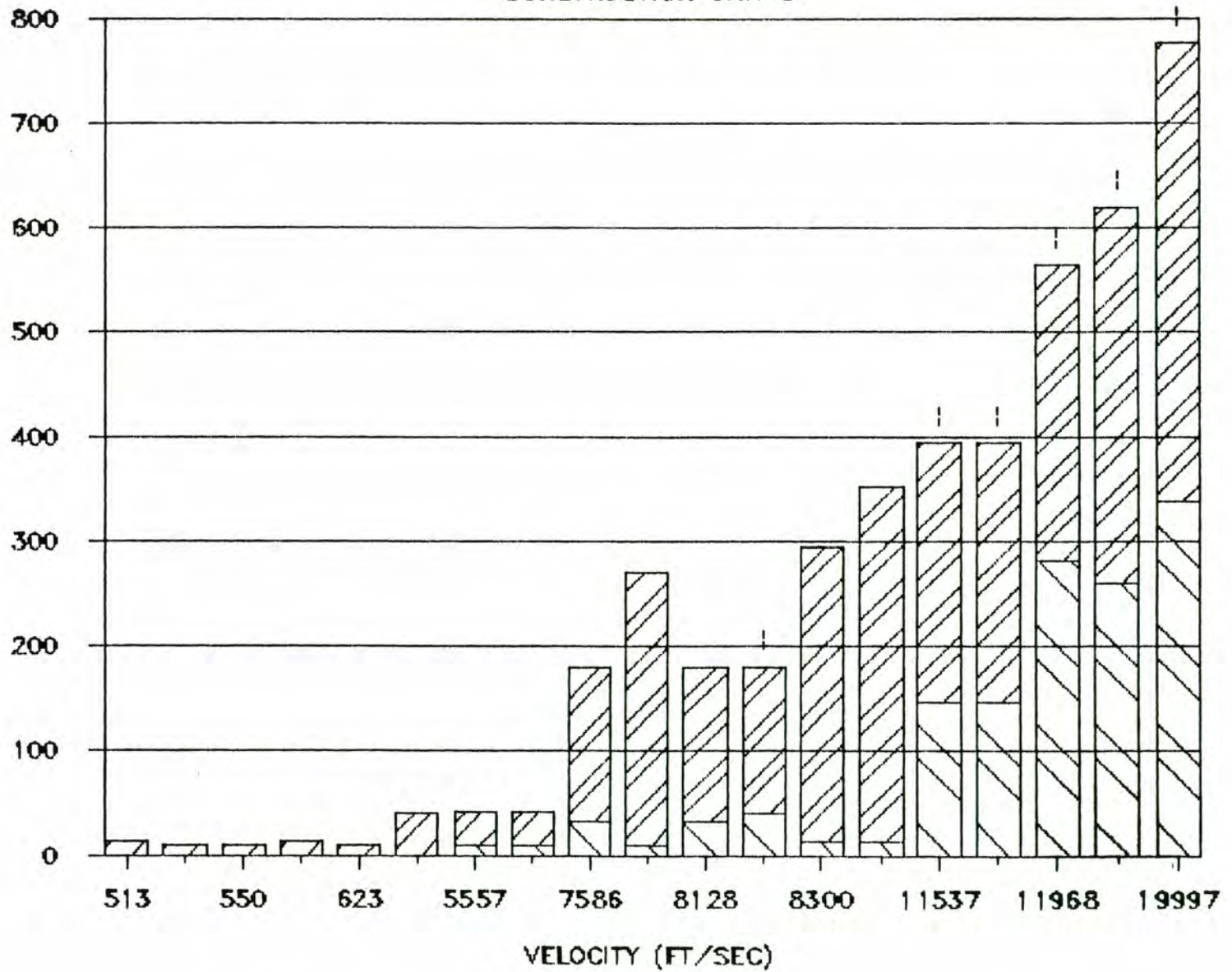


Figure 35. Seismic Velocities Versus Depth, Construction Unit 5

SEISMIC VELOCITIES VS DEPTH

CONSTRUCTION UNIT 6

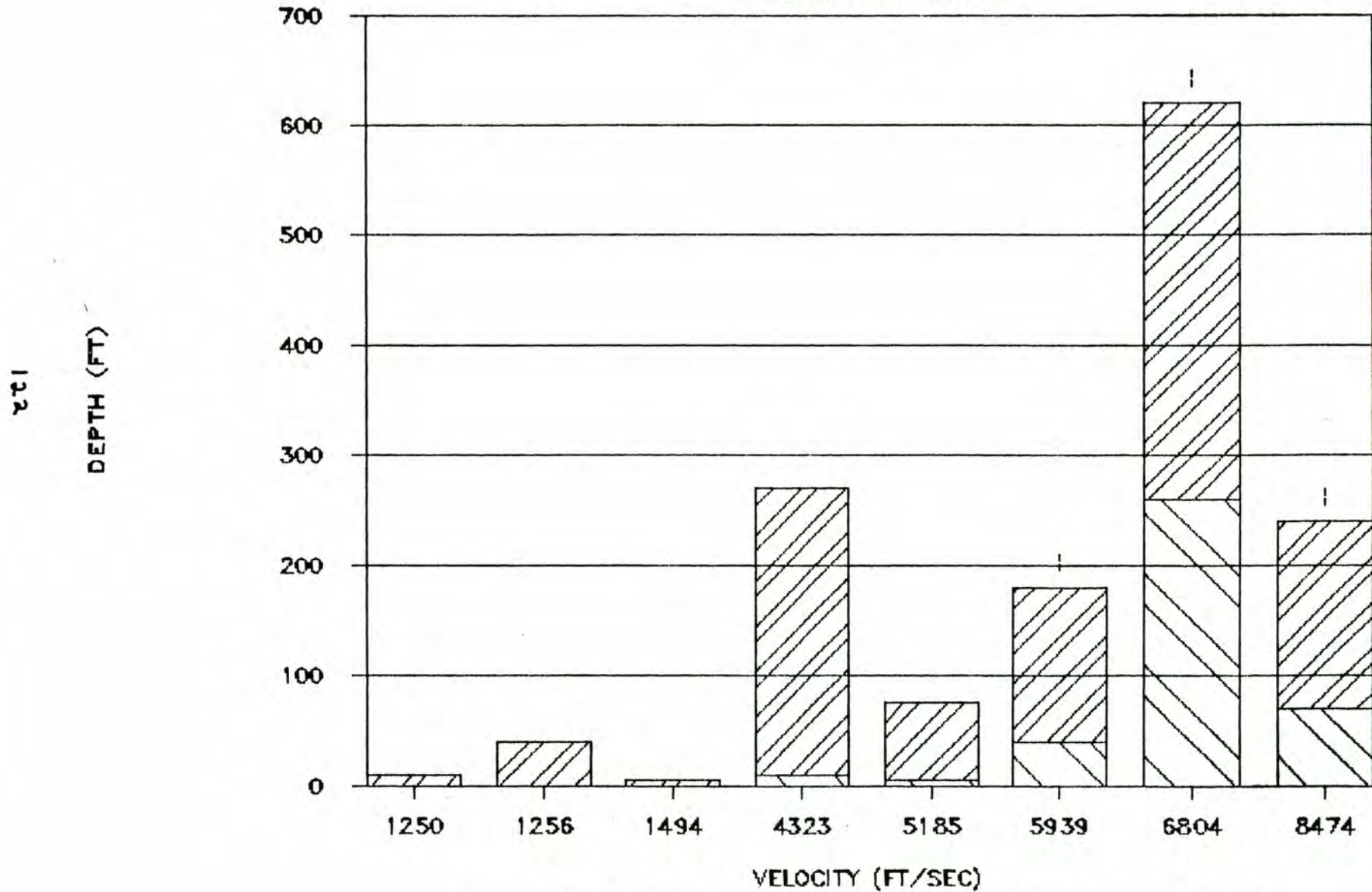


Figure 36. Seismic Velocities Versus Depth, Construction Unit 6

SEISMIC VELOCITIES VS DEPTH

CONSTRUCTION UNIT 7

123

DEPTH (FT)

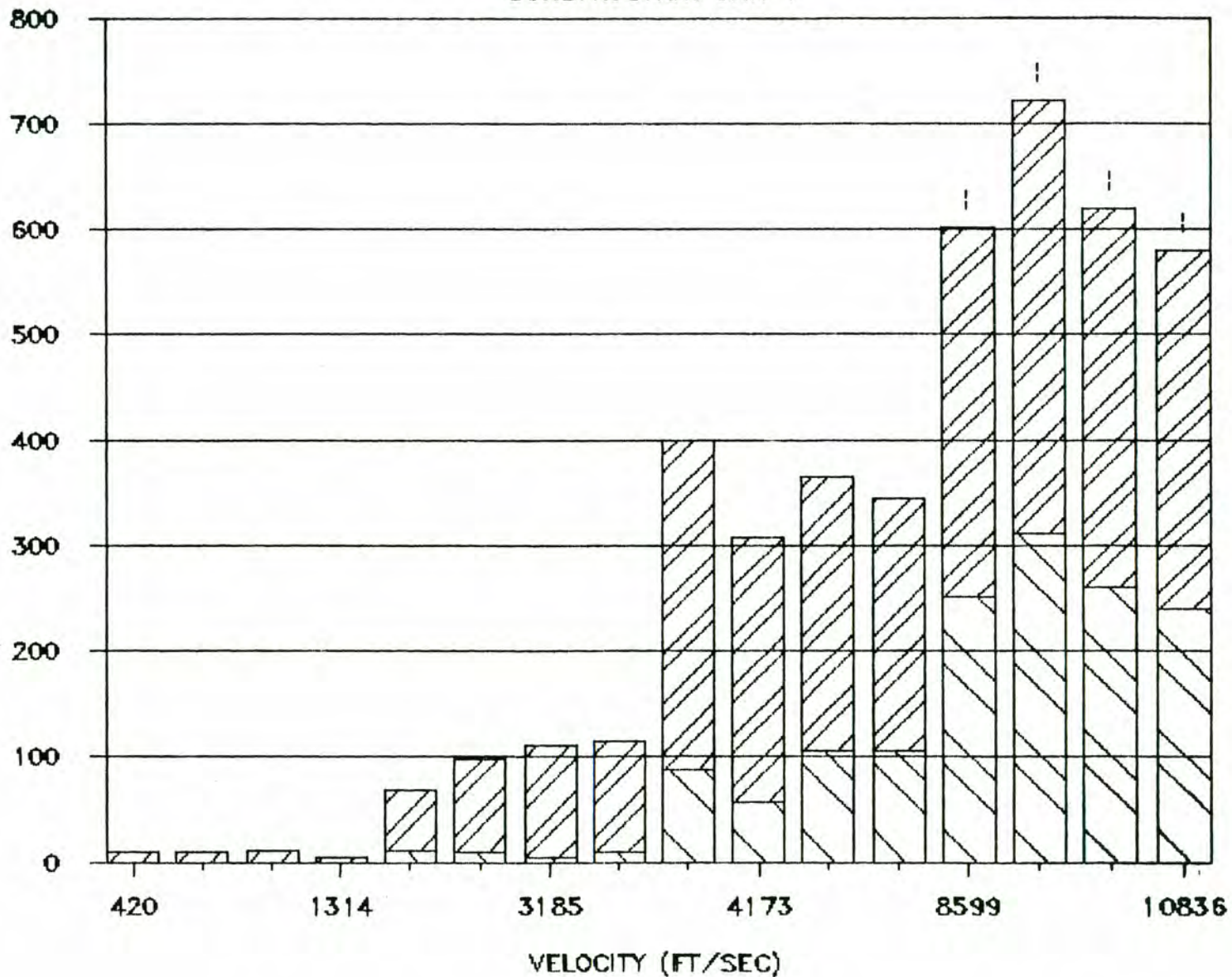


Figure 37. Seismic Velocities Versus Depth, Construction Unit 7

Figure 37, for CU 7, shows that most of the open cut will be constructed in competent fanglomerate in the 2,000-4,000 ft/s range, except for very thin, near surface deposits of weaker material. The fanglomerate is expected to consist of sands, silts, and fine gravels. Northeast of mile 31 a reverse circulation rotary borehole, MD6, penetrated 258 ft of material identified visually as sandy clay and silty sand. No groundwater was encountered. Approximately 39% of the sediments were classified as fine sandy clays and 60% as silty fine sands. A trace of gravel is found as thin lenses. All sediments in Borehole MD6 are weakly to moderately lime cemented. This overall fine-grained character shows that sediments of the upper basin-fill become finer to the southeast in the Bosque Basin and to the west toward Gila Bend. The fine-grained character of these sediments, coupled with the presence of thin lenses of gravel, suggest that they were deposited as overbank flood sediments or as playa or playa-edge sediments. The lateral extent of these fine-grained sediments is currently unknown.

At mile 39.5, Borehole MA6 penetrated 70 ft of indurated sediment, consisting of 4% silt, 66% silty or clayey sand, and 30% sandy gravel (visual classification). The presence of varying amounts of gravel throughout all units of Borehole MA6, the extremely poor sorting of sediments, and the vertical variability of sediment textures suggest that Borehole MA7 penetrated intermittent channel, sheetflood, and overbank deposits in the medial portion of an alluvial fan. Sand and gravel deposits between 12 and 33 ft in thickness probably represent intermittent channel deposits. Clayey sands probably represent mixed sheetflood and overbank sediments, possibly with some accumulation of paleosol clays.

At mile 41, a 42-in large-diameter auger hole (MA5) penetrated 70 ft of cemented silty to gravelly sand. The extremely poor sorting of these deposits, which range in grain size from clays to cobbles, the apparently local derivation from granitic source rock, and the general lack of vertical variability suggest that Borehole MA5 penetrated intermittent channel and sheetflood deposits on the proximal portion of a small alluvial fan. The lower percentages of gravel here may be accounted for by provenance. The granitic bedrock appears to weather more readily than the metamorphic source rocks of Borehole MA6 because of the granite's mineralogical composition and larger grain size.

Construction Unit 8 (Mile 41.5 to 45.0).

At mile 41.5 the ring enters porphyritic granite and returns to fanglomerate at mile 42.3. The fanglomerate in this area is derived from granite and is expected to consist of lime-cemented, fine-grained sands, silts, and gravels.

Figure 38 shows the distribution of seismic velocities pertaining to CU 8. As in other CUs, the lowest velocity represented below 100 ft depth is in the neighborhood of 3,000 ft/s, but most of the velocities deeper than 100 ft will be near 7,000 ft/s or greater. The velocities at the lower end of this range are strongly grouped in between 3,000 and 4,000 ft/s or so, indicating a prevalent fanglomerate layer. Since the TBM tunnel in this CU will be about 120 ft deep at its shallowest and will deepen consistently to

around 325 ft at its downstation (north) end, velocities less than 4,000 ft/s are not likely to be encountered. The highest velocity identified within the range of tunnel depth on Figure 38 is about 12,500 ft/s which is indicative of moderately-weathered granite. Velocities higher than this were only detected below tunnel depth.

As was pointed out in earlier discussions, a transition through weathered bedrock is the normal condition in passing from fanglomerate to granite, and this will tend to mitigate mixed face concerns. Of course, more granite of high velocities might have been indicated at tunnel depth if refraction surveys had been run on outcrop. However, as several surveys showed that were run over very shallowly-buried granite, velocities too high for a TBM are unlikely.

At mile 42.5, a 6.5-inch hollow stem auger hole (MA4) penetrated 100 ft of texturally-diverse sediments. One 4-ft-thick unit of sandy clay makes up 4% of the section. Beds of silty, clayey and gravelly sand from 5 ft to 27 ft thick make up 84% of the section. A 12-ft-thick silty sandy gravel makes up the final 12% of the section. All identifications were made visually in the field. The extremely poor sorting, rapid vertical variability in sediment texture, unit thicknesses, and grain size range suggest deposits from intermittent streams, sheetflood, and overbank flooding on the medial part of a moderately-sized alluvial fan.

The ring enters porphyritic granite near mile 45, where 450 ft of weakly-foliated porphyritic granite were sampled in Borehole MD5.

Construction Unit 9 (Mile 45.0 to 52.2).

From mile 45 to mile 51.25, the ring passes through porphyritic granite. Seismic refraction profiles (Figure 39) indicate that only thin veneers of fanglomerate (no thicker than 100 ft or so) are present from mile 47.5 to 48.75 and mile 50.25 to 51.25. Figure 39 clearly shows an intermediate range of velocities (6,000-10,000 ft/s) that probably represent variation from older fanglomerate to weathered bedrock. This CU reaches greater depth (1300 ft) than any other, but rock encountered at that depth will be of generally high velocity. At mile 51.25 the ring may pass through a leucocratic, tan to cream, fine to medium-grained muscovite-biotite granite. This granite is not porphyritic and intrudes the porphyritic granite as both concordant and discordant masses. From mile 51.25 to the junction with CU 1, the ring passes through fanglomerates as described in CU 1. Chapters 2 and 4 of this report detail the geology and engineering characteristics of the granite, and the distribution of rock mass strengths.

Construction Unit 10 (Mile 35.5 to 43.5)

From mile 35.5 to 43.5 a bypass tunnel will be constructed. This facility is treated as a separate CU because the geologic and topographic characteristics of this length are most efficiently and cost-effectively constructed by a single TBM designed for weak-rock applications separate from CUs 6, 7, and 8. Geologic descriptions for the materials that will be penetrated are the same as for CUs 6, 7, and 8.

SEISMIC VELOCITIES VS DEPTH

CONSTRUCTION UNIT 8

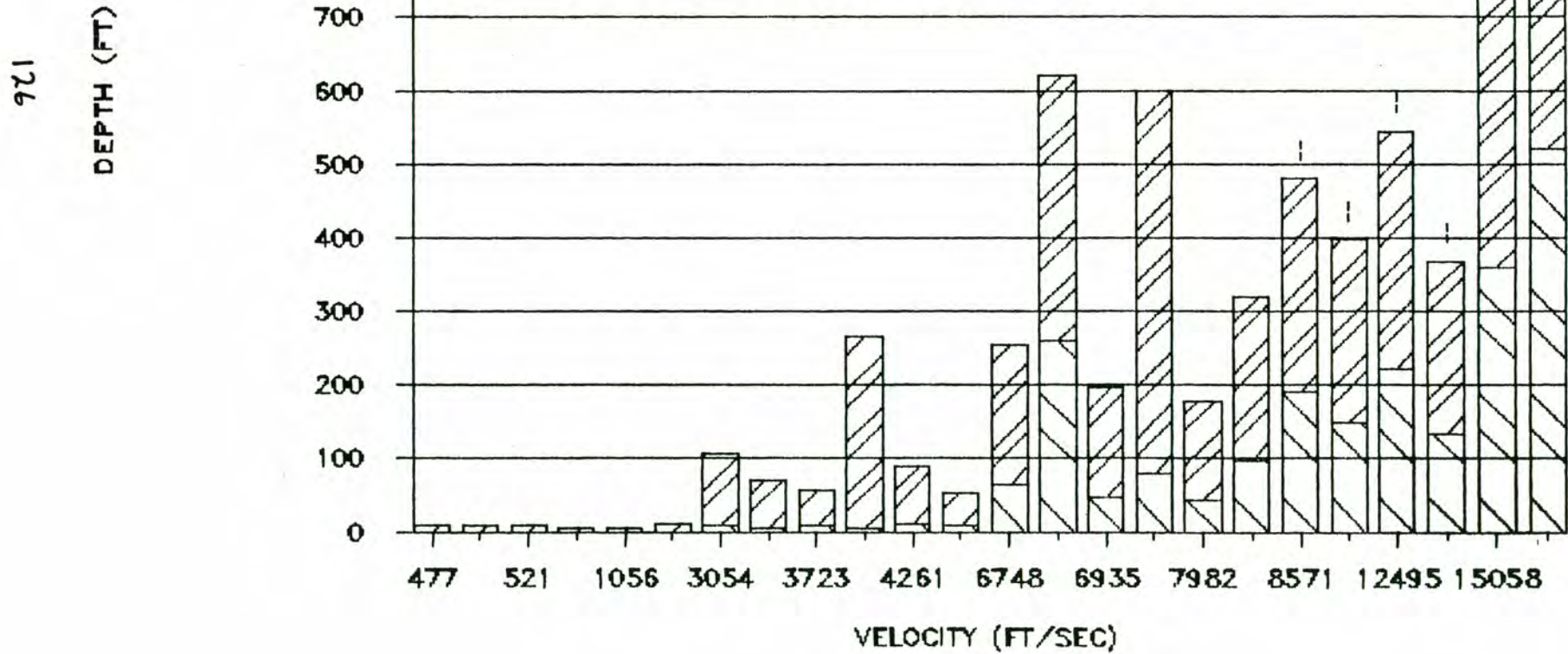


Figure 38. Seismic Velocities Versus Depth, Construction Unit 8

SEISMIC VELOCITIES VS DEPTH

CONSTRUCTION UNIT 9

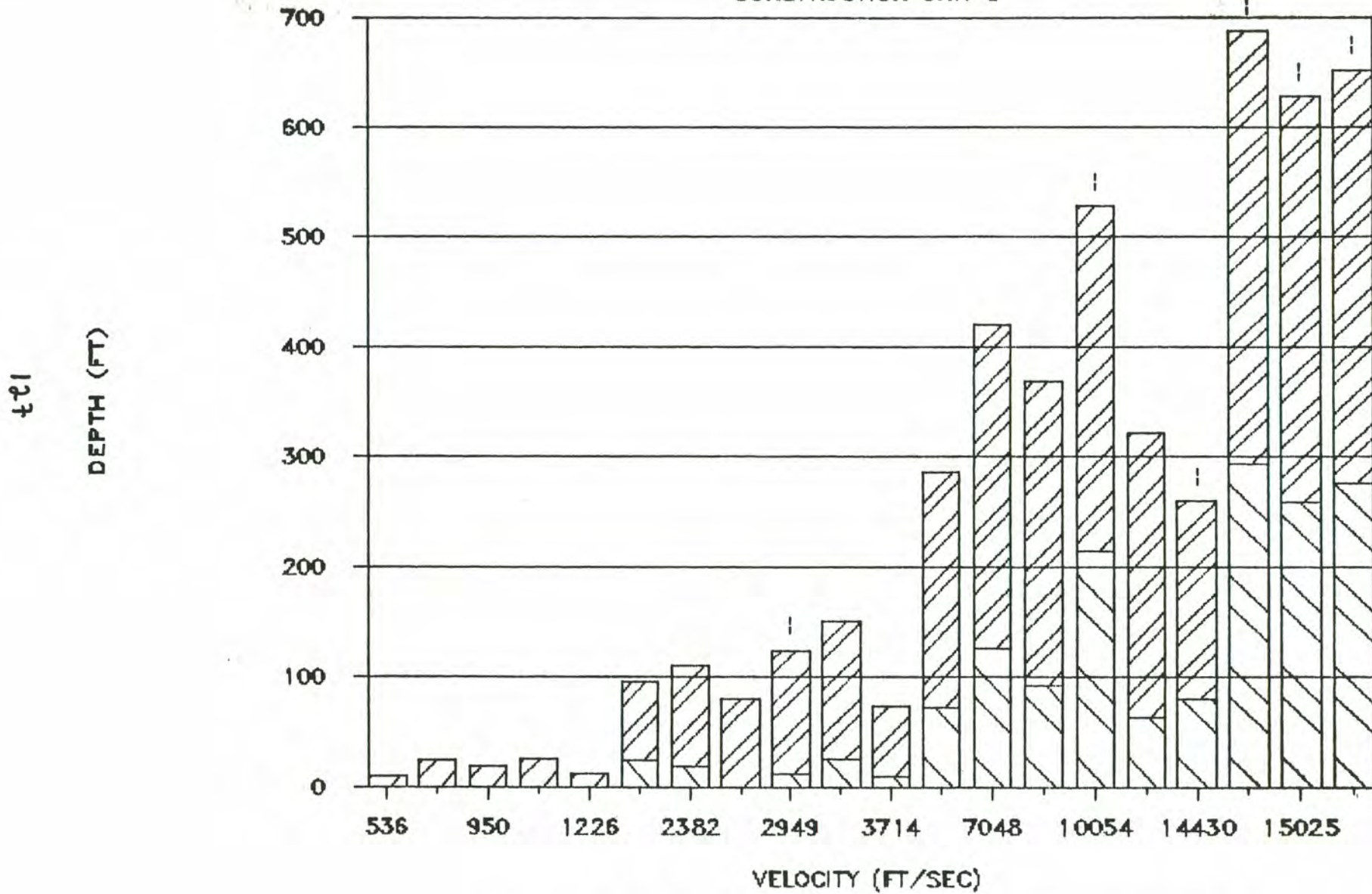


Figure 39. Seismic Velocities Versus Depth, Construction Unit 9

7.2 Construction Costs

In 1985 the Arizona SSC Project assembled a site evaluation team to define the geotechnical studies required to locate the SSC in Arizona. The evaluation team recommended that a heavy construction estimate be developed to quantify the site's advantages using the appropriate site-specific geotechnical data.

Accordingly, heavy-construction cost and scheduling estimates were used for cut-and-fill and TBM tunnels and shafts. Building estimates were used for surface facility construction. This method was recommended by the central Design Group in the Conventional Facilities Report.

During screening studies, alternative construction methods were evaluated for each of the CUs. Alternative configurations for the CUs were also evaluated. This earlier work defined the CUs and construction methods used to develop costs and schedules for this proposal. A Work Breakdown Structure (WBS) identifies costs by sector, and separates costs of cut-and-fill and TBM tunnels, shafts, and other major features.

Heavy construction estimates for each construction method alternative in each CU were input to a computer model for evaluation of total facility costs, schedules, and resource requirements. The computer model used by the Arizona SSC Project is called a Decision Support System (DSS). The DSS permitted an unbiased evaluation of construction alternatives in sufficient detail to define project constraints. This evaluation allowed the examination of multiple interlocking alternatives, and a flexible approach to minimizing costs and schedules.

The DSS developed for Arizona's SSC program has evolved over the past 10 years on various mining projects (Miller and Milligan, 1987). Its basis is Project/2 software developed by Project Software Development Incorporated (PSDI). The DSS was adapted specifically for Arizona SSC Project analysis requirements and compatibility with the central Design Group's work breakdown structure. The level of detail for Arizona's site-specific estimates met or exceeded that required for the DOE generic models.

Arizona's model allows total integration of cost and schedule with summation of cost and schedule by CU, by construction method, and sector. The model can monitor up to 99 geologic and geotechnical conditions for both ground support and instantaneous penetration rate of the TBM for each tunnel contract, regardless of the sectors that the tunnel crosses. This allows an accurate evaluation of the impact of changing geotechnical conditions as well as a realistic definition of contract lengths by economic, geologic, and topographic considerations. Another benefit of this approach is the reliable evaluation of the merits of alternative construction methods as they apply to individual construction units and to the project as a whole. The sensitivity of the Maricopa Site to innovations can be quantified to investigate the benefits of Arizona's construction conditions.

Construction costs can be entered as a unit price, or as a detailed estimate. The program allows the user to mix various estimating systems or methods in a single model.

Site-specific heavy-construction estimates were developed for all facets of construction except utility tie-ins and site infrastructure, which account for 19% of the total cost. These non-site-specific sections of the cost estimate are based upon the CDG Conventional Facilities Report.

7.2.1. Cut-and-Fill for Ring and Injector Tunnels.

Heavy construction estimates were developed for each of the cut-and-fill sections assuming the construction methodology described in 5.5.7.1. Summations of this estimate are given in Tables 19 and 20. Table 19 summarizes the characteristics of the CUs in length, estimated daily production, and geotechnical contingency. "Geotechnical contingency" is the possible range of an estimate that could occur due to incomplete knowledge of geotechnical conditions. It is presented here as a subjective estimate, based on the quantity of present data versus the expected geotechnical variation in a given CU. Table 20 summarizes the costs of cut-and-fill construction at various depths.

7.2.2. TBM for Ring and Injector Tunnels

Estimates were developed for each of the TBM tunnels using the construction methods described in 4.4.5. and 5.5.7.2. Summations of this estimate are presented in Tables 21 and 22. Table 21 summarizes the TBM costs for CU 3 which is typical of the Maricopa Site. Table 22 lists examples of unit costs for the three tunneling methods to be used at the Maricopa Site.

7.2.3. Comparison of TBM Versus Cut-and-Fill

For purposes of this proposal, use of a TBM was assumed for ring depths greater than 60 feet. The experience of local contractors with the fanglomerate demonstrates, however, stable open-cut excavations to depths of between 80 and 100 feet. Table 23 lists a cost of \$660/foot for a TBM tunnel in fanglomerate. Table 20 lists a cost of \$630/foot for a cut-and-fill tunnel in fanglomerate at a depth of 100 feet. Considering construction cost alone, the breakeven point between cut-and-fill and TBM tunneling occurs at a depth of about 100 feet. Assuming an 80-foot depth, there are seven additional miles of cut-and-fill construction at the Maricopa Site, and 15 additional miles at a 100-foot depth. The injector complex, by-pass tunnel, and 63% of the collider ring may be constructed with cut-and-fill methods by deepening the cuts. To be conservative in the estimates, a depth of 60 feet is assumed. However, experience shows there are significant increased flexibility and reduced costs in using cut-and-fill as an alternative to TBM tunneling down to a depth of 100 feet.

7.2.4. Experimental Chambers

Heavy construction estimates were developed for the experimental chambers and injector complex using methods described in Section 6.2. Summations of this estimate are presented in Table 23.

7.2.5. Shafts

Heavy construction estimates were developed for the shafts using methods described in Section 6.1. Table 24 compares the unit cost of shaft construction at the Maricopa Site. The projected total cost of an "average" shaft is presented in Table 25.

Further details on cost estimates for individual components or for the facility as a whole were provided in Arizona's site proposal (State of Arizona, 1987, Appendix B).

Table 19 - Construction Method Summary of Construction Units

<u>Description</u>		<u>Construction Unit Length</u>	<u>Predicted Average Production %</u>	<u>Geotechnical Contingency</u>
Unit 1	TBM	29,568	201	10
Unit 2	Cut-and-Fill	41,184	97*	5
Unit 3	TBM	13,200	145	15
Unit 4	TBM	31,680	185	15
Unit 5	TBM	39,600	182	20
Unit 6	TBM	45,408	204	5
Unit 7	Cut-and-Fill	21,648	95*	5
Unit 8	TBM	18,480	168	15
Unit 9	TBM	38,016	123	10
Unit 10	TBM	42,600	201	5
Weighted Average for TBM			180	11
Weighted Average for Cut-and-Fill			96	5
Weighted Average for Project			164	10

*Cut-and-fill advance rates vary with depth and length of cut. Rather than providing faster advance rates, cut-and-fill construction allows construction to begin sooner, and construction can proceed at several points along a contact length simultaneously. It is possible for cut-and-fill construction to be completed before a TBM can be purchased and installed, despite the apparent slower advance rates.

Table 20 - Estimated Cut-and-Fill Construction Cost Per Foot*

<u>DESCRIPTION</u>	<u>DEPTH OF CUT IN FEET</u>				
	<u>60</u>	<u>70</u>	<u>80</u>	<u>90</u>	<u>100</u>
Excavation Volume cu.yd.	121	157	196	240	288
Excavation \$/ft.	49.61	64.37	80.36	98.40	114.80
Regular Backfill \$/ft.	57.02	75.02	94.521	16.52	140.52
Select Backfill \$/ft.	7.66	7.66	7.66	7.66	7.66
Cast-in-Place Pipe Cost	253.47	253.47	253.47	253.47	253.47
G & A + Tax @ 12%	44.13	48.06	52.32	57.13	61.97
Profit @ 10%	36.78	40.05	43.60	47.61	51.64
Total \$/ft.	448.67	488.63	531.93	580.79	630.06

* The tunnel excavation cost estimates assume using a Holland Loader system with a 60 degree slope profile.

Cost estimates are in 1987 dollars.

Table 21 - Summary of TBM Costs*

COST	TOTAL COST	COST/FOOT OF TUNNEL
Direct**	\$9,672,893	\$327
Plant & Equipment***	\$5,225,393	\$178
Indirect****	\$4,618,710	\$156
TOTAL	\$19,546,996	\$661

*The displayed costs are for Constuction Unit 1 which is typical of the Maricopa Site TBM Construction Units. The tunnel length of 29,568 feet in weak rock.

**See Table 3-21 for a detailed listing of Construction Unit 1 direct costs.

***See table 3-22 for a detailed listing of Construction Unit 1 plant and equipment costs.

****See Table 3-23 for a detailed listing of Construction Unit 1 indirect costs.

Table 22 - TBM Unit Cost Per Foot

DESCRIPTION	WEAK ROCK TBM	HARD ROCK TBM	DRILL AND BLAST
Tunnel Length	29,568	43,100	2,400
Advance Rate, Ft/Day	202	132	18
Direct Cost \$/Ft	327	290	890
Plant and Equipment \$/Ft	178	170	570
Indirect Cost \$/Ft	156	190	830
Total Cost \$/Ft	660	650	2,290

NOTE: Cost estimates are in 1987 dollars.

Table 23 - Experimental Chambers and Injector Complex
 Estimated Construction Cost (x \$1,000,000)

DESCRIPTION	MARICOPA	CDG**	PERCENT SAVINGS
Site & Infrastructure	70	90	22
Campus	26	45	42
Injector Complex	56	42	0
Experimental Chambers	63	61	0
TOTAL	215	238	10

*Cost estimates are in 1987 dollars.

**CDG generic site "C" 1986 cost estimate inflated by 5%

Table 24 - Estimated Shaft Unit Costs

SHAFT*	COSTED DEPTH**	COST \$/FT
E 3	250	5,784
F 2	100	12,869
E 2	80	9,988
F 1	60	18,617
E 1	60	12,067
F 10	240	6,808
E 10	180	5,822
F 9	210	8,638
E 9	330	4,867
F 8	380	5,650
E 8	350	4,891
F 7	400	7,093
E 7	270	5,356
F 6	160	9,906
E 6	110	9,027
F 5	70	15,957
E 5	120	7,775
F 4	370	5,803
E 4	800	3,298
F 3	470	6,130

*E shafts are 20 feet in diameter.

F shafts are 30 feet in diameter.

**Depths shown were used to estimate cost.

Actual depths are given in Table 17.

Cost estimates are in 1987 dollars.

Table 25 - Access Shaft E7 Cost Summary

ACTIVITY	ESTIMATED COST
Mobilize and Set-Up	\$195,000
Collar	\$127,000
Shaft	\$854,000
Furnish	\$ 56,000
Clear and Demobilize	\$ 94,000
Drifts	\$120,000
Total	\$1,446,000

*Access shaft E 7 is "typical" of shafts to be constructed at the Maricopa Site. The depth used for estimating cost is 270 feet; whereas the actual depth is 250 feet.

Cost estimates are in 1987 dollars.

REFERENCES

Abdullatif, A.A., 1969, Physical testing of engineering properties of collapsing soil in the City of Tucson, Arizona:Tucson, University of Arizona, M.S. Thesis.

Alfi, A.A.S., 1984, Mechanical and electron optical properties of a stabilized collapsible soil in Tucson, Arizona: Tucson, University of Arizona, Ph.D. Dissertation.

Ali, M.M., 1987, A probabilistic Analysis of the Distribution of Collapsing Soil in Tucson Using Kriging Method, PhD. Dissertation, The University of Arizona, Department of Civil Engineering and Engineering Mechanics.

American Association of State Highway and Transportation Officials, 1983, Guide specifications for seismic design of highway bridges:Washington, D.C.

American National Standards Institute, 1982, Minimum Design Loads for Buildings and Other Structures, ANSI A58.1-1982, New York.

Anderson, F., 1968, Collapsing soils and their basic parameters in an area in the Tucson, Arizona vicinity:Tucson, University of Arizona, M.S. Thesis.

Applied Technology Council, 1978, Tentative Provisions for the Development of Seismic Regulations for Buildings, Report ATC-3-06 Prepared for the National Bureau of Standards and National Science Foundation, Second Printing, 1984, April.

Arizona, State of (Arizona Department of Commerce), 1987, Volume 3, Geology and Tunneling, Maricopa SSC Site, State of Arizona, Proposal to U.S. Department of Energy, September.

ASTM, 1985, Soil and rock; building stones in Annual Book of ASTM Standards:Philadelphia, v.4, u8.

Barton, N., Lien, R., and Lunde, J., 1974, Engineering classification of rock masses for the design of tunnel support:Rock Mechanics, v. 6, no. 4, p. 189-236.

Beckwith, G.H., and Hanse, L.A., 1982, Calcareous soils of the southwestern United States in Demars, K.R., and Chaney, R.C. eds., Geotechnical Properties, behavior, and performance of calcareous soils:Philadelphia, ASTM, STP 777.

Beckwith, G.H. and Bedenkop, D.V., 1973, An Investigation of the Load Bearing Capacity of Drilled, Cast-in-Place Concrete Piers Bearing on Coarse Granular Soils and Cemented Alluvial Fan Deposits, Sergeant, Hauskins & Beckwith Engineers, Report AHD-RD-10-122, Prepared for the Arizona Department of Transportation.

Beckwith, G.H., Weeks, R.E., and Cheng, S.S., 1988, The Preliminary Geotechnical Investigation:Main Campus Area, Maricopa SSC Site, Technical Report, SHB Consulting Geotechnical Engineeres, Phoenix, Arizona.

Bieniawski, Z.T., 1973, Engineering classification of jointed rock masses:- Transactions of the South African Institute of Civil Engineers, v. 15, no. 12, p. 335-344.

Bishop, A.W., 1955, The Use of the Slip Circle in the Stability Analysis of Slopes, Geotechnique, Vol. 5, pp. 7-17.

Bowles, J.E., 1987, Elastic Foundation Settlements on Sand Deposits, Journal of Geotechnical Engineering, ASCE, Vol. 113, No. 8, pp. 846-860, August.

Brooks, S.J., 1987, Ground water occurrences and aquifer properties for the Maricopa SSC Site, Maricopa County, Arizona:University of Arizona, Arizona SSC Project, unpublished manuscript.

Bruce, D.A., and Jewell, R.A., 1986, Soil Nailing:Application and Practice-Part 1, Ground Engineering, Vol. 19, November.

Cockran, B. 1987, M.M. Sundt Co.,:private communication to R.M. Miller 11 May 1987.

Crossley, R.W., 1969, A geologic investigation of foundation failures in small buildings in Tucson, Arizona:Tucson, University of Arizona, M.S. Thesis.

Crossley, R.W. and Beckwith, G.H., 1978, Subgrade Modulus for Arizona Pavements, Prepared for Arizona Department of Transportation, Report No. FHWA/AZ-75/142, January.

Cunningham, W.D., DeWitt, E., Haxel, G., Reynolds, S.J., and Spencer, J.E., 1987, Geologic map of the Maricopa Mountains, central Arizona:Arizona Bureau of Geology and Mineral Technology Open-File Report 87-4, scale 1:62,500.

Deere, D.U., 1963, Technical description of rock cores for engineering purposes: Rock Mech. Eng. Geol., v. 1, p. 18-22

Deere, D.U., 1968, Chapter 1, Geological Considerations, Rock Mechanics in Engineering Practices, John Wiley & Sons, New York.

DeNatale, J., and Nowatzki, E.A., 1987, Geotechnical engineering investigations for Arizona's SSC Sites:Arizona Bureau of Geology and Mineral Technology Open-File Report 87-7. 75p.

DeNatale, J.S., 1986, Program CSLIP1:For Slope Stability Analysis by Bishop's Modified Method, with a Search Routine Based on the Simplex Method of Nelder and Mead, Technical Report, The University of Arizona, Department of Civil Engineering and Engineering Mechanics.

DeNatale, J.S., Nowatzki, E.A., and Welty, J.W., 1987, Geotechnical Engineering Investigations for Arizona's SSC Sites, Arizona Bureau of Geology and Mineral Technology Open-File Report 87-7.

Dowding, 1979, Earthquake Stability of Rock Tunnels, Tunnels and Tunneling, Vol. II, No. 5, June.

- Farmer, I. W., 1968, Engineering Properties of Rocks, Spar, London
- Farmer, Ian Associates, Ltd. (1987) Development of an in-situ stress measuring device. Contract Progress Report. UX/96/151
- GAI Consultants, Inc., 1982a, Laterally Loaded Drilled Pier Research, Volume I: Design Methodology, EPRI-EL 2197 Report Prepared for Electric Power Research Institute.
- GAI Consultants, Inc., 1982b, Laterally Loaded Drilled Pier Research, Volume II: Research Documentation, EPRI-EL 2197 Report Prepared for Electric Power Research Institute.
- Gassler, G. and Gudehaus, G., 1981, Soil Nailing -Some Aspects of a New Technique, Proceedings of the 10th International Conference on Soil Mechanics and Foundation Engineering, Vol. 1, Stockholm.
- Gibbs, H.J. and Bara, J.P., 1962, Predicting Surface Subsidence from Basic Soil Tests, ASTM Special Technical Publication No. 322, American Society of Testing and Materials.
- Gibbs, H.J., 1961, Properties Which Divide Loose and Dense Uncemented Soils, U.S. Bureau of Reclamation Report No. EM-608.
- Glynn, M.E., 1987, Geotechnical Investigations of Two Potential Sites for the Proposed Arizona Superconducting Super Collider, M. S. Thesis, University of Arizona.
- Glynn, M.E., 1987, Geotechnical data--Sierrita and Maricopa Sites: University of Arizona, Arizona SSC Project Report, 15 p.
- Graham, P. C., 1976, Rock Exploration for Machine Manufacturers, Proc Symposium Exploration for Rock Engineering, Johannesburg, pp 173-180
- Hansen, J.B., 1961, The Ultimate Resistance of Rigid Piles Against Transversal Forces, Danish Geotechnical Institute Bulletin, 12.
- Hoek, E. and Brown, E.T., 1980, Underground Excavations in Rock, The Institution of Mining and Metallurgy, London.
- Hovland, H.J. 1977, Three-Dimensional Slope Stability Analysis Method, Journal of Geotechnical Engineering, ASCE, Vol. 103, No. GT-9, pp. 971-986.
- Hunt R. E. (1984) Geotechnical engineering investigation manual McGraw-Hill, New York p. 228 et seq.
- Hunter, P.W., 1987, Excavation of a major tunnel by double shielded TBM through mixed ground of basalt and clayey soil, in Jacobs, J.M., and Hendricks, R.S., eds., Proceedings of the rapid excavation and tunneling conference: Society of Mining Engineers, v. 1, p. 526-551
- International Conference of Building Officials, 1982, Uniform Building Code, 1982 Edition, Whittier, California.

Janbu, N. 1973, "Slope Stability Computations," Embankment Dam Engineering, Casagrande Volume, pp 47-86.

Jennings, J.E. and Knight, K., 1975, A Guide to Construction on or with Materials Exhibiting Additional Settlement Due to Collapse of Grain Structure, Proceedings of the 6th Regional Conference for Africa on Soil Mechanics and Foundation Engineering, Vol. 1, pp. 99-105.

Jones, C., 1985, Earth Reinforcement and Soil Structures, Butterworths Advanced Series in Geotechnical Engineering, London.

Judd, W. R., and Huber, C., 1961, Correlation of Rock Properties by Statistical Methods, in Clark, G. B., ed., International Symposium on Mining Research, Pergamon, Oxford.

Kahle, K., Conway, D., and Haxel, G., 1987, Preliminary Geologic map of the Ajo 1 degree x 2 degree quadrangle, Arizona:U.S. Geological Survey Open-File Report 78-1096, scale 1:250,000.

Koerner, R.M. 1986a, Designing for Flow, Civil Engineering, Vol. 56, No. 10, October.

Koerner, R.M. 1986b, Designing With Geosynthetics, Prentice Hall International, New Jersey.

Kulhawy, F.H. and Goodman, R.W., 1987, Chapter 55 -Foundations in Rock, Ground Engineer's Reference Book, Butterworth and Co. Publishers, Ltd., London.

Kulhawy, F.H. and Others, 1983, Transmission Line Structure Foundations for Uplift-Compression Loading, EPRI-EL 2870, Report Prepared for Electric Power Research Institute.

Machette, M.N., 1985, Calcic Soils of the Southwestern United States, Soils and Quaternary Geology of the Southwestern United States, D.L. Weide, Ed., Special Paper 203, Geological Society of America, Boulder, Colorado.

McBean, R.P., Escalante, L.E., and Shively, A.W., 1983, Intermountain Power Project Seismic Criteria, Journal of Technical Topics in Civil Engineering, ASCE, Volume 109, No. 1.

McCreath, D.R., 1984, Golder Associates, Inc., Seattle, WA, Rock Engineering Short Course, Anchorage, Alaska.

Source:Norwegian Institute of Technology, 1983, Hard Rock Tunnel Boring, Project Report No. 1-83, Department of Geology/ Division of Construction Engineering, University of Trondheim, 159 pp.

Menard L. R. (1975) Interpretation and application of pressuremeter test results Soils-Soils Vol 26 pp.1-43.

Miller, R.M., Sperry, P.E., Milligan, J., Hynd, J.S.G., and Heuer, R., 1987, Arizona Superconducting Super Collider Program; analysis of construction

methods and site specific cost and schedules: Consulting report submitted to the Arizona Department of Commerce, 50p. This report is available from the Arizona SSC Project.

Miller, R.M., and Milligan, J., Decision support system for underground construction--a mining case study in Jacobs, J.M., and Hendricks, R.S., eds., Proceedings of the rapid excavation and tunneling conference: Society of Mining Engineers, v. 2, p. 1329-1342.

Morgenstern, N.R. and Price, V.E. 1965, The Analysis of the Stability of General Slip Surfaces, Geotechnique, Vol. 15, No. 1, pp. 79-93.

Nowatzki, E.A., 1981b, Settlement estimates in collapse susceptible soils-: Journal of Civil Engineering Design, v. 2, no. 2.

Nowatzki, E.A., 1980, Settlement Estimates in Collapse-Susceptible Soils, Journal of Civil Engineering Design, Vol. 2, pp 121-148.

Nowatzki, E. E., Muller, E., DeNatale, J., Ibarra-Encinas, G. A., and Al-Ghanem, A. M., 1988, Additional Geotechnical Engineering Investigation of Maricopa SSC Site, Arizona Bureau of Geology and Mineral Technology Open-File Report, Tucson.

Newlin, C.W., 1968, Report of Lateral Load Tests Single-Pole Transmission Tower Foundations, Kyrene Receiving Station Test Site Near Kyrene, Arizona, Report Prepared for the Salt River Project.

Poulos, H.G. and Davis, E.H., 1980, Pile Foundation Analysis and Design, John Wiley and Sons, Inc., New York.

Poulos, H.G. and Davis, E.H., 1974, Elastic Solutions for Soil and Rock Mechanics, John Wiley & Sons, Inc., New York.

Quiros, G.W. and Reese, L.C., 1977, Design Procedures for Axially Loaded Shafts, Research Report 176-5F, Center for Highway Research, The University of Texas at Austin.

Reese, L.C., Cooley, L.A. and Radhakrishnan, N., 1984, Laterally Loaded Piles and Computer Program COM 624G, Technical Report K-84-2, U.S. Army Waterways Experiment Station, Vicksburg, Mississippi.

Reynolds, S. J., 1987. Arizona Geological Survey: Private communication to J.W. Welty 20 April 1987.

SSC Central Design Group, 1986, Conceptual Design of the Superconducting Supercollider, Universities Research Association, Washington, D.C., March.

Sabbagh, A.O., 1982, Collapsing soil and their clay mineralogy in Tucson:- Tucson, University of Arizona, M.S. Thesis.

Seed, H.B. and Others, 1984, Moduli and Damping Factors for Dynamic Analysis of Cohesionless Soils, Report No. UCB/EERC-84/14, University of California, Berkeley, California, September.

Seed, H.B. and Others, 1970, Soil Moduli and Damping Factors for Dynamic Response Analysis, Report No. EERC 70-10, University of California, Berkeley, California, December.

Sergent, Hauskins and Beckwith, Inc., 1987, Geotechnical site characterization, Superconducting Super Collider (SSC), Maricopa and Sierrita Mountains, Arizona: Report No. E87-113.

Sergent, Hauskins, and Beckwith, Inc. 1988, Preliminary Geotechnical Investigation Report, Main Campus Area, SHB job No. E88-11, available through Sergent, Hauskins, and Beckwith, Inc., Phoenix, AZ, or through the Arizona SSC project.

Sperry, P.E., 1987, Tunneling Consultant: private communication to R.M. Miller, 20 January 1987.

Sternberg, B.K., 1987, Report on seismic survey during August, 1986 for Desertron Sierrita Site: University of Arizona Laboratory for Advanced Subsurface Imaging Report LASI-86-1, 215 p.

Sternberg, B.K., and Esher, J.E., 1987, Report on seismic surveys during December, 1986, January, 1987, and March, 1987, for the Desertron Maricopa Site: University of Arizona Laboratory for Advanced Subsurface Imaging Report LASI-87-1, 239 p.

Sternberg, B.K., and Sutter, T.C., 1987, Report on gravity surveys for Desertron Maricopa Site, October, 1986; March, 1987: University of Arizona Laboratory for Advanced Subsurface Imaging Report LASI-87-2, 96 p.

Sternberg, B.K., and Thomas, S.J., and Fink, J.B., 1987, Report on electrical resistivity and induced polarization (IP) surveys for the Desertron Maricopa and Sierrita Sites: University of Arizona Laboratory for Advanced Subsurface Imaging Report LASI-87-3, 65 p.

Sternberg, B.K., Bryan, W.C., Burchard, G.C., Byrne, R.W., Condit, T.B., DeHart, B.J., DuPass, M.K., Loy, K.L., Thomas, S.J., Umholtz, A.C., and Wilkosz, M.E., 1987: University of Arizona Laboratory for Advanced Subsurface Imaging Report LASI-87-4, 188 p.

Sternberg, B.K., Esher, J.E. and Poulton, M.M., 1988, Report on Seismic Surveys During December, 1987 and January, 1988, for the Arizona SSC Maricopa Site, Laboratory for Advance Subsurface Imaging, The University of Arizona, Tucson, February.

Trautmann, C.H. and Kulhawy, F.H., 1987, CUFADA Computer Program for Compression and Uplift Foundation Analysis and Design, Report EL-4540-CCM, Vol. 16, Electric Power Research Institute, Palo Alto, CA.

Tucker, K.D., 1987, Uplift Behavior of Drilled Shaft and Driven Piles in Granular Materials, Foundations for Transmission Lines, J.L. Briaud, Ed., Geotechnical Special Publication No. 8, ASCE, New York.

U.S. Army Corps of Engineers, Sternberg, B.K., 1960, The Unified Soil

Classification System:Vicksburg, MS, Technical Memorandum no. 3-357

USNCTT (U.S. National Committee on Tunneling Technology), 1976, Executive presentation--recommendations on better contracting for underground construction:Washington, D.C., National Academy of Sciences, 21 p.

Wang, F. D. and Ozdemir, L., 1978, Tunnel Boring Penetration Rates and Machine Design, Tunnelling and Underground Structures, Trans. Res. Record, 684.